2019

Assessing the Safety and Operational Benefits of Connected and Automated Vehicles: Application on Different Roadways, Weather, and Traffic Conditions

Md Sharikur Rahman
University of Central Florida

ASSESSING THE SAFETY AND OPERATIONAL BENEFITS OF CONNECTED AND AUTOMATED VEHICLES: APPLICATION ON DIFFERENT ROADWAYS, WEATHER, AND TRAFFIC CONDITIONS

by

MD SHARIKUR RAHMAN

B.Sc., Bangladesh University of Engineering and Technology, Bangladesh, 2014

M.Sc., University of Central Florida, USA, 2018

A dissertation submitted in partial fulfillment of the requirements
for the degree of Doctor of Philosophy
in the Department of Civil, Environmental and Construction Engineering
in the College of Engineering and Computer Science
at University of Central Florida
Orlando, Florida

Summer Term

2019

Major Professor: Mohamed Abdel-Aty

ABSTRACT

Connected and automated vehicle (CAV) technologies have recently drawn an increasing attention from governments, vehicle manufacturers, and researchers. Connected vehicle (CV) technologies provide real-time information about the surrounding traffic condition (i.e., position, speed, acceleration) and the traffic management center's decisions. The CV technologies improve the safety by increasing driver situational awareness and reducing crashes through vehicle-to-vehicle (V2V) and vehicle-to-infrastructure (V2I). Vehicle platooning with CV technologies is another key element of the future transportation systems which helps to simultaneously enhance traffic operations and safety. CV technologies can also further increase the efficiency and reliability of automated vehicles (AV) by collecting real-time traffic information through V2V and V2I. However, the market penetration rate (MPR) of CAVs and the higher level of automation might not be fully available in the foreseeable future. Hence, it is worthwhile to study the safety benefits of CAV technologies under different MPRs and lower level of automation. None of the studies focused on both traffic safety and operational benefits for these technologies including different roadway, traffic, and weather conditions. In this study, the effectiveness of CAV technologies (i.e., CV /AV/CAV/CV platooning) were evaluated in different roadway, traffic, and weather conditions. To be more specific, the impact of CVs in reduced visibility condition, longitudinal safety evaluation of CV platooning in the managed lane, lower level of AVs in arterial roadway, and the optimal MPRs of CAVs for both peak and off-peak period are analyzed using simulation techniques. Currently, CAV fleet data are not easily obtainable which is one of the primary reasons to deploy the simulation techniques in this study to evaluate the impacts of CAVs in the roadway. The car following, lane changing, and the platooning behavior of the CAV technologies were modeled in the C++ programming language by considering realistic car following and lane

changing models in PTV VISSIM. Surrogate safety assessment techniques were considered to evaluate the safety effectiveness of these CAV technologies, while the average travel time, average speed, and average delay were evaluated as traffic operational measures. Several statistical tests (i.e., Two sample t-test, ANOVA) and the modelling techniques (Tobit, Negative binomial, and Logistic regression) were conducted to evaluate the CAV effectiveness with different MPRs over the baseline scenario. The statistical tests and modeling results suggested that the higher the MPR of CAVs implemented, the higher were the safety and mobility benefits achieved for different roadways (i.e., freeway, expressway, arterials, managed lane), weather (i.e., clear, foggy), and traffic conditions (i.e., peak and off-peak period). Interestingly, from the safety and operation perspective, at least 30% and 20% MPR were needed to achieve both the safety and operational benefits of peak and off-peak period, respectively. This dissertation has major implications for improving transportation infrastructure by recommending optimal MPR of CAVs to achieve balanced mobility and safety benefits considering varying roadway, traffic, and weather condition.

ACKNOWLEDGMENT

I would like to express the deepest appreciation and gratitude to my honourable supervisor Professor Mohamed Abdel-Aty, for his invaluable guidance, advice, support, and encouragement toward successful completion of the doctorate degree. Without his help and persistent guidance, my PhD Student life can not be smooth.

I would also like to gratefully acknowledge Signal Four Analytics (S4A) and Florida Department of Transportation (FDOT) for providing access to Florida traffic data for building, calibration, and validation of the simulation network. I also acknowledge the funding support of UTC SAFER-SIM, SAFER-SIM is a RITA funded UTC Center lead by the University of Iowa. I wish to acknowledge the support of my respectable committee members, Dr. Naveen Eluru, Dr. Samiul Hasan, and Dr. Xin Yan. The course they offered were among the most taught courses I have had. Meanwhile, I also want to acknowledge Dr. Ling Wang, Dr. Jaeyoung Lee, and Dr. Yina Wu for providing valuable suggestion for my research work. Additionally, I am thankful to all of my lab mates for helping me towards the successfully completion of my Ph.D. degree.

I would also like to thank my beloved parents (Father: Md Ataur Rahman, Mother: Nazmin Nahar) and elder brother (Md Shakilour Rahman) who always encourage me a lot. Last but not the least, many thanks to my beloved wife Laizu Akter. She always stood by me and cheered me up through good and bad times. Without her support and encouragements, I cannot achieve anything.

TABLE OF CONTENTS

LIST OF FIGURES

LIST OF TABLES

CHAPTER ONE: INTRODUCTION

1.1 Background

Connected and automated vehicle (CAV) technologies have been considered as a vital strategy for both traffic operation and safety improvement. The combination of connected and automated vehicle technologies has generated high expectations regarding traffic safety by minimizing drivers' errors, which is considered a major cause solely or in combination with other factors for more than 94% of traffic crashes (Singh, 2015; Yue et al., 2018). By leveraging vehicle-to-vehicle (V2V) and vehicle-to-infrastructure (V2I) communications, connected vehicle (CV), automated vehicle (AV), CAV, and CV platooning technologies are expected to provide cooperative movements and thus increase freeway/expressway traffic safety and operations (Kockelman et al., 2016; Papadoulis et al., 2019; M. S. Rahman et al., 2019d; Rahman and Abdel-Aty, 2018). Nevertheless, the evaluation of their safety and operational benefits has still been a major challenge due to the lack of real-world CAV data. Recent studies have attempted two directions of CAV research to predict the effectiveness of CAV technologies: (1) real-world CAV data (2) simulation techniques. The former one focuses on real-world CAV data extracted from the Safety Pilot Model Deployment (SPMD). The latter one has focused on CAV simulation during the past few years. A very limited portion of the SPMD CAV test data is available to the public and was used in some recent studies. This is one of the primary reasons to deploy the simulation techniques in the existing part of the literature to evaluate the impacts of CAV fleets (Fagnant and Kockelman, 2015; Kim et al., 2015; Papadoulis et al., 2019). More recently, researcher has relied on simulation techniques which might be the only viable alternative method to evaluate the impacts of CAV and can provide the initial insights into the implementation of CAVs.

This dissertation has focused both traffic safety and operational benefits of multiple CAV technologies including different roadway, traffic, and weather conditions. The impact of CV in fog condition, longitudinal safety evaluation of CV platooning in the managed lane, lower level of AVs on arterials, and the optimal MPRs of CAV for both peak and off-peak periods are analyzed using simulation techniques. The CAV will not be available 100% in the near future. Hence, the market penetration rate (MPR) of CAVs are also considered due to the unavailability of CAV in the foreseeable future. The different roadway types including freeway, expressway, arterial, and the managed lane were designed, calibrated, and validated based on real-world traffic data in PTV VISSIM. From the modeling standpoint, capturing the effects of driving behaviors of CAV in the simulation software are a very challenging task (M. S. Rahman et al., 2019d). The driving behavior of CAVs and standard vehicles are significantly different from each other. Therefore, the understanding of the driving behavior of CAV technologies are essential for studying the impact on traffic operations and safety benefits considering different roadway, weather, and traffic conditions. A driving behavior model for all the CAV technologies (CV, AV, CAV, and CV platooning) were modeled in VISSIM using C++ programming language which overrides the VISSIM default driving behavior. To the best of our knowledge, this is the first study which utilizes different types of CAV technologies to evaluate both traffic safety and operation characteristics considering multiple conditions sets including roadway, weather, and traffic conditions.

Both traffic safety and operational characteristics were evaluated in order to observe the CAV benefits in the transportation infrastructure. Surrogate safety assessment techniques were considered as safety indicators, while average travel time, speed, and delay were assessed as traffic mobility indicators. Some statistical testing and modelling were conducted to obtain the

significance of the safety and mobility indicators. The optimal MPRs of CAV were also quantified by conducting statistical modelling techniques.

1.2 Objectives of the Research

The specific objectives for the dissertation are described here:

Objective 1. *Understanding the Highway Safety Benefits of Different Approaches of Connected Vehicles in Reduced-Visibility Conditions*

The dissertation examines the effectiveness of CV technologies in adverse visibility conditions using microscopic traffic simulation. Under fog condition, traffic flow characteristics change significantly compared to the normal weather condition which might result in high crash risk. In order to improve safety in fog condition, this study tested CV technologies in microsimulation at the segment of I-4, Florida. The technologies included connected vehicles without platooning and connected vehicles with platooning which were applied in fog condition to reduce the crash risk in terms of surrogate measures of safety. The standard deviation of speed, the standard deviation of headway, and rear end crash risk index (RCRI) were considered as three surrogate measures of safety in this study. This chapter implemented CVs as a Vehicle-to-Vehicle protocol, which offers Dedicated Short-Range Communication (DSRC) system to acquire real-time traffic data with the help of microsimulation software VISSIM. The car following model was also proposed for both technologies with an assumption that the CVs will follow this car following behavior in fog condition. The impact of traffic safety and operations were evaluated under two approaches of CV technologies.

Objective 2. *Longitudinal safety evaluation of connected vehicles' platooning on expressways*

The main objective this task was to evaluate longitudinal safety of CV platoons by comparing the implementation of managed-lane CV platoons and all lanes CV platoons (with same MPR) over non-CV scenario. This study applied the CV concept on a congested expressway (SR408) in Florida to improve traffic safety. The Intelligent Driver Model (IDM) along with the platooning concept were used to regulate the driving behavior of CV platoons with an assumption that the CVs would follow this behavior in real-world. A high-level control algorithm of CVs in a managed-lane was proposed in order to form platoons with three joining strategies: rear join, front join, and cut-in joint. Results of this study provide useful insight for the management of CV MPR as managed-lane CV platoons based on traffic safety.

Objective 3. *Assessing the Safety Benefits of Arterials' Crash Risk under Connected and Automated Vehicles.*

This section examines the safety benefit of CV and the connected vehicles lower level automation (CVLLA) on arterials' using micro-simulation. Examining the lower level of automation is more realistic in the foreseeable future. This study considered two automated features: automated braking and lane keeping assistance which are available in the market. Driving behaviors of CV and CVLLA were proposed by considering car following models that approximate the decision processes of CV and CVLLA using C++ programming interface in VISSIM. The safety impact of both segment and intersection crash risks were quantified under various MPRs of CV and CVLLA based on surrogate safety assessment techniques.

<u>Objective 4.</u> *Traffic Safety and Operational Benefits of Connected and Automated Vehicles on Expressways under varying traffic conditions*

This task explores the traffic safety and operational benefits of CAVs in expressway. The optimal market penetration rates of CAV technologies for both peak and off-peak periods are also recommended. The CAV applications were tested in the studied simulated network using PTV VISSIM 11. PTV VISSIM 11 has the new capability to model the CAV with validated driving behavior models based on real-word CAV data. The safety and operation performance for various scenarios were evaluated using different measures of effectiveness. Operational measures included average travel time and average delay, while the safety measures considered both time proximity (conflicts) based and evasive action based (jerk) surrogate measures of safety. To achieve balanced mobility and safety benefits from mixed traffic environment, optimal CAV market penetration should be determined at varying traffic conditions.

1.3 Dissertation Structure

In Chapter 2, a detailed literature review is conducted on the effectiveness of different approaches of CAV technologies including CV, AV, CAV, and CV platooning. In recent years, an increased number of studies are undertaking with detailed analysis of CAV technologies. These studies examine traffic safety and mobility characteristics under CAV environment using mostly the traffic simulation techniques.

Chapter 3 examines the impact of CV technologies under reduced visibility conditions. This research estimates traffic safety and mobility benefits under connected vehicle without platooning (CVWPL) and the connected vehicle with platooning condition (CVPL). The car following model was also proposed for both technologies with an assumption that the CVs will follow this car following behavior in fog condition. The model performances were evaluated under different CV market penetration rates (MPRs). The results showed that both CV approaches improved safety significantly in fog conditions as MPRs increase. The results also indicated a significant improvement in the traffic operation characteristics in terms of average speed.

Chapter 4 presents details to evaluate the longitudinal safety evaluation of managed-lane CV platoons on a congested expressway. The simulation experiments are first designed, including deployment of both CV platoons as managed-lane and all lanes in this expressway. Then, a driving behavior model for CVs along with the platooning concept were used with an assumption that the CVs would follow this driving behavior in real-world. From our analysis, it is evident that managed lane CV platoons and all lanes CV platoons significantly improved the longitudinal safety in the studied expressway segments compared to the base condition. In terms of surrogate safety measures, the managed-lane CV platoons significantly outperformed all lanes CV platoons with the same MPR.

Chapter 5 discusses the evaluation of vehicle to vehicle (V2V) and infrastructure-to-vehicle (I2V) communication technologies along with the automated vehicles in an arterial section. The lower level of automation features was considered due to the unavailability of the higher-level automation in the foreseeable future. Driving behavior of connected and lower level of automated

vehicles were modeled in the C++ programming languages. The safety impact on both segment and the intersection crash risk were explored through surrogate safety assessment techniques.

Chapter 6 explores both safety and operational benefits of CAV with considering different market penetration rates and traffic condition. The optimal market penetration rates were calculated based on both traffic safety and operational characteristics. Tobit and negative binomial models were developed for traffic operation and traffic safety, respectively, to investigate the market penetration rate (MPR) and the traffic condition (peak, off-peak) effectiveness.

Finally, Chapter 7 summarizes the dissertation and raises potential improvement for future applications and proposes studies in the era of CAV technologies.

CHAPTER TWO: LITERATURE REVIEW

CAV technologies which have the potential to reduce traffic congestion, road crashes and vehicle emissions have been drawn an increasing attention recently (Fagnant and Kockelman, 2015; Poczter, 2014). Most of the recent studies attempted two directions of CAV research to predict the effectiveness of CAV technologies: (1) real-world CAV data (2) simulation techniques. The former one focused on real-world CAV data extracted from the Safety Pilot Model Deployment (SPMD). The latter one focused on CAV simulation during the past few years. A very limited portion of the SPMD CAV test data is available to the public and was used in some recent studies. These studies have been evaluated the safety and operation benefits of CAV data using volatile measures, surrogate safety assessment techniques, and traffic operation characteristics. It is beyond the scope of this paper for exhaustive review of these studies using real-world CAV data (see (Arvin et al., 2019; Kamrani et al., 2018, 2017, Liu and Khattak, 2018, 2016; Xie et al., 2019; Zhang and Khattak, 2018; Zheng and Liu, 2017) for detailed review).

Despite the real-world CAV deployment data is available, CAV fleet data are not easily obtainable. However, the SPMD deployment data are not enough to evaluate the CAV impact on traffic safety and operations because of their limited scope of data. This is one of the primary reasons to deploy the simulation techniques in the existing part of literature to evaluate the impacts of CAV fleets (Fagnant and Kockelman, 2015; Kim et al., 2015; Papadoulis et al., 2019). More recently, several studies have relied on simulation techniques which might be the only viable alternative method to evaluate the impacts of CAV and can provide initial insights of the CAVs implementation. However, the recent attempts in CAV simulations have some limitations. The driving behaviors of CAV are significantly different from conventional vehicles. From the modeling standpoint,

capturing the effects of driving behaviors of CAV in the simulation software are very challenging tasks (M. S. Rahman et al., 2019d; Talebpour and Mahmassani, 2016a). Most of the previous studies employed the Intelligent Driver Model (IDM) to replicate the behavior of CAVs in simulation as the IDM has the validated car following models for CAV data (Li et al., 2016a; M. S. Rahman et al., 2019c; Rahman and Abdel-Aty, 2018; Talebpour et al., 2015; Talebpour and Mahmassani, 2016a; Wu et al., 2019a) using very limited real-world public test track. However, they are solely focused on the longitudinal driving behaviors (i.e., car following model) of CAV without considering the lateral behaviors (i.e., lane changing model). Moreover, modeling the interaction between CAVs and conventional vehicles are very challenging tasks which are also not validated in the previous studies.

Florida is among the highest ranked states in the United States with regards to traffic safety problems resulting from adverse weather conditions, especially in fog. As an example, a fog related severe crash caused 5 fatalities, several injuries, and left a pileup of 70 vehicles on I-4, Polk County, Florida (Hassan et al., 2011). The injury and death rates (per 100 crashes) for fog-related crashes were found to be 3.75 and 2.25 times of the corresponding type of crashes occurring in normal weather conditions, respectively (Al-Ghamdi, 2007). This study has examined previous studies to evaluate the traffic characteristics in fog conditions. Abdel-Aty et al. (Abdel-Aty et al., 2014) conducted a comprehensive study with an effort to examine the traffic characteristics in fog conditions. The study concluded that speed and headway decreased significantly under reduced visibility conditions. Furthermore, the standard deviation of speed and headway increased in fog conditions compared to the clear conditions. A more recent study by Peng et al. (Peng et al., 2017) identified that reduced visibility would significantly increase the standard deviation of speed and

headway which intensifies traffic crash risk. It was also observed that time to collision decreased significantly in reduced visibility conditions, which means that the crash risk would be higher under reduced visibility conditions. They also found that the impact of low visibility on crash risk was different for different vehicle types and for different lanes. The crash risk is higher for passenger vehicles compared to the heavy vehicles, and the inner lane (close to the median) has higher crash risk compared to the middle and outer lanes. Other studies also pointed out that headway distance was reduced in fog conditions and sometimes reduced headway would have a perceptual control benefit to the driver in terms of reduction in response time under fog conditions (Broughton et al., 2007; Caro et al., 2009). Brooks et al. (Brooks et al., 2011) examined the effect of fog conditions on the lane-keeping ability using driving simulator. It was shown that lane keeping performances were significantly degraded by the existence of fog.

There is relatively little work in the literature describing the countermeasures in reduced visibility conditions. The findings of the previous studies provided several recommendations as guidelines to improve safety in reduced visibility conditions. Based on a questionnaire survey, Hassan et al. (Hassan et al., 2011) suggested that changeable message signs can be a good countermeasure to reduce the driving speed. Pang et al. (Pang et al., 2015) used a simulation based study to examine the traffic safety and operation in fog conditions. The study showed that fog-related crashes were reduced by controlling upstream traffic flow (decreasing upstream traffic volume) and implementing VSL. Peng et al. (Peng et al., 2017) suggested that implementing the algorithms in real-time with Intelligent Transport System (ITS) measures, such as VSL and VMS, can reduce the crash risk in reduced visibility conditions. Speed variance would be lower with the implementation of VSL, which in turn decrease crash risk (Abdel-Aty et al., 2009, 2006; Lyles et

al., 2004; Wang et al., 2017). In terms of safety, VSL has been used during the inclement weather in order to decrease both the mean and the standard deviation of speed (Perrin et al., 2002; Rämä, 1999). However, the success of the VSL application is more dependent on the compliance level. In the low level of compliance, the VSL might fail to improve traffic safety (Hellinga and Mandelzys, 2011; Lee et al., 2006; Yu and Abdel-Aty, 2014). The research by Abdel-Aty et al. (Abdel-Aty et al., 2009) also evaluated that the implementation of VSL might reduce the rear-end and lane-change crash risks at uncongested traffic conditions but not successfully reduce the crash risk in the congested situation. Hence, the success of the VSL is also dependent on the level of congestion.

The new ITS technologies, CV, has been recently recognized as an auspicious approach which proved its potential to improve traffic safety, including mitigating crash severity and declining the possibility of crashes by offering vehicle to vehicle (V2V) and vehicle to infrastructure (V2I) communication. The majority of the previous research was concerned about the mobility and the traffic operations under CV environment but did not focus on traffic safety. Fyfe and Sayed (Fyfe and Sayed, 2017) combined VISSIM and the Surrogate Safety Assessment Model (SSAM) with the application of the Cumulative Travel Time (CTT) algorithm which evaluates the safety under CV environment. The study showed a 40 percent reduction of rear-end conflicts' frequency at a signalized intersection with the application of CV. Olia et al. (Olia et al., 2016) experimented with CV technologies in PARAMICS and estimated that the safety index improved up to 45% under CV environment. Paikari et al. (Paikari et al., 2014) also used PARAMICS which combined the V2V and V2I technologies and obtained higher safety and mobility enhancement on freeways under the CV environment. Vehicle platooning with CV technologies is another key element of

the future transportation systems which help us to enhance traffic operations and safety simultaneously. Tian et al. (Tian et al., 2016) proposed a stochastic model to evaluate the collision probability for the heterogeneous vehicle platoon which can deal with the inter-vehicle distance distribution. The results have the great potential to decrease the chain collisions and alleviate the severity of chain collisions in the platoon at the same time. However, until this point, no researcher has potentially analyzed CV technologies which are expected to decrease the crash risk in reduced visibility conditions. When compared to the previous studies, this study is unique in a sense that it reflects the fog conditions in microscopic simulation and apply CV technologies which are expected to improve traffic safety in reduced visibility conditions.

Vehicle platooning with CV technologies is another key element of the future transportation systems which help us to enhance traffic operations and safety simultaneously. Recent research (Tian et al., 2016) proposed a stochastic model to evaluate the collision probability for the heterogeneous vehicle platooning which can deal with the inter-vehicle distance distribution. The results showed great potential in decreasing the chain collisions and alleviating the severity of chain collisions in the platoon at the same time. The platoon-based driving may significantly improve traffic safety and efficiency because a platoon has closer headways and lower speed variations compared to traditional traffic flow. The platoon-based cooperative driving system has been widely studied. However, there have not been enough studies that allocate managed-lane CV platoons which is highly related to CV MPR. The safety benefits of managed-lane CV platoons are expected to be positive because of the dissociation of conventional vehicles and CVs in the same lane. Most of the researches in CV technologies were related to the implementation of CV in all the lanes of the entire roadway with different MPRs. However, until this point, no researcher

has potentially analyzed the managed-lane CV platoons which are expected to decrease the crash risk.

Moreover, CAV technologies have great potentials to reduce crash costs all over the world. Those technologies are expected to reduce crash risk as the majority of the crashes are owing to driver's human error. However, very little research has been conducted to estimate the safety impacts of connected and automated vehicles on arterials. The CV technologies would inform a vehicle about the traffic conditions from its surrounding environment, such as a nearby vehicle's position, speed, acceleration, signal status, and other traffic information through V2V and I2V communications. According to the National Highway Traffic Safety Administration (NHTSA), CV technologies will annually prevent 439,000 to 615,000 crashes with adoption of full V2V communication (National Highway Traffic Safety Administration, 2016; Rahman and Abdel-Aty, 2018). Yue et al., (Yue et al., 2018) conducted a comprehensive study with an effort to examine the exact safety benefits when all vehicles are equipped with these technologies. This research effort found that the CV technologies could lead to the reduction of light vehicle and heavy truck involved crashes by at least about 33% and 41%, respectively. However, the safety impact of implementing I2V communication has not been sufficiently explored. Li et al., (Li et al., 2016b) investigated the I2V communication technology along with variable speed limit strategy under adaptive cruise control environment. This simulation-based study indicated that I2V communication system provides significant safety benefits in terms of surrogate measures of safety under adaptive cruise control environment.

The CV technologies can also further increase the efficiency and reliability of automated vehicles by collecting real time traffic information through V2V and I2V communications. There are considerable amount of work in the literature describing the effectiveness of automated vehicle (Mirheli et al., 2018; Talebpour et al., 2017; Talebpour and Mahmassani, 2015, 2016b). Morando et al., (Morando et al., 2018) investigated full level of automated vehicle and found the reduction of the number of conflicts by 20% to 65% with the penetration rates of between 50% and 100%. None of the studies focus on lower level of automation features under connected vehicle environment which are available in the market with low penetration rates. Kockelman et al., (Kockelman et al., 2016) conducted a comprehensive study about the adoption of automated vehicles in United States based on questionnaire survey. Most respondents were interested about lower level automation technologies which would be the most promising for US over the next 25 years. This research team also anticipated that, lower levels of automation technologies are estimated to have adoption rates of more than 90% by 2045. Hence, it is worthwhile to study the safety benefits of lower level automation under connected vehicle environment using V2V and I2V communication technologies. CAVs can also reduce the vulnerable road user crashes which is the most active forms of transportation (i.e., walking and bicycling) using vehicle-to-pedestrian (V2P) connectivity (M. S. Rahman et al., 2019a, 2019b; Rahman, 2018; Saad et al., 2019a).

As mentioned earlier, the driving behavior of connected and automated vehicle are significantly different from conventional vehicles. From the modeling standpoint, capturing the effects of driving behavior of connected and automated vehicles are very challenging task. An exhaustive summary of earlier studies employing simulation based connected and automated vehicle effectiveness in transportation literature are presented in Table 1 (Fernandes and Nunes, 2010;

Genders and Razavi, 2016; Guériau et al., 2016; Ilgin Guler et al., 2014; Jin et al., 2014, 2013; Lee and Park, 2012; Letter and Elefteriadou, 2017; Li et al., 2013; Mirheli et al., 2018; Qian et al., 2014; Rahman et al., 2018a; Rahman and Abdel-Aty, 2018; Tajalli and Hajbabaie, 2018; Talebpour and Mahmassani, 2016b; Wan et al., 2016; Wu et al., 2015). The information provided in the table includes the simulation software used, the car following behavior employed, the area of interest (connected vehicle/automated vehicle or both), and the measure of effectiveness. The following observations can be concluded from the table. From the Table 1, it is evident that most of the existing literature used VISSIM as their simulation platform for the connected and automated vehicle. However, some study used SUMO, PARAMICS, CORSIM, MOVSIM, and MATLAB in order to approximate the behavior of connected and automated vehicle. Those studies evaluated the effectiveness of connected and automated vehicle technologies considering full road networks of freeway and arterial section but did not focus the segments and intersections safety concurrently. It is also noticed that most of the studies used their default car following behavior except for six studies (Genders and Razavi, 2016; Guériau et al., 2016; Jin et al., 2013; Rahman et al., 2018a; Rahman and Abdel-Aty, 2018; Talebpour and Mahmassani, 2016b). Among these six studies, three of them have been used validated car following model for CAV, however no study considers validated lane changing model based on the real-world CAV data. It is worth noting that default car following behavior would not approximate the behavior of connected and automated vehicle in real-world. Some studies used deterministic acceleration modeling framework such as Intelligent Driver Model (IDM) which is considered to be more suitable to approximate the connected vehicle behaviors in the real world (Rahman et al., 2018a; Rahman and Abdel-Aty, 2018; Talebpour and Mahmassani, 2016b). However, none of the studies implement the IDM model to simulate the connected vehicle behaviors on an arterial section.

Table 1 Summary of Previous Simulation Based Study for Connected and Autonomous Vehicles

Studies	Car Following Model Used	Lane Changing Model Used	Simulation Software Used	Area of Interest	Analysis Area	Measure of Effectiveness
Talebpour et. al, (2016)	IDM	Platooning algorithm	NA	Connected and Autonomous Vehicle	Freeway	Traffic Operations
Rahman et. al, (2017)	IDM	VISSIM Default	VISSIM	Connected Vehicle	Freeway	Traffic Safety
Guler et. al, (2014)	NA	VISSIM Default	MATLAB	Connected Vehicle	Arterial	Traffic Operations
Rahman et. al, (2018)	IDM	Platooning algorithm	VISSIM	Connected Vehicle	Freeway	Traffic Safety and Operations
Tajalli et. al, (2018)	VISSIM Default	MOBIL lane change model	VISSIM	Connected Vehicle	Arterial	Traffic Safety
Mirheli et. al, (2018)	VISSIM Default	PARAMICS Default	VISSIM	Connected vehicle	Arterial	Traffic Safety and Operations
Guériau et. al, (2016)	IDM	PARAMICS Default	MOVSIM	Connected Vehicle	Freeway	Traffic Operations and Safety
Lee et. al, (2012)	VISSIM Default	NA	VISSIM	Connected Vehicle	Arterial	Traffic Operations
Li et. al, (2015)	VISSIM Default	NA	VISSIM	Connected Vehicle	Arterial	Traffic Operations
Fernandes et. al, (2010)	Gipps-model extension	Sumo Default	SUMO	Autonomous Vehicle	Freeway	Traffic Operations
Jin et. al, (2013)	Sumo Default	Optimal driving behavior algorithm	SUMO	Connected Vehicle	Arterial	Traffic Operations and fuel consumption
Qian et. al, (2013)	Sumo Default	VISSIM Default	SUMO	Connected and Autonomous Vehicle	Arterial	Traffic Operations
Jin et. al, (2013)	Optimal driving behavior algorithm	CORSIM Default	SUMO	Connected Vehicle	Arterial	Traffic Operations and fuel consumption
Wan et. al, (2016)	PARAMICS Default	VISSIM Default	PARAMICS	Connected Vehicle	Arterial	Traffic Operations and fuel consumption
Genders et. al, (2015)	Modified driving behavior	Default lane changing model	PARAMICS	Connected Vehicle	Arterial	Traffic Safety
Letter et.al, (2017)	CORSIM Default	Gap-acceptance based lane-changing model	CORSIM	Autonomous Vehicle	Freeway	Traffic Operations
Li et. al, (2013)	VISSIM Default	NA	VISSIM	Autonomous Vehicle	Arterial	Traffic Safety and Operations

Previous studies have shown that parameters of the default car-following model of a microsimulation software can be modified to model the behaviors of automated vehicle (Atkins, 2016; Kockelman et al., 2016; Morando et al., 2018). Those studies applied fully automated vehicle behavior in VISSIM with changing only the parameters of default car following model (Wiedmann-99) but did not focused on the lane changing model. However, it is intuitive that the lane changing behavior of fully automated vehicle would also be significantly different from the conventional vehicles. Therefore, a more realistic driving behavior model is required to simulate the behavior of fully automated vehicles under connected vehicle environment. This study proposed a car following model to simulate CVLLA in simulation based on a recent study by Wen-Xing et al., (Wen-Xing and Li-Dong, 2018) along with lane keeping assistance feature adopted in VISSIM which would approximate the decision processes of CVLLA.

PTV VISSIM has been using Wiedemann car following model to simulate the roadway network under human-driven vehicles for the last three decades (VISSIM, 2017). Very few studies have utilized the default car-following model of VISSIM to simulate the behavior of CAV (Atkins, 2016; Kockelman et al., 2016; Morando et al., 2018). However, they did not consider the calibrated parameters of Weidmann model based on real world CAV data. Those studies tried to approximate CAV behavior in VISSIM without considering the lane changing model. Moreover, the interaction between CAV and conventional vehicles (passenger cars, trucks, etc.) were largely unknown in the Weidmann car following model. Recently, PTV VISSIM (version 11.0) offers validated car following and lane changing models with multiple additional attributes using real-world CAV data. To the best authors' knowledge, this is the first application of validated CAV driving behavior model (both car following and lane changing) provided in the commercially available software using real-world CAV data. The interaction between the CAVs and conventional vehicles have also

been validated based on time headway. This study also utilized the real world validated driving behavior models to simulate CAV in simulation which would better replicate the decision processes of CAVs.

In summary, the current study contributes to the traffic safety and mobility impacts in the CAV research along some directions: (1) first application of CV technologies under reduced visibility conditions (2) evaluate the effectiveness of managed lane CV platooning in expressway segments (3) application of lower automated vehicle in arterials under V2V and V2I technologies (4) first application of validated driving behavior model in VISSIM to approximate the CAV behavior on an expressway using real-word CAV data (5) evaluate the both safety and operational benefits of CAV for both peak and off-peak hours traffic (6) provide recommendation of the optimal market penetration rates of CAV for both peak and off-peak hours to achieve balanced mobility and safety benefits with varying traffic condition.

CHAPTER THREE: DIFFERENT APPROACHES OF CONNECTED VEHICLES IN REDUCED VISIBILTY CONDITIONS

3.1 Introduction

It is known that reduced visibility due to fog has caused serious traffic safety and flow issues. Florida had experienced a total of 4,954 fog-related crashes between the year of 2008 and 2012, of which 132 crashes were fatal, and about 30% of the total fog-related crashes were fatal and injury crashes (Peng et al., 2017). It is worth mentioning that fog-related crashes tend to result in more severe injuries and involve more vehicles compared to clear conditions crashes (Abdel-Aty et al., 2011; Hassan et al., 2012). Fog affects roadway safety by increasing crash risk. Therefore, it is necessary to evaluate the appropriate countermeasures to enhance traffic safety under fog conditions. There have already been a lot of research conducted on traffic safety under normal weather conditions. On the other hand, traffic safety under fog conditions has attracted much less attention. However, some researchers have already proposed the traditional approach of Variable Speed Limits (VSL) or Variable Message Signs (VMS) to decrease the crash risk in reduced visibility conditions (Hassan et al., 2011, 2012; Peng et al., 2017). It can possibly improve traffic safety and mitigate traffic crashes by adjusting vehicle speeds and decreasing speed variation among vehicles in reduced visibility conditions. Nevertheless, the success of VSL or VMS is dependent on the level of compliance. Therefore, the VSL would not guarantee the improvement of the traffic safety if drivers do not follow the new speed limit.

An innovative feature of this study was to apply the Connected Vehicle (CV) technologies in adverse visibility conditions under microsimulation environment. To be more specific, this research aims to contribute to the implementation of two CV approaches such as connected vehicle

without platooning (CVWPL) and connected vehicle with platooning (CVPL) to improve the traffic safety in reduced visibility conditions. CVPL concept is an extension of CVWPL approach wherein several CVs form a "platoon" that behaves as a single unit. A car following model for both CV approaches was also used in fog conditions with an assumption that applied CVs would follow this car following behavior in the simulation. The most significant difference of CVs driving behavior between two approaches was joining vehicles to maintain a platoon. At the near future, the MPR will not achieve 100%, meanwhile, the penetration will increase gradually. Hence, it is worthwhile to study the safety benefits of CV technologies under different MPRs (Hellinga and Mandelzys, 2011; Yu and Abdel-Aty, 2014).

3.2 Data Preparation

A section of Interstate, a main arterial for the Orlando metropolitan area, was selected for this study. The studied section had experienced severe fog-related crashes (Hassan et al., 2012). Data from two different sources were collected for this study. Weather data were collected from Fog Monitoring System (FMS), a new visibility detection system, installed in the segment of I-4. And, real-time traffic data were collected from Regional Integrated Transportation Information System (RITIS) augmented with a device installed close to the FMS. RITIS indicates the basic traffic characteristics of the selected road segment, while the added device captures both regular traffic parameters and the headway between each vehicle on each lane. The study area along with the FMS and RITIS detectors is shown in Figure 1. The collected weather data contain 21 variables, including visibility distance, air temperature, surface moisture, dew point, wind speed, barometric pressure, rainfall, etc. Among these parameters, visibility distance is significant for fog conditions. The traffic data were collected from RITIS detectors installed in the above-mentioned areas

(Figure 1). The traffic dataset comprises eight important variables related to traffic flow characteristics, including vehicle speed, vehicle length, duration of detection, and lane assignment. In this study, vehicles were classified into two categories: (1) passenger car (PC) and (2) heavy goods vehicle (HGV). A vehicle was considered as a PC if its length is equal to or less than 7.32 meters (24 feet).

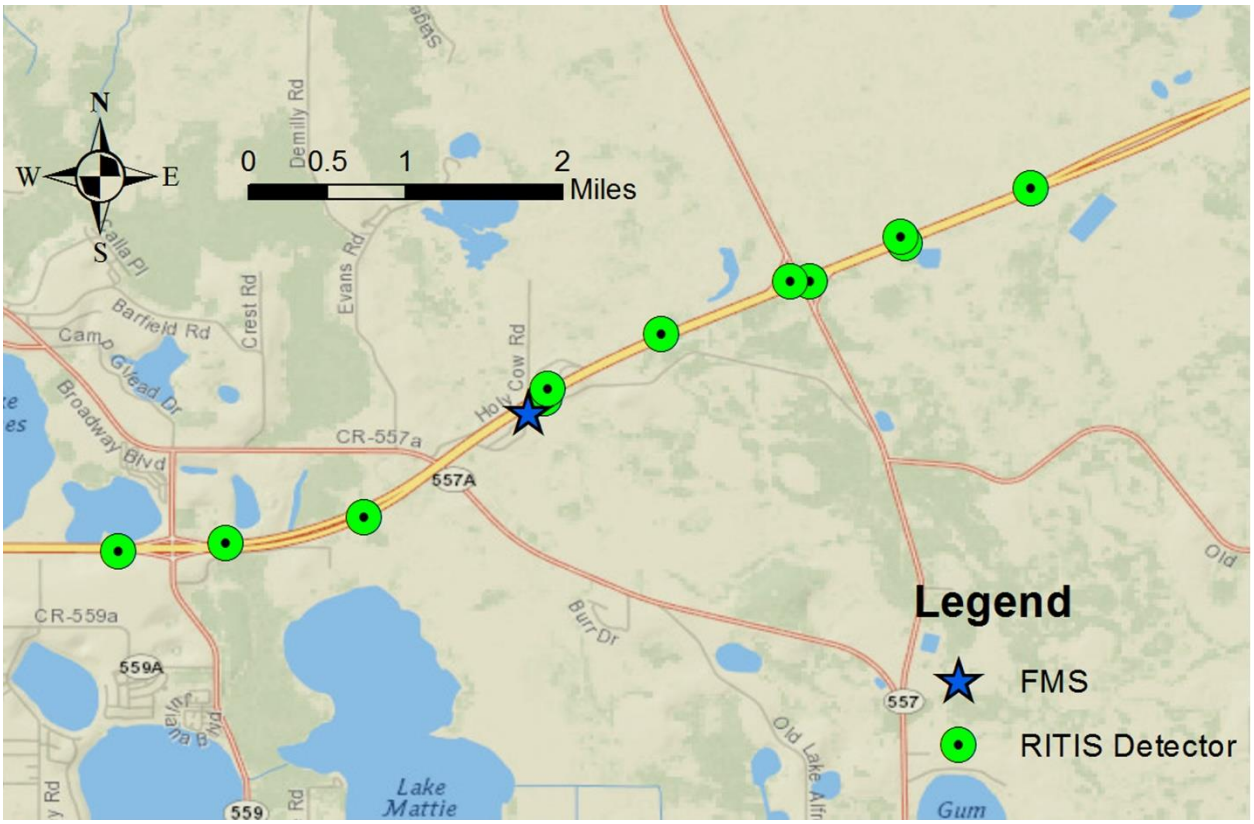

Figure 1 The study area showing Fog Monitoring System (FMS) and Regional Integrated Transportation Information System (RITIS).

According to the weather data, the visibility distance from 6:45 am to 7:45 am on February 2, 2016 (Tuesday) was the lowest among all days of field data collection between the observed months of January to May in 2016. And this hour's maximum and minimum visibility distance were recorded as 88 meters and 45 meters, respectively. Referring to the traffic flow data, the data of traffic

volume and traffic speed in the same time period, 6:45 am to 7:45 am on February 2, were chosen for basic simulation model development.

3.3 VISSIM Simulation Model

A well calibrated and validated VISSIM network replicating the fog conditions was one of the most important parts of this study. Simulations were conducted in PTV VISSIM, version 8.0. The testbed was a 10-miles section of I-4 which had experienced a severe fog-related crash. The traffic information on the simulation network, including traffic volume (aggregated into 15 minutes), PC and HGV percentages, and desired speed distribution were obtained from the RITIS detectors. In addition to that, the "Look Ahead Distance" was changed in VISSIM driving behavior to replicate reduced visibility conditions based on field visibility distance. The simulation time was set from 6:15 A.M. to 8:15 A.M in VISSIM. After excluding first 30 minutes of VISSIM warm up time and last 30 minutes of cool-down time (no statistics were collected during this time), 60 minutes VISSIM data was used for calibration and validation. Geoffrey E. Heavers (GEH) statistic was used to compare the field volumes with simulation volumes. The GEH statistic is a modified Chi-square statistic that incorporates both relative and absolute differences. The definition of GEH is as follows,

$$GEH = \sqrt{\frac{(M_{obs}(n) - M_{sim}(n))^2}{0.5 \times (M_{obs}(n) + M_{sim}(n))}} \quad (1)$$

Where $M_{obs}(n)$ is the observed volume of field detectors and $M_{sim}(n)$ is the simulated volume obtained from the simulation network. The simulated volume would precisely reflect the field volume if more than 85% of the measurement locations GEH values are less than five (Abdel-

Aty et al., 2017; M. H. Rahman et al., 2019; Moatz Saad et al., 2018a; Yu and Abdel-Aty, 2014). As for speed, the absolute speed difference between simulated speeds and field speeds should be within five mph for more than 85% of the checkpoints (Cai et al., 2018; Nezamuddin et al., 2011; Moatz Saad et al., 2018a, 2018b; Saad et al., 2019c). The simulated traffic volumes and speeds were aggregated to 15-minute intervals and then compared with the corresponding field traffic data. Ten simulation runs with different random seeds worth of results showed that 91.25% of observed GEHs were less than five, and 92.50% of the aggregated speeds in the simulation were within five mph of field speeds. The results above proved that the traffic calibration and validation satisfy the requirements and indicate that the network was consistent with that of the field traffic conditions.

3.3.1 Further calibration to reflect fog conditions

To reflect the fog conditions, there was a need to revalidate the VISSIM network with respect to both traffic and safety. For further validation, headway was used to validate the VISSIM network using two-sample t-test and the result showed that the mean simulated headway was significantly different from the mean field headway when all the driver behavior parameters in VISSIM were set as default. Previous studies considered only 'Look Ahead Distance' as one of the most essential simulation parameters in VISSIM to replicate the fog conditions (Abdelfatah et al., 2013; Zhang, 2015). Hence, changing only the "Look Ahead Distance" in VISSIM driving behavior may not reflect the fog conditions. To simplify the further calibration process, a sensitivity analysis was conducted on VISSIM driver behavior parameters in simulation models to reflect the fog conditions. The ten sets of the car following parameters (CC_0 to CC_9) were tried and each set was run ten times with different random seeds. For each parameter, a range of values (9 values), which

includes the default, was determined based on previous studies and engineering judgment (Habtemichael and Picado-Santos, 2013; Lownes and Machemehl, 2006). A total of 730 simulation runs [(1 base-models + 9×8 car-following parameters) times 10 random seeds] were conducted. Toward this end, the standard deviation of speed (significant traffic characteristic in fog condition) was selected in order to compare the field and simulated value with two-sample t-test at 5% significance level. For each value of parameters, the results of t-test with 10 different random seeds proved whether the distribution of the field and simulated standard deviation of speed were identical or not. The sensitivity analysis results showed that three most important parameters were vital to reflect the fog conditions. These include CC0 (standstill distance), CC1 (headway time), and CC2 (following variation). From the results of sensitivity analysis, the safety distance parameters (i.e. CC_0, CC_1, CC_2) decreased compared to the default values in fog conditions. The default value of CC_0, CC_1, CC_2 in VISSIM were 1.5 meters, 0.9 seconds, and 4 meters whereas the calibrated values were found to be 1 meter, 0.7 seconds, and 3 meters, respectively. Thus, the safety distance of calibrated network has lower value compared to the uncalibrated network. Therefore, the safety distance between two vehicles has been reduced in fog conditions. For further validation, headway was again used to validate the new calibrated VISSIM network using two-sample t-test. After replicating the fog conditions, there were no significant difference between the simulated mean headway and the field mean headway. Therefore, the simulation network was well calibrated and validated with respect to both traffic and safety.

3.4. Methodologies

In order to assess the safety performance in fog conditions, this study tested two distinct CV approaches including CVWPL and CVPL on the segment of I-4. Therefore, the understanding of

the car following behavior of CV technologies is essential for studying the impact on traffic safety in fog conditions under microsimulation. A car following model for both CV approaches was used in fog conditions with an assumption that applied CVs would follow this car following behavior in the simulation.

3.4.1 Car following model in fog conditions

A car following model is a prerequisite to regulate the driving behavior of CVs in microsimulation. The desired model should be able to simulate user defined driving behavior significantly differing from the traditional ones (i.e. Wiedemann model). The basic Intelligent Driver Model (IDM) which was proposed by Treiber et al. (Treiber et al., 2000) has been used as machine driving by many researchers (Kesting et al., 2010a; Li et al., 2017a) Many researchers have already used IDM or modified IDM in order to simulate their own machine driving platform named Adaptive Cruise Control (ACC) and Cooperative Adaptive Cruise Control (CACC) (Kesting et al., 2010a, 2008; Khondaker and Kattan, 2015; Li et al., 2017a). The basic IDM model is a nonlinear car following model in which the acceleration ($\dot{v}_{IDM}$) is the function of desired gap distance s^* and the speed difference between leading and following vehicles Δv, expressed by the following Equation 2.

$$\dot{v}_{IDM}(t+t_a) = \max\left\{b_m, a_m\left[1-\left(\frac{v}{v_o}\right)^{\delta}-\left(\frac{s^*}{s}\right)^2\right]\right\}$$
$$\text{Where, } s^* = s_0 + max\left[0, vT + \frac{v\Delta v}{2\sqrt{a_m b}}\right] \quad (2)$$

where, t_a = the perception-reaction time, b_m = the maximum deceleration, a_m = the maximum acceleration, v = the speed of the following vehicle, v_0 = the desired speed, δ = the acceleration exponent, s = the gap distance between two vehicles, s_0 = the minimum gap distance at standstill, T = the safe time headway, b = the desired deceleration

In this study, this IDM model was used for CVs car following behavior in fog conditions. The parameter settings for this model were potentially determined according to previous studies (Kesting et al., 2010a; Li et al., 2017a; Milanés and Shladover, 2014). The desired speed (v_0) , acceleration exponent (δ) , maximum acceleration (a_m), desired deceleration (b), minimum gap distance at standstill (s_0) , Safe time headway (T) , maximum deceleration (b_m) , and Time delay (t_a) were selected 120 km/h, 4, 1 m/sec^2, 2 m/sec^2, 2 m, 0.6 sec, 2.8 m/sec^2, and 1.5 sec, respectively.

Additionally, CVs were implemented as a platooning concept (CVPL), wherein several vehicles form a "platoon" that behaves as a single unit. However, the IDM model was followed by CVs in both approaches (i.e., CVWPL and CVPL) under fog conditions. The most significant difference of CVs driving behavior between two approaches was joining vehicles to maintain a platoon. A minimum five CVs were considered to maintain a platoon in this study. Three grouping schemes for CVs, such as rear, front, and cut-in joins, as depicted in Figure 2 (a), were implemented to maintain the platoon. The rear join leads a new CV following the last vehicle of a CV group driving along the most adjacent lane of the joining vehicle. The front join performs the same process to allow a new CV to join into an existing CV group except that it leads the joining vehicle to the front of the first vehicle in the CV group. The cut-in join method is implemented by cooperatively adjusting the maneuvers of the joining vehicle and a CV in the group. As shown in Figure 2 (a), once the joining vehicle identifies a target CV group, it approaches the group and determines a proper position to be inserted based on its current driving information such as speed, position, etc. Then the deceleration rate of a CV in the target group is adjusted to create a safe gap for the joining vehicle while the leading vehicle maintains its current speed. If the safe gap is satisfied for the lane

change behavior of the joining vehicle, which is governed by VISSIM's lane changing model, the joining vehicle begins to change the lane.

We developed a high-level control algorithm architecture for CVPL approach as shown in Figure 2 (b). It is worth mentioning that the algorithm continuously adjusted the acceleration or deceleration rates using the above-mentioned Equation 4 between the leading and the subject vehicles using two-way communications under CV environment which offers a dedicated short-range communication (DSRC) of 300 meters (1000 feet).

The aforementioned two driving behavior models were implemented as Dynamic Link Library (DLL) plug-in for both approaches, which overrides the VISSIM default driving behavior. This two DLL were written in C++ which offers VISSIM an option to replace the internal driving behavior. During the simulation, the DLL file is called up in each time step and then controls the behavior of the vehicle for all or part of the vehicles depending on the MPRs. Note that the car following and the lane changing behavior of non-CVs were determined by VISSIM's default driving behavior model.

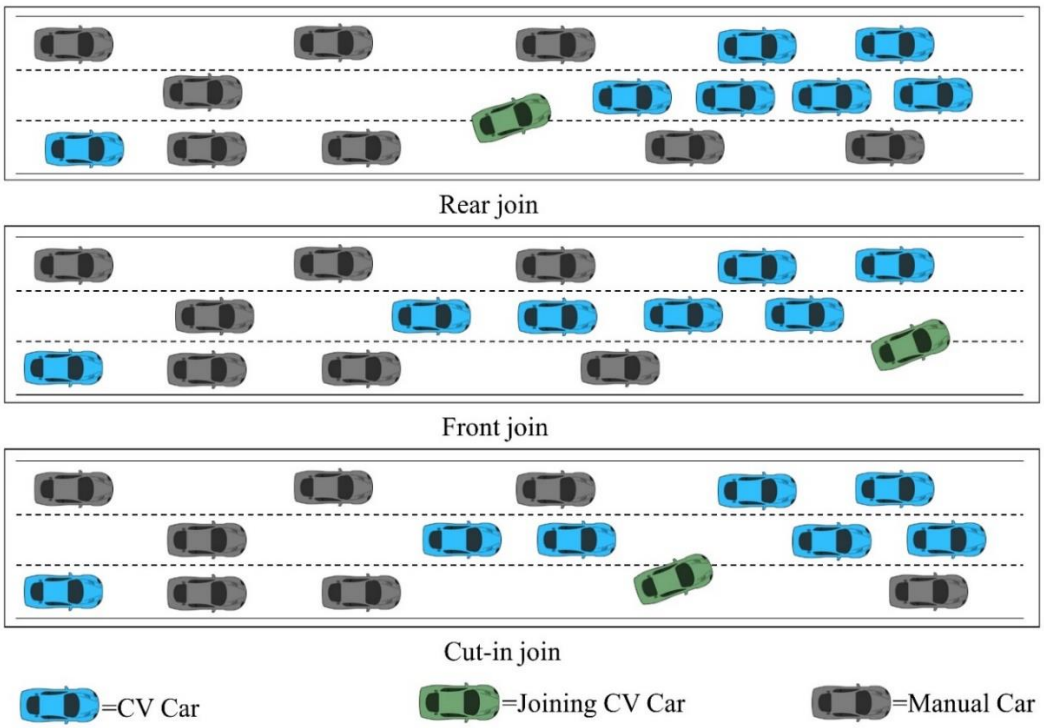

2 (a) Joining of CVs to maintain a platoon.

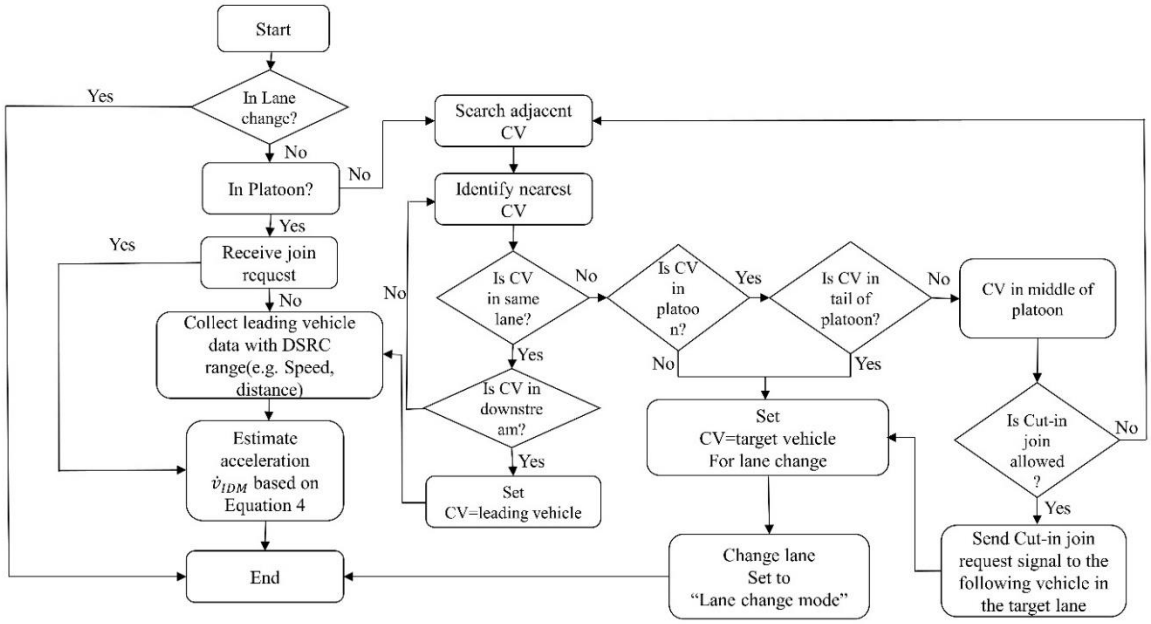

2 (b) Control algorithm of CVs to maintain a platoon.

Figure 2 Platooning behavior of CVs (a) Joining of CVs to maintain a platoon (b) Control algorithm of CVs to maintain a platoon.

3.5 Surrogate Measures of Safety

Traffic crashes are rare events which involve numerous human factors along with the road environment and vehicle factors. A surrogate safety assessment technique should be adopted to measure safety as microsimulation software cannot be directly used to measure crashes or traffic safety. A number of previous studies used surrogate measures including speed variance, headway variance, time to collision, post-encroachment time, and rear-end crash risk index (Abdel-Aty et al., 2009; Gettman and Head, 2003; Peng et al., 2017). From the above-mentioned literature review the crash risk increased in fog conditions compared to normal weather conditions as the standard deviation of speed and headway increased significantly. Additionally, the rear-end crash is the significant type of crash in reduced visibility conditions (Abdel-Aty et al., 2012, 2011; Al-Ghamdi, 2007). A rear-end crash may occur if the leading vehicle stops suddenly, and the following vehicle does not decelerate in time because of the low visibility. Maintaining insufficient safety distance between the leading and the following vehicle is the primary cause of rear-end crashes. To avoid the rear-end crashes, the stopping distance of the following vehicle should be smaller than the leading vehicle. A rear-end crash risk index (RCRI) proposed by Oh et al. (Oh et al., 2006) in which the dangerous condition can be mathematically expressed as:

$$SD_F > SD_L \tag{3}$$

$$SD_L = v_L \times h + \frac{v_L^2}{2 \times a_L} + l_L \tag{4}$$

$$SD_F = v_F \times PRT + \frac{v_F^2}{2 \times a_F} \tag{5}$$

Where SD_L and SD_F are the stopping distance of the leading and the following vehicles, respectively. l_L the length of the leading vehicle, v_L the speed of the leading vehicle, v_F the speed of the following vehicle, PRT is the perception-reaction time, h the time headway, a_L the

deceleration rate of the leading vehicle and a_F is the deceleration rate of the following vehicle. As mentioned earlier, for the VISSIM model, I used two types of vehicles PC and HGV. Therefore, different deceleration rates were employed to estimate the reliable safe distance for the leading and following vehicles. The deceleration rates of PC and HGV were selected as 3.42 m/s^2 and 2.42 m/s^2 respectively, while the PRT was used as 1.5 s, these values are generally accepted by AASHTO (American Association of State Highway and Transportation Officials (AASHTO), 2004). So, the RCRI is defined by the following formula,

$$RCRI = \begin{cases} 1\ (Dangerous) & If\ SDF > SDL \\ 0\ (safe) & Otherwise \end{cases} \quad (6)$$

In a nutshell, the standard deviation of speed, the standard deviation of headway, and RCRI were considered as surrogate measures of safety to evaluate the safety performances in fog conditions in a microsimulation platform.

3.6 Results and Discussions

Three surrogate measures of safety were considered to evaluate the safety performances in fog conditions under two CV approaches. Two sample t-test was applied to compare the differences between two group means and their average variations in two minutes. This technique provides a method for comparing the mean standard deviation of speed and headway between base scenario and CV scenarios. Base scenario comprised of 100% regular vehicles, and CV scenarios were comprised of two types of CV approaches (i.e., CVWPL and CVPL) with different MPRs. The Chi-square test was also applied to analyze the significance in the difference of RCRI between base scenario and CV scenarios. Ten simulation runs, each with a different random number of seeds were conducted to eliminate random effects for each scenario.

Table 2 illustrates the summary of two surrogate measures of safety, (i.e., standard deviation of speed, standard deviation of headway) with the implementation of CVWPL and CVPL techniques. Compared to the base scenario, the standard deviation of speed and headway decreased significantly in both CV approaches. Model performances were evaluated for three different condition sets (Base, CVWPL and CVPL) each under five different MPRs (20%, 30%, 50%, 70%, and 100%). To find out the safety impact of the applied technologies the mean values of the surrogate safety measures were compared with the base condition. In 100% MPR, the standard deviation of speed and the standard deviation of headway were found to be reduced by 28.49% and 18.68%, respectively, in CVWPL compared to base condition. On the other hand, in CVPL, the reductions were found to be 38.90% and 33.22%, respectively. The results revealed that the applied CV technologies enhanced traffic safety by decreasing the surrogate measures of safety in fog conditions. From Table 2 it was found that the maximum significant improvement resulted at 100 % MPR, while the improvement below 30% MPRs was insignificant at 5% level of significance.

For each of the 15 scenarios listed in Table 2, the mean differences of standard deviation of speed and standard deviation of headway were higher for CVPL than CVWPL. It was also found that the CVPL achieved significant reductions in the standard deviation of speed and headway compared to CVWPL when the MPRs were equal or greater than 50%. For instance, standard deviation of speed and standard deviation of headway for CVPL were 14.58% and 17.88% lower respectively than CVWPL at 100% MPR. Thereby, CVPL approach clearly outperformed CVWPL approach in terms of safety improvement. In terms of traffic operation, simulation results demonstrated higher speed for CVWPL and CVPL compared to the base condition. Additionally, compared to

CVWPL, the average speed was higher in CVPL. Hence, for both traffic safety and operation the CVPL approach outperformed CVWPL approach.

Table 2 Summary of Measure of Effectiveness

MPR	Comparisons	Speed (km/h)	Standard deviation of speed in 2 mins (km/h)		Standard deviation of headway in 2 mins (s)	
		Mean difference (P-value)	Mean difference (P-value)	% Reduction	Mean difference (P-value)	% Reduction
20%	Base - CVWPL	-0.288 (0.0322)	0.264# (0.1915)	2.78	0.139# (0.2645)	3.31
	Base- CVPL	-0.398 (0.0030)	0.375# (0.0642)	3.96	0.184# (0.1371)	4.39
	CVWPL -CVPL	-0.108# (0.4062)	0.111# (0.4997)	1.20	0.045# (0.6519)	1.11
30%	Base - CVWPL	-0.570 (<0.0001)	0.597 (0.0042)	6.29	0.344 (0.0060)	8.19
	Base- CVPL	-1.149 (<0.0001)	0.769 (0.0002)	8.12	0.453 (0.0003)	10.79
	CVWPL -CVPL	-0.579 (<0.0001)	0.174# (0.2503)	1.96	0.109# (0.2055)	2.83
50 %	Base - CVWPL	-1.334 (<0.0001)	0.848 (<0.0001)	8.95	0.456 (0.0002)	10.87
	Base- CVPL	-2.457 (<0.0001)	1.476 (<0.0001)	15.57	0.764 (<0.0001)	18.21
	CVWPL -CVPL	-1.125 (<0.0001)	0.626 (0.0005)	7.25	0.308 (<0.0001)	8.24
70 %	Base - CVWPL	-2.395 (<0.0001)	1.745 (<0.0001)	18.41	0.584 (<0.0001)	13.92
	Base- CVPL	-3.275 (<0.0001)	2.536 (<0.0001)	26.76	1.005 (<0.0001)	23.95
	CVWPL -CVPL	-0.880 (<0.0001)	0.793 (<0.0001)	10.24	0.421 (<0.0001)	11.66
100 %	Base - CVWPL	-4.897 (<0.0001)	2.700 (<0.0001)	28.49	0.784 (<0.0001)	18.68
	Base- CVPL	-5.535 (<0.0001)	3.687 (<0.0001)	38.90	1.394 (<0.0001)	33.22
	CVWPL -CVPL	-0.637 (<0.0001)	0.988 (<0.0001)	14.58	0.610 (<0.0001)	17.88

#Difference is insignificant at 5% level

Figure 3 shows the decreasing trend of standard deviation of speed and headway for CVWPL and CVPL approaches with increasing MPRs. As seen from the figure, the higher the percentage of

the CVs implemented, the lower were the standard deviations of speed and headway, and therefore the higher were the safety benefits achieved.

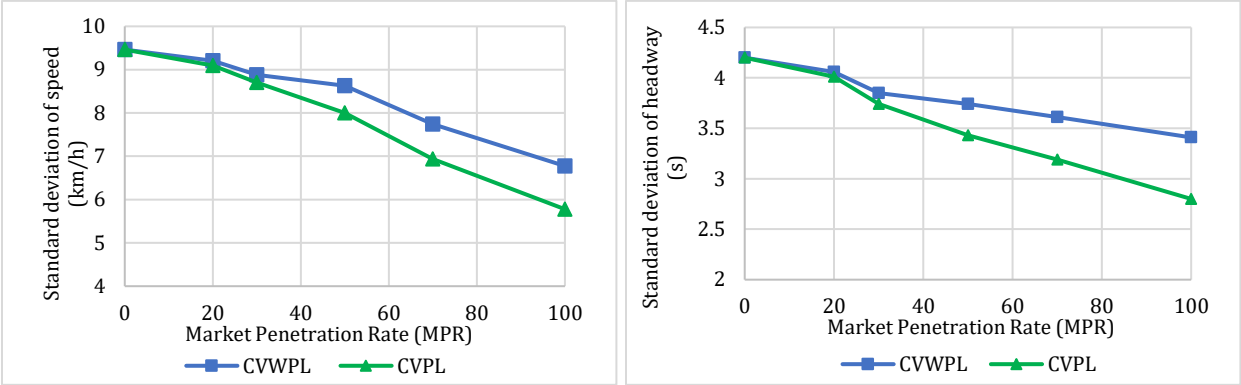

Figure 3 Reduction of surrogate measures of safety with different MPRs.

Apart from statistical significance, Figure 4(a) and 4(b) compares the profile of both the surrogate measures of safety under base, CVWPL and CVPL scenario in 100 % MPR. For every 2-minute time interval which is denoted in the x axis, the standard deviation of speed and standard deviation of headway (denoted in y axis) were calculated. Figure 4 (a) and 4 (b) illustrates that both CV approaches not only reduced the standard deviation of speed and headway but were able also to stabilize the profile. With lower variances in standard deviation of speed and headway these CV technologies are expected to decrease the crash risks.

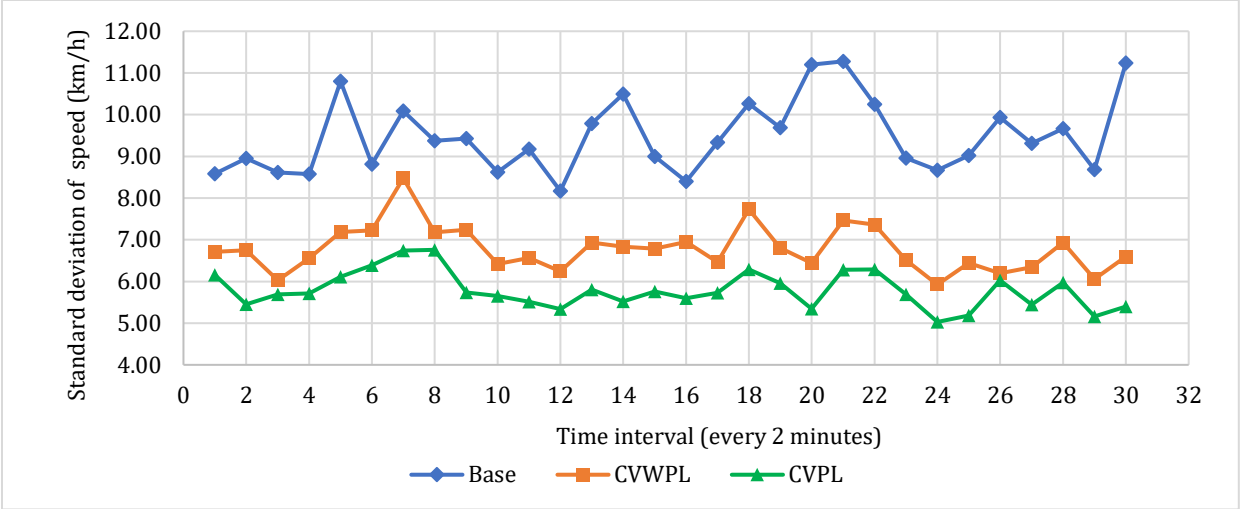

(a)

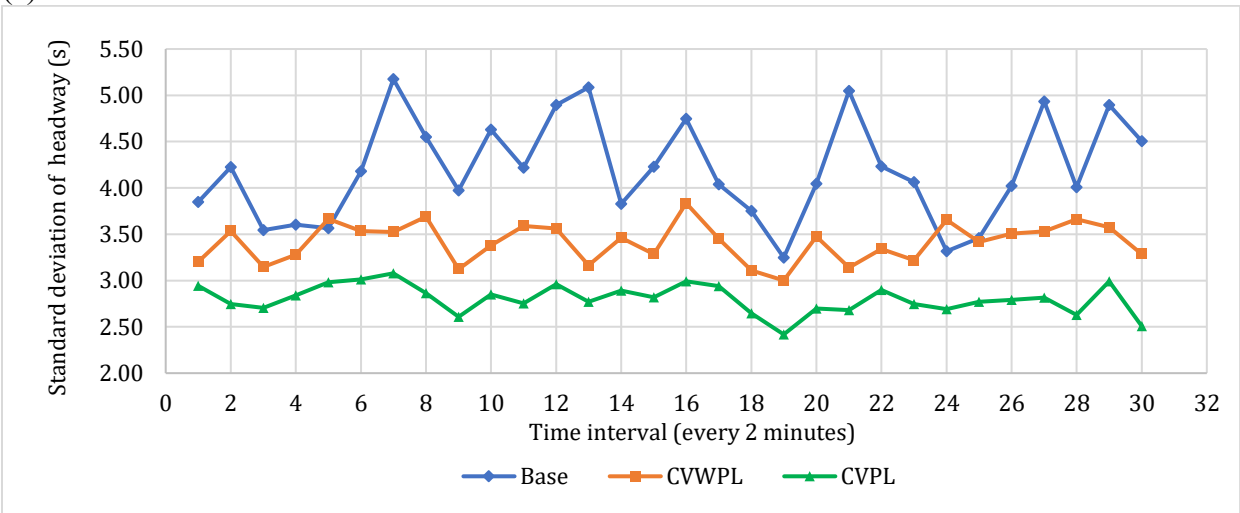

(b)

Figure 4 Stabilize profile of surrogate measures of safety at 100% MPR.

The RCRI was considered as another surrogate measure for rear-end crashes. The Chi-square test was applied to test the significance in differences of RCRI between base scenario and CV scenarios. The percentages of vehicles under potential rear-end crash risk for different scenarios are listed in Table 3 with the Chi-square significance test.

It can be seen from Table 3 that the percentages of potential rear-end crash observations were lower for CVWPL and CVPL than the base condition. At 100% MPR, the percentage of vehicles with potential rear-end crash risks were 11.55% lower in CVWPL and 14.67% lower in CVPL compared to the base condition.

Table 3 Summary of Measure of Effectiveness

MPR	Classification	Total observation	Number of potential rear-end crash observation	Comparison	Chi-square	P-value
20%	Base	10035	4161 (41.46%)	Base vs CVWPL	0.780#	0.3770
	CVWPL	10034	4099 (40.85%)	Base VS CVPL	3.274#	0.0704
	CVPL	10035	4035 (40.21%)	CVWPL VS CVPL	0.858#	0.3544
30%	Base	10035	4161 (41.46%)	Base vs CVWPL	23.487	<0.0001
	CVWPL	10037	3823 (38.12%)	Base VS CVPL	39.848	<0.0001
	CVPL	10030	3725 (37.11%)	CVWPL VS CVPL	2.151#	0.1425
50%	Base	10035	4161 (41.46%)	Base vs CVWPL	75.775	<0.0001
	CVWPL	10035	3561 (35.49 %)	Base VS CVPL	118.091	<0.0001
	CVPL	10035	3414 (34.03 %)	CVWPL VS CVPL	4.704	0.0301
70%	Base	10035	4161 (41.46%)	Base vs CVWPL	169.646	<0.0001
	CVWPL	10035	3270(32.59%)	Base VS CVPL	264.023	<0.0001
	CVPL	10031	3055 (30.46 %)	CVWPL VS CVPL	10.548	0.0012
100%	Base	10035	4161 (41.46%)	Base vs CVWPL	291.941	<0.0001
	CVWPL	10040	3003 (29.91%)	Base VS CVPL	480.641	<0.0001
	CVPL	10037	2689 (26.79%)	CVWPL VS CVPL	24.045	<0.0001

#Difference is insignificant on 5% level

Hence, the rear-end crash risk decreased with the application of CV technologies. Also, the CVPL approach performed better than the CVWPL approach for each MPR in terms of RCRI. It was also found that at least 30% MPR was needed to have significant reduction in rear-end crash risk. Additionally, CVPL achieved higher reductions of RCRI compared to CVWPL when the MPRs were equal or greater than 50%. It is worth mentioning that, the higher the MPRs implemented, the lower were the potential rear-end crash observations, and therefore the higher were the safety benefits achieved.

Overall, the deployment of CVs in reduced visibility conditions would significantly decrease the standard deviation of speed, standard deviation of headway, and RCRI; thereby might decrease the probability of crashes.

3.7 Summary

Traffic flow characteristics deteriorate significantly in fog conditions compared to normal weather conditions which might result in high crash risk. In order to improve traffic safety in fog conditions, two CV strategies were applied in microsimulation. The strategies include connected vehicle without platooning and connected vehicle with platooning. A car following model for both approaches was used with an assumption that the CVs would follow this car following behavior in fog conditions. Three surrogate measures of safety including the standard deviation of speed, the standard deviation of headway, and RCRI were considered as safety indicators in this study. The safety benefits were observed under different MPRs for both approaches. In general, both CV approaches improved safety in fog conditions by providing significant reductions in standard deviation of speed, standard deviation of headway, and RCRI. It was found that the higher the MPRs of CV implemented the higher were the safety benefits achieved. Maximum improvement

was found to be at 100% MPR. A minimum of 30% MPR was needed to observe significant safety benefits of the applied CV approaches compared to the base scenario. The results showed that the CVPL significantly outperformed CVWPL in terms of three surrogate measures of safety. It was also found that at least 50% MPR was needed to achieve the safety benefits for the CVPL compared to CVWPL. To be more specific, both approaches of CV technologies achieved significant safety benefits over the base scenario with at least 30% MPR. Additionally, CVPL achieved higher safety benefits compared to CVWPL when the MPRs were equal or greater than 50%. From the profiles of standard deviation of speed and headway, it was found that the variances of these values decreased thereby providing a stabilized flow with fewer crash risk. On the other hand, simulation results asserted that speed was higher in both CV approaches compared to the base scenario. Therefore, the CV technologies not only improved traffic safety but also enhanced traffic operation. However, the average speed was higher in CVPL compared to CVWPL. Hence, taking both traffic safety and operation into consideration, the CVPL approach performed better than CVWPL approach.

For the car following model, this study considered several parameters implemented in previous studies. However, the optimization of these parameters was out of the scope for this study. This study can be a good platform for further analysis with a combination of VSL and CV technologies. With this regard, V2I protocol might be useful with combination of V2V communication under CV environment.

As a follow-up study, it may consider a full-scale field experiment. Nevertheless, the experiment will be limited for several reasons. First of all, this study tested the effects of CV by market

penetration rate (MPR) in this study. Nevertheless, the full market penetration of CVs will not be accomplished in the near future. Thus, it is difficult to incorporate the effective full-scale field experiment with V2V communication. A full-scale field experiment with a small group of experimental cars with V2V communication might be needed to substantiate and extend the results of this simulation study. That would be very important to policy makers or researchers working toward the implementation of CV technologies.

CHAPTER FOUR: EFFECTIVENESS OF MANAGED LANE CONNECTED VEHICLES' PLATTONING IN EXPRESSWAY'S

4.1 Introduction

Connected vehicles (CV) technologies has recently drawn an increasing attention from governments, vehicle manufacturers, and researchers. One of the biggest issues facing CVs popularization associates it with the market penetration rate (MPR). The full market penetration of CVs might not be accomplished recently. Therefore, traffic flow will likely be composed of a mixture of conventional vehicles and CVs. In this context, the study of CV MPR is worthwhile in the CV transition period. The overarching goal of this study was to evaluate longitudinal safety of CV platoons by comparing the implementation of managed-lane CV platoons and all lanes CV platoons (with same MPR) over non-CV scenario. This study applied the CV concept on a congested expressway (SR408) in Florida to improve traffic safety. The Intelligent Driver Model (IDM) along with the platooning concept were used to regulate the driving behavior of CV platoons with an assumption that the CVs would follow this behavior in real-world. A high-level control algorithm of CVs in a managed-lane was proposed in order to form platoons with three joining strategies: rear join, front join, and cut-in joint. Five surrogate safety measures, standard deviation of speed, time exposed time-to-collision (TET), time integrated time-to-collision (TIT), time exposed rear-end crash risk index (TERCRI), and sideswipe crash risk (SSCR) were utilized as indicators for safety evaluation. The results showed that both CV approaches (i.e., managed-lane CV platoons, and all lanes CV platoons) significantly improved the longitudinal safety in the studied expressway compared to the non-CV scenario. In terms of surrogate safety measures, the managed-lane CV platoons significantly outperformed all lanes CV platoons with the same MPR. Different time-to-collision (TTC) thresholds were also tested and showed similar results on traffic

safety. Results of this study provide useful insight for the management of CV MPR as managed-lane CV platoons. Figure 5 illustrates the managed-lane CV concept along with the regular vehicles' lanes.

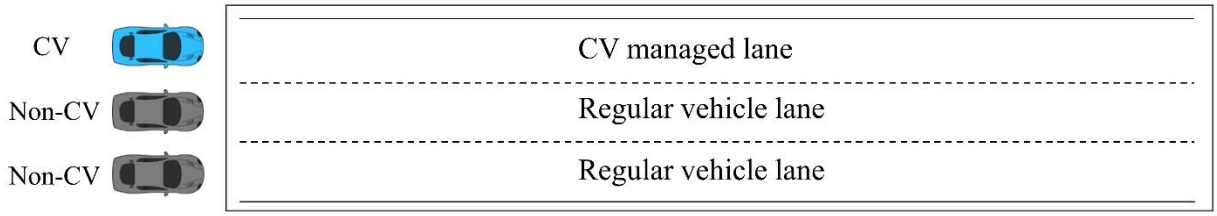

Figure 5 Illustration of CV managed lane and regular vehicle lane

The overarching goal of this study was to evaluate the longitudinal safety evaluation of managed-lane CV platoons on a congested expressway. To have better understanding of managed-lane CV effectiveness, this study selected a congested expressway SR408 which has 17 weaving segments. The simulation experiments are first designed, including deployment of both CV platoons as managed-lane and all lanes in this expressway. Then, a driving behavior model for CVs along with the platooning concept were used with an assumption that the CVs would follow this driving behavior in real-world. Five surrogate safety measures, standard deviation of speed, time exposed time-to-collision (TET), time integrated time-to-collision (TIT), time exposed rear-end crash risk index (TERCRI), and sideswipe crash risk (SSCR) were utilized as indicators for safety evaluation. Sensitivity analysis were also conducted for the different time-to-collision (TTC) thresholds. Results of this study provide useful information for expressway safety when CVs are applied as managed-lane concept for the management of CV MPR in the near future.

4.2 Data Preparation

A congested expressway Holland East-West Expressway (SR408) in Orlando, Florida was selected as a testbed for this study. The testbed was a 22-miles section of SR408 with 17 weaving segments from West Colonial Drive, Orlando to Challenger Parkway, Orlando. This expressway is monitored by Microwave Vehicle Detection System (MVDS), and almost all ramps have an MVDS detector to provide ramp traffic information. MVDS indicates the basic traffic characteristics of the selected road segment. The study area along with the MVDS detectors is shown in Figure 6.

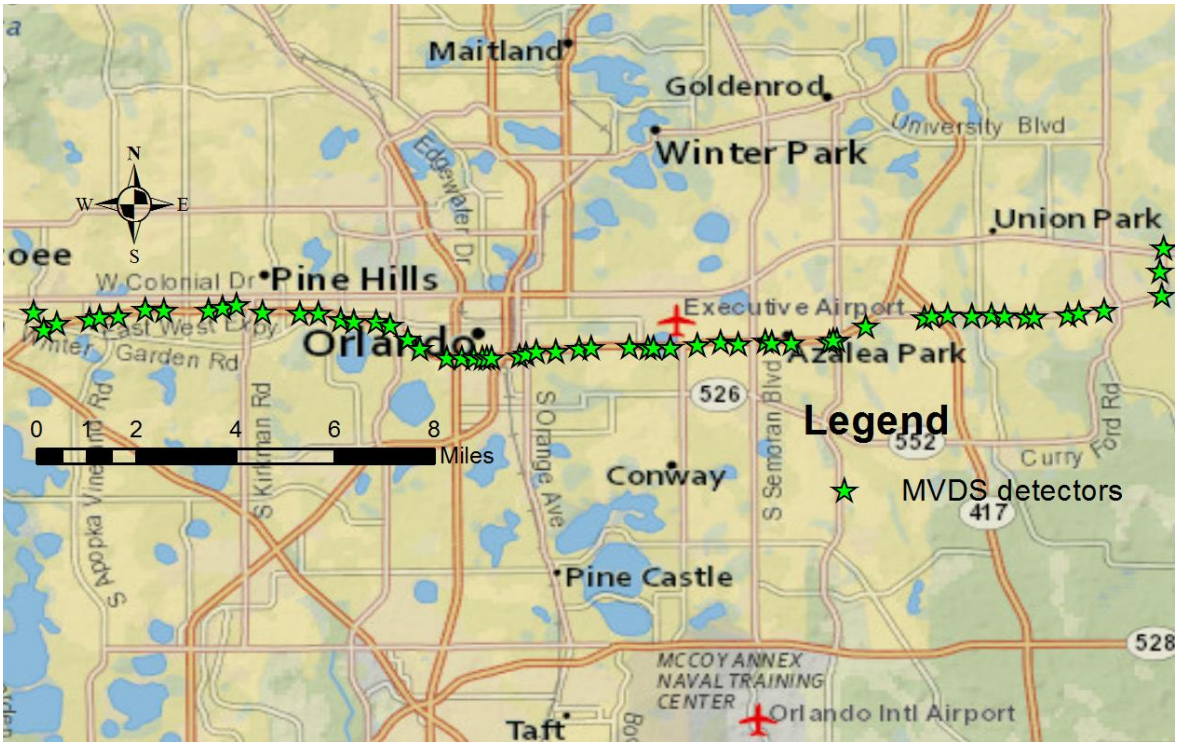

Figure 6 The study area showing MVDS detectors.

The collected traffic dataset contains seven important variables including volume, speed, and lane occupancy for each lane at 1-minute interval, and also categorizes vehicles into four types according to their length; type 1: vehicles 0 to 3 meters in length, type 2: vehicles 3 to 7.5 meters

in length, type 3: vehicles 7.5 to 16.5 meters in length, type 4: vehicles over 16.5 meters in length. The type 3 and type 4 vehicles in MVDS data were considered to be heavy goods vehicles (HGV) whereas the type 1 and type 2 vehicles were passenger vehicles (PC). The traffic data were collected from MVDS detectors installed in the above-mentioned areas (Figure 6).

4.3 VISSIM Simulation Model and Calibration

A well calibrated and validated VISSIM network replicating the field condition is the prerequisite of microsimulation-based study. Simulations were conducted in PTV VISSIM, version 9.0. The testbed was around 22-miles section of SR 408. The traffic information on the simulation network including, traffic volume aggregated into 5 minutes intervals, PC and HGV percentages, and desired speed distribution were obtained from the MVDS detectors. The simulation time was set from 6:30 A.M. to 9:30 A.M in VISSIM. After excluding first 30 minutes of VISSIM warm up time and last 30 minutes of cool-down time, 180 minutes VISSIM data was used for calibration and validation. Geoffrey E. Heavers (GEH) statistic was used to compare the field volumes with simulation volumes. The GEH statistic is a modified Chi-square statistic that takes into account both the absolute difference and the percentage difference between the modelled and the observed flows. The definition of GEH is as follows,

$$GEH = \sqrt{\frac{(M_{obs}(n) - M_{sim}(n))^2}{0.5 \times (M_{obs}(n) + M_{sim}(n))}} \tag{7}$$

Where $M_{obs}(n)$ is the observed volume from field detectors and $M_{sim}(n)$ is the simulated volume obtained from the simulation network. The simulated volume would precisely reflect the field volume if more than 85% of the measurement locations GEH values are less than five (M

Saad et al., 2018; Wang et al., 2017; Wu et al., 2019a; Yu and Abdel-Aty, 2014). It is worth mentioning that, for GEH < 5, flows can be considered a good fit; for 5 < GEH < 10, flow may require further investigation; and for 10 < GEH, flow cannot be considered a good fit. To validate the simulation network, average speeds from the field and simulation have been utilized. Mean, minimum, and maximum values of the average speeds from in-field detectors were calculated. As for speed, the absolute speed difference between simulated speeds and field speeds should be within five mph for more than 85% of the checkpoints (Lee et al., 2018; Nezamuddin et al., 2011). The simulated traffic volumes and speeds were aggregated to 5-minute intervals and then compared with the corresponding field traffic data. Ten simulation runs with different random seeds worth of results showed that 93.23% of observed GEHs were less than five, and 92.92% of the aggregated speeds in the simulation were within five mph of field speeds. The results above proved that the traffic calibration and validation satisfy the requirements and indicate that the network was consistent with that of the field traffic conditions.

Traffic safety deteriorated significantly in weaving segments compared to non-weaving segments which increase crash risk in weaving segments (Glad, 2001; Golob et al., 2004; Kim and Park, 2016; Pulugurtha and Bhatt, 2010; Saad et al., 2019b; Yuan et al., 2019a). So, there was a need to revalidate the weaving segment VISSIM network with respect to both traffic and safety. To simplify the further validation process, a sensitivity analysis was conducted on VISSIM driver behavior parameters in simulation models to reflect the weaving segments condition. Based on the literature review, six parameters were chosen for VISSIM calibration and validation for weaving segments (Jolovic and Stevanovic, 2012; Koppula, 2002; Woody, 2006; Wu et al., 2005). They were DLCD (desired lane change distance), CC0 (standstill distance), CC1 (headway time), CC2

(following variation), waiting time per diffusion, and safety distance reduction factor. For each parameter, a range of values (9 values), which includes the default, was determined based on previous study and engineering judgment (Habtemichael and Picado-Santos, 2013). A total of 490 simulation runs [(1 base-models + 6×8 car-following parameters) times 10 random seeds] were conducted. For sensitivity analysis, standard deviation of speed was calculated in 5 minutes of each run and compared it with the corresponding field standard deviation of speed in 5 minutes by two sample t-test. The sensitivity analysis results showed that three most important parameters were vital to reflect the safety in weaving segment. These include DLCD, CC1, and safety distance reduction factor. The default value of DLCD, CC_1, and safety distance reduction factor in VISSIM were 200 meters, 0.9 seconds, and 0.60, respectively whereas the calibrated values were found to be 400 meters, 0.8 seconds, and 0.50, respectively.

4.4 Methodology

The overview of whole methodology is expressed in Figure 7. The CV platoon was deployed in the simulation experiments in a fashion of managed-lane CV platoons and the all lanes CV platoons with same MPR of 40%. For the managed lane simulation experiment, CV platoons were dedicated only in the inner lane (close to the median) and all other lanes were implemented as regular vehicles. While the simulation experiment for all lanes, CV platoons were implemented all the lanes of the expressway along with regular vehicles. To be more specific, this simulation experiment tested two scenarios including managed-lane CV platoons and all lanes CV platoons which would be compared with the base condition (non-CV scenario). All the CVs behavior are controlled by a car following model and the control algorithm of the CV platoons will be described in the next section. The outputs of the CV platoons' behavior model were microscopic simulation

traffic data, such as position, speed, occupancy, time interval, vehicle length, and acceleration. Based on surrogate safety measures, a relation can be established between these microscopic data and longitudinal safety.

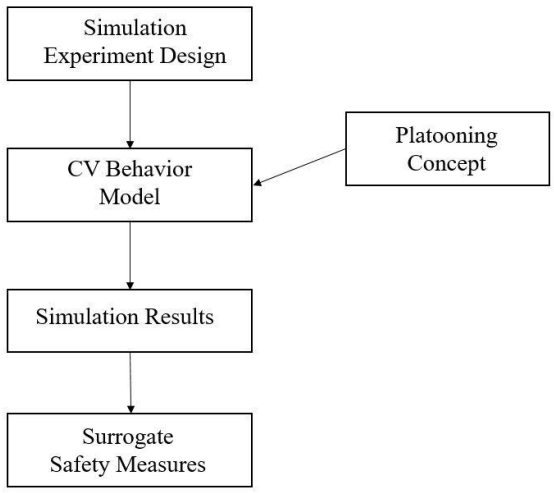

Figure 7 A flowchart of entire methodology.

4.4.1 CV with platooning behavior model

A car following model is a prerequisite to regulate the driving behavior of CVs in microsimulation. The intelligent driver model (IDM), introduced by (Treiber et al., 2000), is a non-linear car following model for which the acceleration ($\dot{v}_{IDM}$) is calculated by the speed differences (Δv) and the dynamic desired gap distance (s^*). Most researchers used IDM as machine driving platform in order to simulate their own driving behavior such as adaptive cruise control (ACC) and cooperative adaptive cruise control (CACC) in microsimulation (Kesting et al., 2010b, 2008; Khondaker and Kattan, 2015; Li et al., 2017a). The acceleration ($\dot{v}_{IDM}$) is expressed in Equation 8.

$$\dot{v}_{IDM}(t + t_a) = \max\left\{b_m, a_m\left[1 - \left(\frac{v}{v_o}\right)^{\delta} - \left(\frac{s^*}{s}\right)^2\right]\right\} \quad (8)$$

$$s^* = s_0 + max\left[0, vT + \frac{v\Delta v}{2\sqrt{a_m b}}\right]$$

where, t_a = the perception-reaction time, b_m = the maximum deceleration, a_m = the maximum acceleration, v = the speed of the following vehicle, v_0 = the desired speed, δ = the acceleration exponent, s = the gap distance between two vehicles, s_0 = the minimum gap distance at standstill, T = the safe time headway, and b = the desired deceleration

All the model parameters of this IDM model were potentially determined according to previous studies (Kesting et al., 2010b; Li et al., 2017a, 2017b; Milanés and Shladover, 2014). The main reason of the selection of model parameter values based on previous research is the unavaiability of empirical data of CVs so that parameter calibrations are intractable. The parameters of CVs behavior model are presented below in Table 4.

Table 4 Model Parameter Setting

Model Parameters	Connected Vehicle
Desired speed, v_0	120 km/h
Acceleration exponent, δ	4
Maximum acceleration, a_m	1 m/sec^2
Desired deceleration, b	2 m/sec^2
Minimum gap distance at standstill, s_0	2 m
Safe time headway, T	0.6 sec
Maximum deceleration, b_m	2.8 m/sec^2
Time delay, t_a	1.5 sec

Additionally, CVs were implemented as a platooning concept (CVPL), wherein several vehicles form a “platoon” that behaves as a single unit. In this study, three joining schemes for CVs, such as rear, front, and cut-in joins were implemented to maintain the platoon. For managed- lane CV platoons’ scenario, platoons form in the lane dedicated for CV managed lane. While all lanes CV

platoons' scenario, platoons form in any lane of the designated roadway. The joining scheme of CVs in CV manage-lane and all lanes CV scenarios are presented in Figures 8 and 9, respectively to maintain a platoon. The rear join leads a new CV from regular vehicle lane following the last vehicle of a CV group in a managed lane driving along the most adjacent lane of the joining vehicle (Figure 8). For the all lanes CV scenario, the rear join leads a new CV following the last vehicle of a CV group in any lane driving along the most adjacent lane of the joining vehicle (Figure 9). Thus, the joining process is similar between the managed-lane CV platoons and all lanes CV platoons. The only difference is that platooning occurs at the designated managed lane in the managed-lane CV platoons. While the simulation experiment for all lanes, CV platoons were implemented at all the lanes of the expressway along with regular vehicles. The front join performs the same process as rear join to allow a new CV from regular vehicle lane to join into an existing CV group in CV managed lane except that it leads the joining vehicle to the front of the first vehicle in the CV group. The cut-in join method is implemented by cooperatively adjusting the maneuvers of the joining vehicle from regular lane and a CV of managed lane in the group. As shown in Figure 8, once the joining vehicle identifies a target CV group in the CV managed lane, it approaches the group and determines a proper position to be inserted based on its current driving information such as speed, position, etc. Then the deceleration rate of a CV in the target group is adjusted to create a safe gap for the joining vehicle while the leading vehicle maintains its current speed. If the safe gap is satisfied for the lane change behavior of the joining vehicle, which is governed by VISSIM's lane changing model, the joining vehicle begins to change the lane.

We developed high-level control algorithm architecture for managed-lane and all lanes CV platoons as shown in Figures 10 and 11, respectively. The all lanes CV platoon's scenario is almost

the same as the managed lane CV platoon's scenario. The same car following model (IDM) along with the platooning concept were used in both scenarios to simulate the behavior of CVs. The only difference is that CVs were allowed to occupy all the lanes of the roadway in the all lanes CV platoon's scenario. Moreover, platooning can form at any lane of the roadway in the all lanes CV platoon. For managed-lane CV platoon's scenario, CVs were allowed only in the designated managed lane of the roadway. The platoons were also formed in the managed-lane only. It is worth mentioning that the algorithm continuously adjusted the acceleration or deceleration rates using the above-mentioned IDM equation between the leading and the subject vehicles using dedicated short-range communication (DSRC) system of 300 meters (1000 feet). The main assumption is that all the CV vehicles will follow the control algorithm in the real-world.

The driving behavior model of CV platoons for both approaches (i.e., managed-lane CV platoons, all lanes CV platoons) were implemented as Dynamic Link Library (DLL) plug-in, which overrides the VISSIM default driving behavior. The DLL were written in C++ which offers VISSIM an option to replace the internal driving behavior and create the V2V communication system. Note that the car following and the lane changing behavior of non-CVs were determined by VISSIM's default driving behavior model.

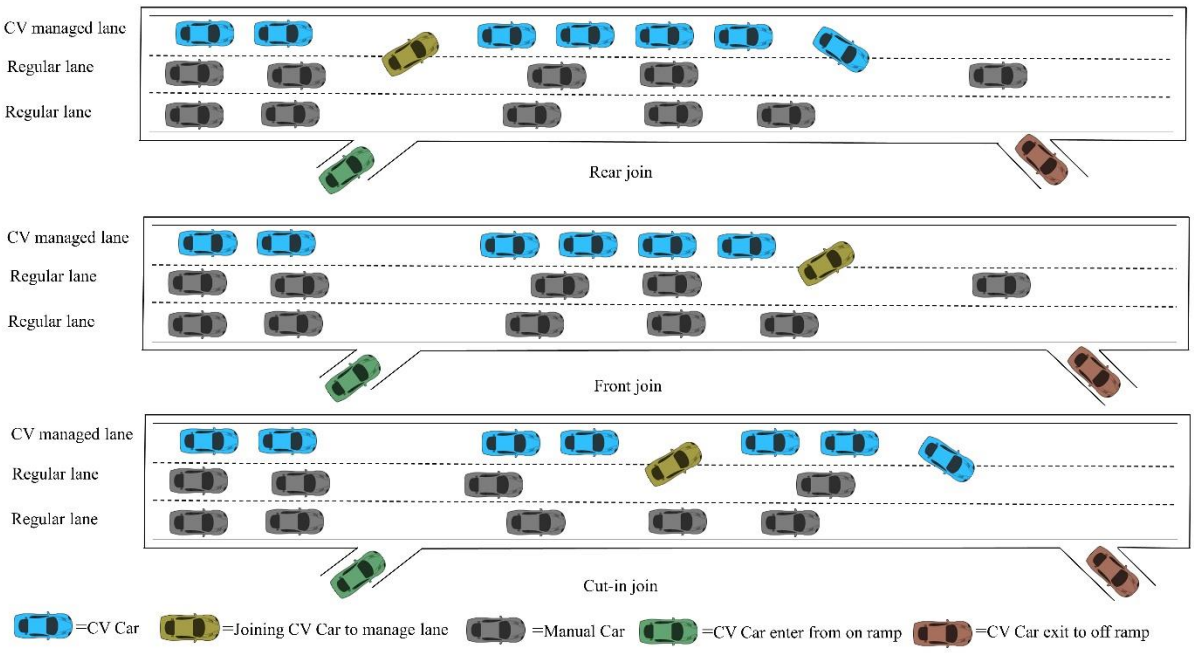

Figure 8 Illustration of CV join to maintain a platoon in managed-lane CV scenario.

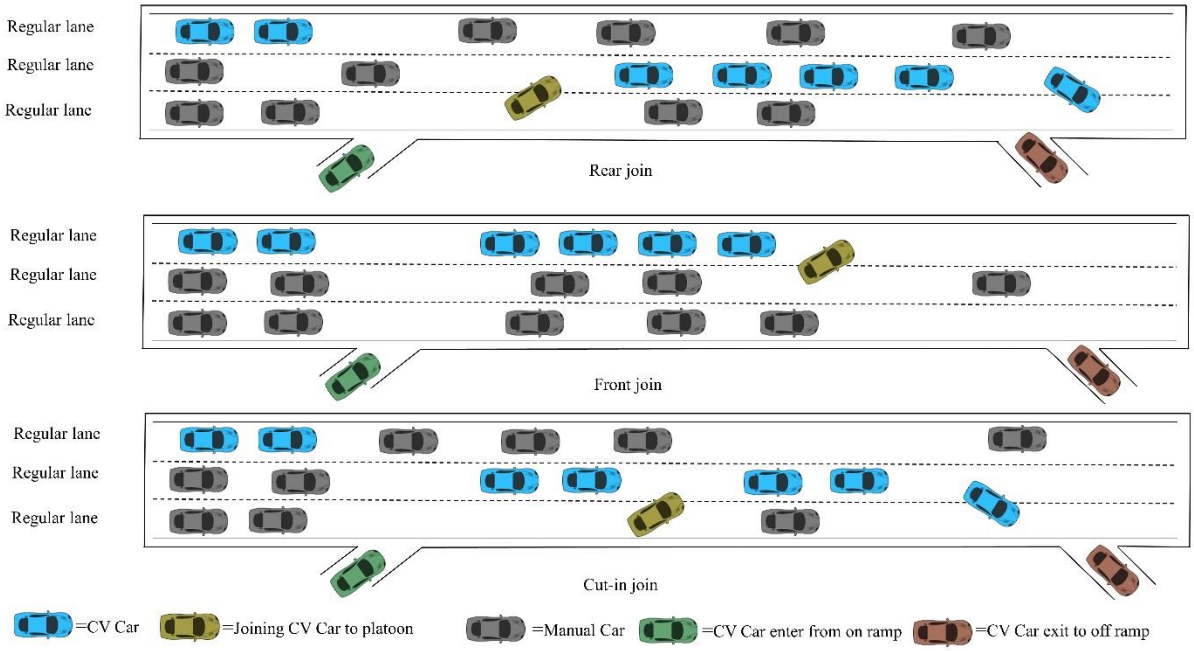

Figure 9 Illustration of CV join to maintain a platoon in all lanes CV scenario.

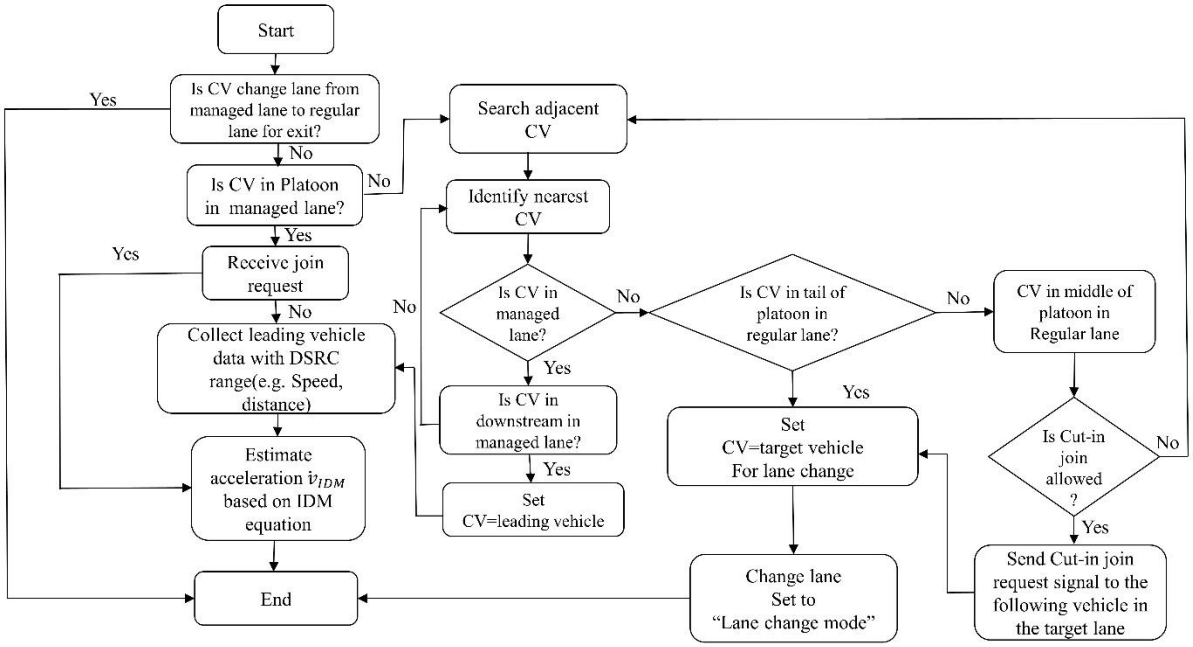

Figure 10 Control algorithm of CVs to maintain a platoon in the managed-lane CV scenario.

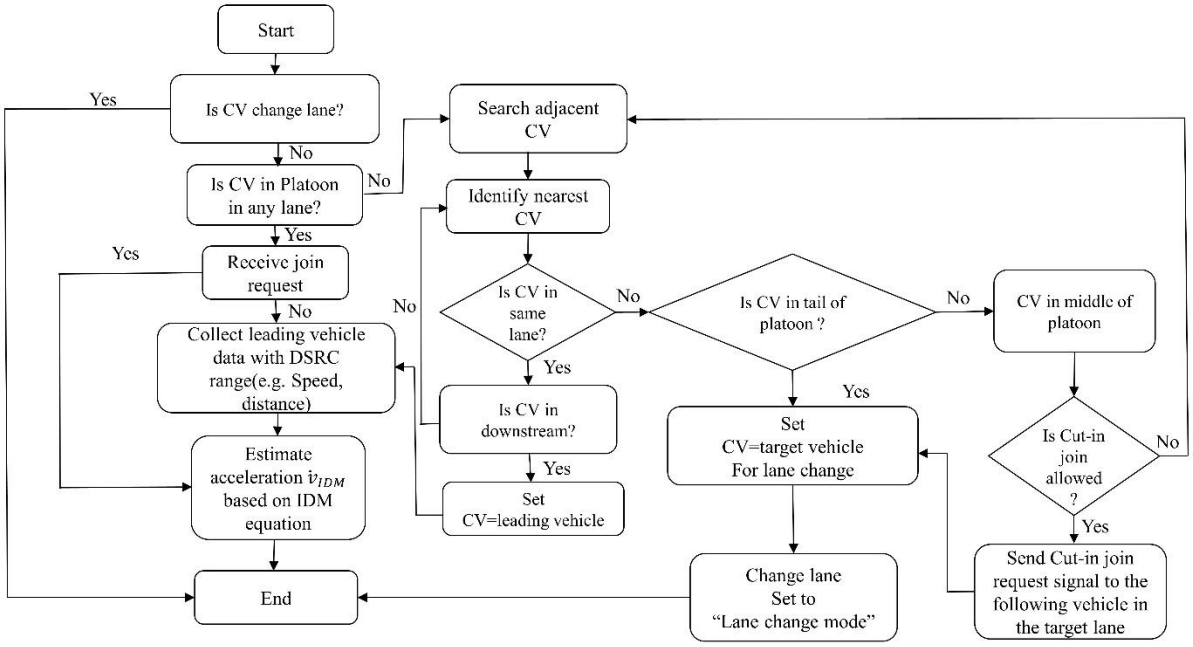

Figure 11 Control algorithm of CVs to maintain a platoon in the all lanes CV scenario.

The comparison among these three scenarios (base, all lanes CV platoons', and managed-lane CV platoons' scenarios) are presented in Table 5.

Table 5 Comparisons among the Three Scenarios (Base, All lanes CV, Managed-lane CV).

Attributes	**Base Scenario**	**All lanes CV platoon's Scenario**	**Managed-lane CV platoon's scenario**
Car following model	Wiedemann 99 (VISSIM Default)	IDM model (Equation 1)	IDM model (Equation 1)
Parameters	VISSIM default	Presented in Table 4	Presented in Table 4
Communication	No communication	V2V	V2V
Control method (Platooning)	No platooning	Platooning (Figures 9 and 11)	Platooning (Figures 8 and 10)

4.4.2 Surrogate measures of safety

Traffic crashes are rare events which involve numerous human factors along with the road environment and vehicle factors. A surrogate safety assessment technique should be adopted to measure safety as microsimulation software cannot be directly used to measure crashes or traffic safety. So, the surrogate measures of safety are widely used as proxy indicators to evaluate the crash risk in microsimulation. A number of previous studies used surrogate measures including speed variance, time to collision, post-encroachment time, and rear-end crash risk index (Abdel-Aty et al., 2009; Gettman and Head, 2003; Peng et al., 2017). In this study, four surrogate measures of safety were considered to evaluate the traffic safety. Standard deviation of speed was considered one of the surrogate measures of safety. Two surrogate measures of safety, derived from TTC and denoted as time exposed time-to-collision (TET) and time integrated time-to-collision (TIT), are utilized to establish relation between microscopic traffic data and longitudinal safety of CVs.

The TTC is firstly introduced by (Hayward, 1972), referring to the time that remains until a collision between the leading and following vehicles will occur if the speed difference is maintained. To be more specific, the TTC represents the time required for two successive vehicles,

occupying the same lane, to collide if they continue at their present speed when vehicle n moves faster than the preceding vehicle (n-1). The TTC notion can be expressed as Equation 9:

$$TTC_n(t) = \begin{cases} \frac{x_{n-1}(t) - x_n(t) - L_{n-1}}{v_n(t) - v_{n-1}(t)}, & if\ v_n(t) > v_{n-1}(t) \\ \infty, & if\ v_n(t) \leq v_{n-1}(t) \end{cases} \tag{9}$$

where $TTC_n(t)$ = the TTC value of vehicle n at time t, x = the positions of vehicles, v= the velocities of vehicles, L_{n-1}= Length of preceding vehicles.

Furthermore, two types of TTC are usually utilized in traffic safety analysis: TTC1 and TTC2. TTC1 assumes the preceding vehicle maintains its speed, while TTC2 describes situations when the preceding vehicle stops suddenly, which is also called TTC at braking (Peng et al., 2017; Wu et al., 2019b). During the simulation, traffic data was collected at eighteen detectors in the VISSIM network, and few small TTC1 was observed during the simulation. Thus, TTC at braking (TTC2) is employed in this study to evaluate traffic safety in different situations. In this study, the definition of the TTC at braking (TTC_{brake}) is as follows (Peng et al., 2017):

$$TTC_{brake}(t) = \frac{x_{n-1}(t) - x_n(t) - L_{n-1}}{v_n(t)} \tag{10}$$

The smaller TTC_{brake} value indicates the lager risk at a certain time instant. The TET and TIT, two aggregate indictors developed by (Minderhoud and Bovy, 2001), are potentially used in this study as surrogate safety measures. The TET refers to the total time spent under dangerous traffic conditions, determined by TTC_{brake} value below the threshold value of TTC (TTC*).

$$TET\ (t) = \sum_{n=1}^{N} \delta_t \times \Delta t, \quad \delta_t = \begin{cases} 1, & 0 < TTC_{brake}(t) \leq TTC^* \\ 0, & otherwise \end{cases} \tag{11}$$

$$TET = \sum_{t=1}^{Time} TET(t) \tag{12}$$

where t = the time ID, n = the vehicle ID, N = the total number of vehicles, δ = the switching variable, Δt = the time step, which was 0.1 s in simulation, Time = the simulation period, and $TTC*$ = the threshold of TTC. The TTC* is used to differentiate the unsafe car following conditions from ones considered safe. According to previous studies, the values of TTC* varies from 1 to 3 s (Li et al., 2016a, 2014; Sultan et al., 2002).

The TIT notion refers to the entity of the TTC_{brake} lower than the threshold. The reciprocal transformation was made considering that a lower TTC means a higher collision risk:

$$TIT(t) = \sum_{n=1}^{N} \left[\frac{1}{TTC_{brake}(t)} - \frac{1}{TTC^*}\right] . \Delta t, 0 < TTC_{brake}(t) \leq TTC^* \tag{13}$$

$$TIT = \sum_{t=1}^{Time} TIT(t) \tag{14}$$

Additionally, rear end crashes are the most common type of crashes in any roadway. A rear-end crash may occur if the leading vehicle stops suddenly, and the following vehicle does not decelerate in time. So, maintaining insufficient safety distance between the leading and the following vehicle is the primary cause of rear-end crashes. To avoid the rear-end crashes, the stopping distance of the following vehicle should be smaller than the leading vehicle. A rear-end crash risk index (RCRI) proposed by Oh et al. (Oh et al., 2006) in which the dangerous condition can be mathematically expressed as:

$$SD_F > SD_L \tag{15}$$

$$SD_L = v_L \times h + \frac{v_L^2}{2 \times a_L} + l_L \tag{16}$$

$$SD_F = v_F \times PRT + \frac{v_F^2}{2 \times a_F} \tag{17}$$

Where SD_L and SD_F are the stopping distance of the leading and the following vehicles, respectively. l_L the length of the leading vehicle, v_L the speed of the leading vehicle, v_F the speed of the following vehicle, PRT is the perception-reaction time, h the time headway, a_L the deceleration rate of the leading vehicle and a_F is the deceleration rate of the following vehicle. As mentioned earlier, for the VISSIM model, we used two types of vehicles PC and HGV. Therefore, different deceleration rates were employed to estimate the reliable safe distance for the leading and following vehicles. The deceleration rates of PC and HGV were selected as 3.42 m/s^2 and 2.42 m/s^2 respectively, while the PRT was used as 1.5 s, these values are generally accepted by AASHTO (American Association of State Highway and Transportation Officials (AASHTO), 2004). I proposed one surrogate measures of safety, derived from RCRI and denoted as time exposed rear-end crash risk index (TERCRI).

$$TERCRI\ (t) = \sum_{n=1}^{N} RCRI_n(t) \times \Delta t, \quad RCRI_n\ (t) = \begin{cases} 1, & SDF > SDL \\ 0, & Otherwise \end{cases} \tag{18}$$

$$TERCRI = \sum_{t=1}^{Time} TERCRI(t) \tag{19}$$

Moreover, the rear-end crash type is not the only crash type on expressways. Sideswipe crashes are another type of frequent crashes on expressways. It is worth mentioning that the most common way of a sideswipe crash occurs during the lane changing maneuver. However, it can also happen in a lane changing maneuver on ramps. Therefore, the lane changing conflict can be a surrogate

measure of the sideswipe crash risk (SSCR). It is difficult to find out the surrogate measures of sideswipe crashes analytically. Therefore, the Surrogate Safety Assessment Model (SSAM), developed by the Federal Highway Administration, was applied to analyze the lane changing conflict which can be related to the surrogate measures of the sideswipe crashes. The experimental VISSIM model generated several groups of traffic trajectory data files. The vehicle conflicts' data were stored in these trajectory data files which, contains the conflict locations' coordinates, conflict time, time-to-conflict, and post-encroachment-time among other measures. Hence, the SSAM was applied to analyze these conflict data in order to compare the SSCR among the three scenarios.

In a nutshell, the standard deviation of speed, TET, TIT, and TERCRI were considered as surrogate measures of safety in order to evaluate the longitudinal safety of managed-lane CV platoons.

4.5 Results and Discussion

Five surrogate measures of safety were considered to evaluate the safety performances of managed-lane CV platoons in an expressway. To have a better understanding, this particular study introduced CV platoons in all the lanes and only in a managed-lane on the expressway with similar MPR. These two CV scenarios were compared with the base scenario (non-CV scenario) in order to observe the effectiveness of CV platoons. As mentioned earlier standard deviation of speed, TET, TIT, TERCRI, and SSCR are the five surrogate measures of safety considered in this study. Each scenario (base scenario, all lanes CV platoons, and managed-lane CV platoons) was repeatedly simulated for 20 times in order to consider random effects of simulation and the preliminary results are shown in Figure 12. The TTC threshold was considered 2 seconds for the

preliminary analysis and then a sensitivity analysis is conducted for different TTC thresholds from 1 to 3 seconds.

As shown in Figure 12, the distribution of standard deviation of speed, TET, TIT, TERCRI, and SSCR of each scenario approximately followed the normal distribution because of the random effect of simulation. However, the magnitudes (minimum value, maximum value) were significantly different for each scenario. The values (minimum, maximum) of standard deviation of speed, TET, TIT, TERCRI, and SSCR of base scenario were found to be ranged between [12, 16], [4400, 4725], [2175, 2475], [2700, 2925], and [1212, 1310] respectively.

While the five indicators of all lanes CV platoons' scenario were within approximately [12, 14], [3485, 3725], [1725, 1970], [2125, 2375], and [712, 787] respectively and the scenario with managed-lane CV platoons were within approximately [10.75, 11.5], [3250, 3450], [1600, 1775], [1910, 2060], and [538, 612] respectively. The larger values of each surrogate safety indicator imply the more dangerous situations. Hence, there are the higher longitudinal crash risks in base scenario compared to managed-lane CV platoons and all lane CV platoons. Among the three scenarios, all five indicators had the lowest values for managed-lane CV platoons representing a safer situation.

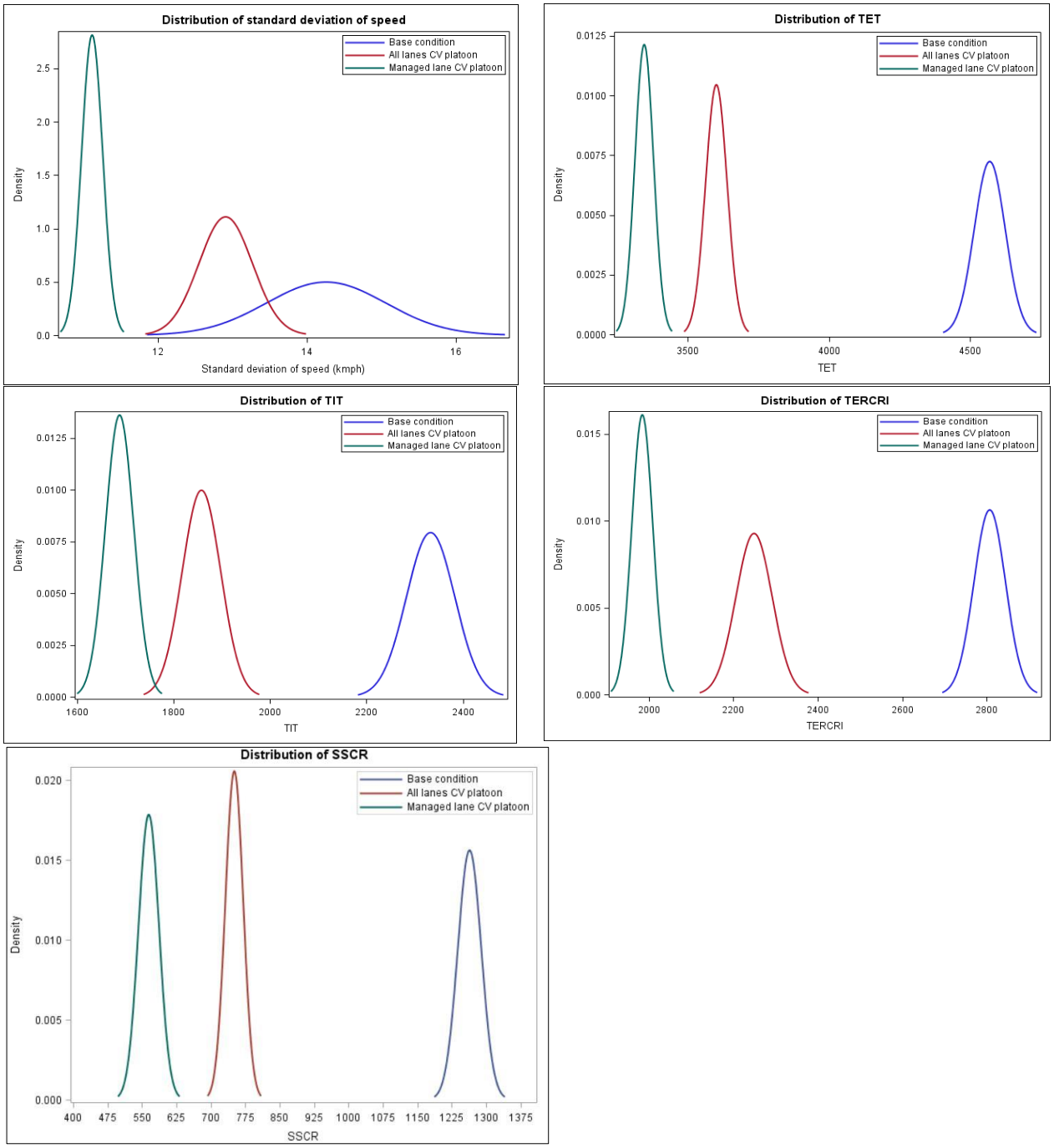

Figure 12 Standard deviation of speed, TET, TIT, TERCRI, and SSCR distribution with different scenarios.

The descriptive statistics of standard deviation of speed, TET, TIT, TERCRI, and SSCR in three scenarios are presented in Table 6. The non-CV scenario has the largest mean value of each

standard deviation of speed (14.26), TET (4569.45), TIT (2333.05), TERCRI (2807.40), and SSCR (1263.80) followed by the all lanes CV platoons with 12.91 of standard deviation of speed, 3601.15 of TET, 1857.90 of TIT, 2249.00 of TERCRI, and 751.30 of SSCR, respectively.

Table 6 Summary Statistics of Standard Deviation of Speed, TET, TIT, TERCRI, and SSCR.

Scenarios	Measures	Number of Runs	Minimum	Maximum	Mean	Standard Deviation
Base	SD of speed (Km/h)	20	13.04	15.83	14.26	0.80
	TET (s)	20	4482	4692	4569.45	55.10
	TIT (s)	20	2258	2440	2333.05	50.28
	TERCRI (s)	20	2734	2881	2807.40	37.51
	SSCR	20	1212	1310	1263.80	25.56
All lane CV	SD of speed (Km/h)	20	11.98	13.56	12.91	0.36
	TET (s)	20	3512	3675	3601.15	38.16
	TIT (s)	20	1801	1934	1857.90	39.97
	TERCRI (s)	20	2103	2301	2249.00	42.99
	SSCR	20	712	787	751.30	19.41
CV managed lane	SD of speed (Km/h)	20	10.83	11.32	11.12	0.14
	TET (s)	20	3307	3417	3345.60	32.88
	TIT (s)	20	1645	1756	1688.10	29.31
	TERCRI (s)	20	1947	2036	1984.25	24.77
	SSCR	20	538	612	564.95	22.37

*SD of speed=standard deviation of speed

The mean value of five surrogate indicators of managed-lane CV platoons were lowest with mean standard deviation of speed (11.12), TET (3345.60), TIT (1688.10), TERCRI (1984.25), and SSCR

(564.95), respectively. Therefore, the scenario with managed-lane CV platoons has the lowest longitudinal crash risks compared to all lane's CV platoon, while the scenario with base condition has the highest crash risk.

The One-way ANOVA analysis are also presented in Table 7 which indicates significant differences among these three scenarios and infer that managed-lane CV platoons significantly outperformed all lane CV platoon.

Table 7 One-way ANOVA Analysis of Standard Deviation of Speed, TET, TIT, TERCRI, and SSCR.

Measures	Attribute	Sum of squares	DF	Mean Squares	F-value	Significance
Standard deviation of Speed (km/h)	Between Groups Within Groups Total	99.32 15.03 114.35	2 57 59	49.66 0.26	188.33	<0.0001
TET (s)	Between Groups Within Groups Total	16671463.43 105898.30 16777361.73	2 57 59	8335731.72 1857.86	4486.73	<0.0001
TIT (s)	Between Groups Within Groups Total	4470400.43 94714.55 4565114.98	2 57 59	2235200.22 1661.66	1345.16	<0.0001
TERCRI (s)	Between Groups Within Groups Total	7063193.63 73514.55 7136708.18	2 57 59	3531596.82 1289.73	2738.25	<0.0001
SSCR	Between Groups Within Groups Total	5238492.63 29084.35 5267576.98	2 57 59	2619246.32 510.25	5133.24	<0.0001

A heat map is also represented in Figure 13 which shows the effectiveness of managed-lane CV platoons and all lanes CV platoon over non-CV scenario. Managed-lane CV platoons has the highest safety improvement in terms of five surrogate measures of safety presented in heat map.

In managed-lane CV platoons' scenario, the values of standard deviation of speed, TET, TIT, TERCRI, and SSCR were lowest with lighter color in heat map.

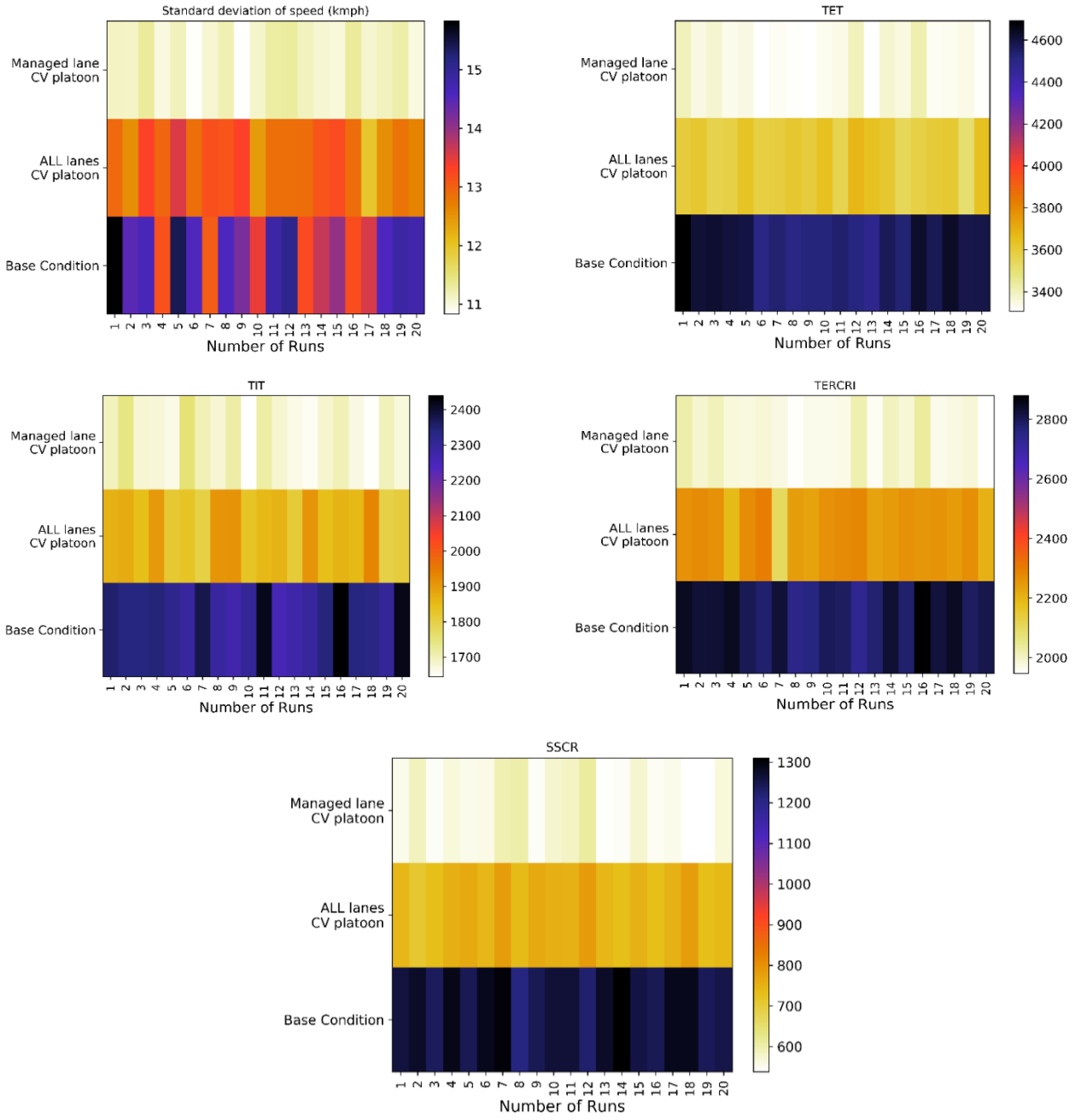

Figure 13 Heat map of surrogate measures of safety.

On the other hand, the values of five surrogate measures of safety were largest representing higher crash risk in non-CV scenario with darker color. In all lanes CV platoons' scenario, the values of aforementioned surrogate measures of safety are smaller than base scenario but larger than the managed-lane CV platoons' scenario. From the above discussion, it is inferred that managed-lane CV platoons clearly outperformed the all lanes CV platoons in terms of surrogate measures of safety.

Table 8 Sensitivity Analysis of Different Values of TTC Threshold

TTC* (s)	**Scenarios**	**Base condition**		**Scenario 1 (All lane CV)**		**Scenario 2 (Managed-lane CV)**	
	Measures	**TET**	**TIT**	**TET**	**TIT**	**TET**	**TIT**
1.0	Average value	2238	674	1765	539	1602	497
	Changing proportion	-	-	21%	20%	28%	26%
1.5	Average value	3634	1654	2921	1326	2647	1182
	Changing proportion	-	-	19%	19%	27%	29%
2.0	Average value	4569	2333	3601	1858	3346	1688
	Changing proportion	-	-	21%	20%	27%	28%
2.5	Average value	5290	2824	4222	2251	3820	2045
	Changing proportion			20%	20%	28%	28%
3.0	Average value	5889	3205	4634	2554	4227	2313
	Changing proportion	-	-	21%	20%	28%	28%

The above results of TET and TIT are mainly based on the same parameter setting of TTC threshold is 2 s. Sensitivity analysis of TTC thresholds were also conducted. The various values TTC threshold do not affect the results of simulations. The five values of TTC threshold ranging from 1 to 3 seconds have almost same results which is presented in Table 8. Compared with base scenario, all the reductions of TIT and TET values maintain within 19% to 21% for all lanes CV

platoons with different values of TTC threshold. And the TIT and TET values are all reduced within 26% to 28% of managed-lane CV platoons compared with that of base condition.

Overall, the deployment of CV platoon of all lanes and managed lane in studied congested expressway would significantly decrease the standard deviation of speed, TET, TIT, TERCRI, and SSCR; thereby might decrease the probability of crashes. Moreover, it is clearly seen that managed- lane CV platoons significantly outperformed all lanes CV platoons with same MPR.

4.6 Summary

The primary objective of this study was to evaluate longitudinal safety of managed-lane CV platoons on expressways based on simulation results. The simulation experiments were designed, by deploying managed-lane CV platoons and all lanes CV platoons on a congested expressway. Then, a vehicle behavior model for CV platoon was used based on the IDM model and five surrogate safety measures, standard deviation of speed, TET, TIT, TERCRI, and SSCR were measured as safety indicators. Sensitivity analysis were also conducted for different TTC thresholds to compare the results among the three scenarios.

The distribution of five surrogate measures of safety approximately follow the normal distribution because of the stochastic nature of simulation. The values of standard deviation of speed, TET, TIT, TERCRI, and SSCR were largest for the base (non-CV) scenario. The results showed that both CV platoons scenarios improved safety significantly over non-CV scenario. However, the surrogate safety measures were smaller in managed lane CV platoons compared to all lanes CV platoons. Hence, traffic stream with managed-lane CV platoons has lower longitudinal crash risks

compared to all lanes CV platoons. One-way ANOVA analysis showed significant differences among the three tested scenarios and inferred that managed-lane CV platoons significantly outperformed all lanes CV platoons. And, the results of sensitivity analysis indicated that the TTC threshold ranging from 1 to 3 seconds have almost the same results. Hence, the different TTC thresholds did not affect the simulation results.

From our analysis, it is evident that managed lane CV platoons and all lanes CV platoons significantly improved the longitudinal safety in the studied expressway segments compared to the base condition. In terms of surrogate safety measures, the managed-lane CV platoons significantly outperformed all lanes CV platoons with the same MPR. The study is not without limitations. In our research effort, we considered several IDM parameters that were implemented in previous studies. The parameters should be calibrated based on the empirical data of CVs which are unavailable, thus parameter calibrations are currently intractable. However, the optimization of these parameters was out of the scope for this study. This study can be a good platform for further analysis with a combination of variable speed limit, ramp metering, and CV technologies in any congested expressway.

CHAPTER FIVE: SAFETY BENEFITS OF ARTERIALS' CRASH RISK UNDER CONNECTED AND AUTOMATED VEHICLES

5.1 Introduction

Connected and automated vehicles are the most recent development of information and communication technologies that can significantly improve the safety and efficiency of the transportation road network. In general, connected vehicle (CV) technologies utilize two main types of communications (1) vehicle-to-vehicle (V2V), and (2) infrastructure-to-vehicle (I2V) through various possible ways, mostly dedicated short-range communication system (DSRC). With reliable connectivity of V2V communication, each CV would receive information about other CVs' statuses (i.e., position, speed, acceleration, etc.). On the other hand, CV would receive information from I2V such as signal status, signal timing, etc. With the advent of V2V and I2V communications along with automated driving features, traffic safety and efficiency are expected to improve significantly in the transportation road network. The combination of connected and automated vehicle technologies are capable to minimize drivers' errors, which is considered a major cause solely or in combination with other factors for more than 94% of traffic crashes (Singh, 2015; Yue et al., 2018). The driving environment and associated driver-vehicle behaviors are expected to change with the introduction of connected and automated vehicles. At the operational level, these technologies are intended to help drivers and vehicles make safe and reliable decisions about acceleration choice, lane keeping assistance, and lane changing decisions etc.

Automated vehicles are expected to decrease crash risk on urban arterial roads under connected vehicle environment with the adoption of both V2V and I2V communication technologies. This study considered two automated features (1) automated braking and (2) lane keeping assistance

which are currently available in many vehicles in the market. Examining lower level of automation is feasible since it will be the most realistic in the context of connected and automated vehicles in the foreseeable future. To be more specific, this research aims to contribute to the safety literature by evaluating connected vehicle (CV) and connected vehicle lower level automation (CVLLA) to improve the traffic safety of both segments and intersections on an arterial section through VISSIM microsimulation. To the best of our knowledge, this is the first study which utilizes lower level of automation under connected vehicle environment to reduce the crash risk of both segments and the intersections on arterials. However, the realistic driving behavior models are prerequisite to approximate the decision processes of these technologies. Towards this end, the Intelligent Driver Model (IDM) (Kesting et al., 2008) was applied to model the CV behavior while the modified Bando's model (Wen-Xing and Li-Dong, 2018) along with lane keeping assistance was developed to model the CVLLA behavior through C++ programming language in microsimulation. In the immediate future, the MPRs will not achieve 100%, meanwhile, the penetration will increase gradually. Hence, it is worthwhile to study the safety benefits of CV and CVLLA technologies under different MPRs.

5.2 Simulation Test Bed and Data

Alafaya Trail is an arterial near the University of Central Florida, Orlando, Florida, was selected as the testbed. This testbed is approximately 3.8 miles in length and includes nine signalized intersections. The testbed is often heavily congested because of the presence of the University of Central Florida, which is one of the largest universities in the United States, in terms of undergraduate enrollment. The simulation model used in this study was VISSIM Version 10.0. The study period spans 2 hours of the A.M. peak, from 7:00 A.M. to 9:00 A.M. on October 11, 2017,

and the field traffic data (i.e. flow) was aggregated into 15-minute traffic counts. Speed and travel time data were also collected on the same day which were used for the calibration and the validation of the VISSIM baseline simulation model. Traffic counts, speed, and travel time data were collected from Bluetooth detectors. Moreover, further traffic information for building the simulation network including passenger car (PC) and heavy goods vehicle (HGV) percentages, and desired speed distribution were also calculated for the input of the VISSIM model. The signal timing for the nine signals in the simulation network were also coded in VISSIM from the signal timing data obtained from the county. The simulation time was set from 6:30 A.M. to 9:30 A.M in VISSIM. After excluding first 30 minutes of VISSIM warm up time and last 30 minutes of cool-down time (no statistics were collected during this time), 120 minutes VISSIM data was used for model calibration and validation.

5.2.1 Model Calibration and Validation

The most important part of any simulation model is calibrating the model by defining or fine-tuning the values of the parameters so that the difference between observed and simulated traffic measurement (i.e., traffic counts, speed, travel time, etc.) is minimum (Duell et al., 2016; FHWA, 2012; Gong et al., 2019; Hadi et al., 2016, 2015; Luo and Joshua, 2011; Pravinvongvuth and Loudon, 2011; Shafiei et al., 2017; Tokishi and Chiu, 2013; Ziliaskopoulos et al., 2004; Zitzow et al., 2015). In this regard, calibration criteria are formulated by the general optimization framework as follows.

$$\min f\left(M^{obs}, M^{sim}\right) \tag{20}$$

Which is subjected to the constraints:

$$l_{\theta_i} \leq \theta_i \leq u_{\theta_i}, \quad i = 1,2, \dots, n \tag{21}$$

Where,

θ_i=the vectors of continuous variable (i.e. model parameters to be calibrated)

$f(.)$ =Objective function (or fitness function).

M^{obs}, M^{sim}=Observed and simulated traffic measurements.

$l_{\theta_i}, u_{\theta_i}$=the respective lower and upper bounds of model parameter

n = number of parameters.

In this study, we used mean absolute normalized error (MANE) as objective function (fitness function) using both traffic counts and speeds. The specification of minimizing MANE is given as follows:

$$Minimize\ MANE(q,v) = \frac{1}{N}\sum_{j=1}^{N}\frac{(|q_{obs_j} - q_{sim_j}|)}{q_{obs_j}} + \frac{(|v_{obs_j} - v_{sim_j}|)}{v_{obs_j}} \qquad (22)$$

q_{obs_j}, v_{obs_j}=actual traffic counts and speed for a given time interval j.

q_{sim_j}, v_{sim_j}=simulated traffic counts and speed for a given time interval j.

N =total number of observations.

VISSIM uses two car following models developed by Rainer Wiedemann named Wiedmann-74 and Wiedmann-99, which captures psychophysical driver behavior model (Brackstone and McDonald, 1999). The former one (Wiedemann-74) is suitable for urban traffic while the latter one (Wiedmann-99) is designed for freeway segments. The base calibration parameters for VISSIM that have been considered in this research are the driver behavior parameters of Wiedmann-74 as the test bed was selected on an arterial section. Wiedmann-74 model includes both car following and lane changing parameters in VISSIM. The parameters are shown in Table 2 with minimum and maximum allowable values that are selected in the calibration procedure which was determined based on previous studies (Cai et al., 2018; Kim et al., 2005; Rahman et al.,

2018a; Rahman and Abdel-Aty, 2018; Moatz Saad et al., 2018b). A sensitivity analysis was conducted on VISSIM driver behavior parameters based on their allowable minimum and maximum values in the simulation model. For each parameter, a range of values between the minimum and maximum (include default value) were chosen to run the VISSIM model and the corresponding values of the objective function MANE were calculated. It is worth mentioning that each parameter value was run ten times with different random seeds and averaged to calculate the simulated traffic measurement which captures the random effects of the simulation. For each parameter, the minimum value of MANE is the corresponding calibrated value for that parameter. The calibrated values of the selected parameter such as average standstill distance, additive part of desired safety distance, multiplicative part of desired safety distance, and lane change distance were found to be 2.5 meters, 3, 4, and 150 meters, respectively, whereas the VISSIM default values were 2 meters, 2, 3, and 200 meters, respectively (see Table 9).

Table 9 VISSIM Calibration Parameters

Parameters	Unit	Default value	Allowable value		Calibrated value based on MANE
			Minimum	Maximum	
Average standstill distance	meter	2	1	4	2.5
Additive part of desired safety distance	N/A	2	1	10	3
Multiplicative part of desired safety distance	N/A	3	1	10	4
Lane change distance	meter	200	50	300	150

NA=not applicable

For the validation of the VISSIM model, the Kolmogorov–Smirnov (KS) test was used to test the hypothesis that whether the distribution of the simulated and the observed travel times are statistically identical or not. The Kolmogorov–Smirnov tests is a nonparametric technique which

can be used to prove that two populations have the same distribution. Let $X_1, \ldots, X_m$ be the field travel time with cumulative distribution function (CDF) F_1, and $Y_1, \ldots, Y_n$ be the travel time from the VISSIM simulation averaging 10 runs (different random seeds) with CDF F_2. The null hypothesis is the distribution between the field and simulated travel time are identical. The Kolmogorov–Smirnov test statistic is defined as follows:

$$D = Max|F_1(x) - F_2(x)| \tag{23}$$

The hypothesis is rejected if the test statistic, D, is greater than the critical value obtained from a KS table which can be found from the statistical textbook (Teukolsky, W. H. et al., 2002). The travel time data for all vehicles are recorded from VISSIM simulation runs and compared with the field observations by KS test. From the KS test result, it is found that the D is less than the critical value with 5% significance level. Hence, the distribution of the simulated and the observed travel times are statistically identical which confirmed the good validation results of the VISSIM model.

5.3 Methodologies

The methodologies of this chapter are mainly focused on the modeling of driving behaviors in VISSIM to simulate the connected vehicles (CV) and the connected vehicles lower level automation (CVLLA). The car following model is a crucial component in simulation which regulates the driving behavior of vehicles to represent the real-world traffic system. The driving behavior of conventional vehicle, CV, and CVLLA should be significantly different from each other. PTV VISSIM uses Wiedemann car following model in order to simulate the road network under human-driven vehicles. This model is not reasonable to represent connected and automated vehicles as it is designated to model human behavior and requiring complex tuning of the multitude of parameters. In order to understand the behavior of introducing CV and CVLLA into the traffic

system, this study utilizes realistic driving behavior models for both CV and CVLLA in accordance with the recent literature that would approximate the decision processes of these technologies.

5.3.1 Driving Behavior Model for CV

To better assess the impact of CV on an arterial, a driving behavior model is prerequisite for micro-simulation studies. The choice of the car following model largely determines the driving behavior of CV to represent the real-world traffic system. The Intelligent Driver Model (IDM) has already been proven as the most realistic car following model in order to simulate the CV in freeway section described in simulation based literature (Guériau et al., 2016; Rahman et al., 2018a; Rahman and Abdel-Aty, 2018; Talebpour and Mahmassani, 2016b). The time-continuous Intelligent Driver Model (IDM) is the simplest complete model that is able to model oscillations, stop-and-go traffic, and start and stop of a vehicle platoon between two traffic lights producing realistic accelerations and braking decelerations profile (Kesting et al., 2010b; Kesting and Treiber, 2013; Treiber et al., 2007). Although this model captures different congestion dynamics, it provides greater realism than most deterministic acceleration modeling frameworks. The most recent simulation study proved that the IDM model can replicate the best driving behaviors compared to the other competing car following models (Pourabdollah et al., 2018). In the literature, there are plenty of safety studies utilizing the IDM as the car following model in microscopic simulation (Derbel et al., 2012; Li et al., 2017b; Plattner et al., 2007). However, the implementation of IDM on an arterial section is significantly different from the freeway traffic because of the presence of signals. In general, there can be two distinct cases of IDM implementation of CV on an arterial section (1) vehicle to vehicle (2) signal to vehicle. The former one is designed for the car following behavior between two vehicles through V2V communication range while the latter on is focused on the vehicle approaching a signalized intersection by I2V

communication. The illustration of the IDM implementation on an arterial section under CV environment (both V2V and I2V) is presented in Figure 14.

The first case in Figure 14(a) shows the car following case of vehicle to vehicle by V2V communication under CV environment. In this case, the IDM model acceleration ($\dot{v}_{IDM}$) is the function of desired gap distance s^* and the speed difference between following ($V_F = v$) and leading (V_L) vehicles ($\Delta v = V_F - V_L$) by offering V2V communication under CV environment, expressed by the following Equation 24.

$$\dot{v}_{IDM}(t + t_a) = \max\left\{b_m, a_m\left[1 - \left(\frac{v}{v_o}\right)^{\delta} - \left(\frac{s^*}{s}\right)^2\right]\right\} \tag{24}$$

Where, $s^* = s_0 + max\left[0, vT + \frac{v\Delta v}{2\sqrt{a_m b}}\right]$

where, t_a = the perception-reaction time, b_m = the maximum deceleration, a_m = the maximum acceleration, v = the speed of the following vehicle, v_0 = the desired speed, δ = the acceleration exponent, s = the gap distance between two vehicles, s_0 = the minimum gap distance at standstill, T = the safe time headway, and b = the desired deceleration.

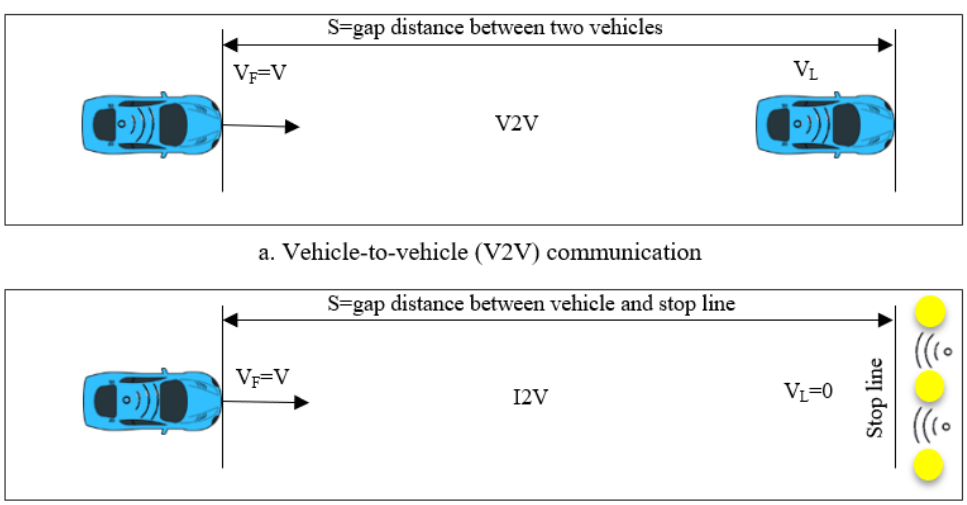

a. Vehicle-to-vehicle (V2V) communication

b. Infrastructure-to-vehicle (I2V) communication

Figure 14 Illustration of the IDM implementation on an arterial.

Figure 14(b) describes the I2V implementation of IDM model in order to assess the impact of infrastructure communication under CV environment. The real-time signal timing status are implemented through I2V communication technologies of CVs. Let's assume a vehicle is approaching a signalized intersection and the traffic lights switches from green to yellow with signal timing information conveyed to CVs through I2V communication technologies as shown in Figure 14(b). Hence, it is necessary to decide whether it is better to cruise over the intersection with unchanged speed, or to stop. Generally, this decision can be estimated by the safety criterion alone (Kesting and Treiber, 2013). The decision to stop is considered as safe if the anticipated braking deceleration will not exceed the desired deceleration at any time of the braking maneuver. In this case, traffic light is considered as a standing virtual vehicle ($V_L = 0$), speed difference between following ($V_F = v$) and leading ($V_L = 0$) vehicles, ($\Delta v = v - 0 = v$) such that s denotes the distance of the front bumpers to the stopping line. In order to decide the cruise or stop when the driver approaches a signalized intersection at his desired speed, the IDM parameters satisfy $a_m = b$ in Equation 24 and the condition become:

$$\begin{aligned} &\text{Cruise, if Where, } s < s^* = s_0 + v_0 T + \frac{v_0^2}{2b} \\ &\text{Stop, Otherwise} \end{aligned} \tag{25}$$

The parameter settings for the aforementioned IDM model were potentially determined according to previous studies (Rahman et al., 2018a; Rahman and Abdel-Aty, 2018) except for desired speed and time delay. Those previous studies had undertaken the CV impact on the freeway for which the desired speed and time delay of 120 km/h and 1.5 seconds, respectively were reasonable, while the arterial section the corresponding values were selected 72 km/h and 1.0 second, respectively based on widely accepted research (Kesting and Treiber, 2013). Therefore, the desired speed (v_0) ,

acceleration exponent (δ) , maximum acceleration (a_m), desired deceleration (b), minimum gap distance at standstill (s_0) , safe time headway (T) , maximum deceleration (b_m) , and time delay (t_a) were selected 72 km/h, 4, 1 m/sec^2, 2 m/sec^2, 2 m, 0.6 sec, 2.8 m/sec2, and 1 sec, respectively. The aforementioned car following behavior of CV was coded in C++ programming language which overrides the VISSIM default car following behavior in order to approximate the decision processes of CV. Note that the car following behavior of non-CVs was determined by VISSIM's default car following model depending on the different MPRs.

5.3.2 Driving Behavior Model for CVLLA

In this study, we have implemented lower level automation features under connected vehicle environment which is already available in many vehicles in the market with relatively lower level of penetration rate. Towards that end, this chapter have considered automated braking control and lane keeping assistance as two specific automated functions for CVLLA. Therefore, a driving behavior model is prerequisite to simulate the CVLLA which is significantly different from the normal human driving. To approximate the behavior of CVLLA, a car following model is required for the automated braking feature in the form of acceleration choice while lateral behavior model would represent the lane keeping assistance feature. However, there are very limited studies describing the decision processes of automated vehicle with calibrated parameters of car following model. In a recent study, to describe the driving behavior of automated vehicles, a dynamical car following model was developed considering mean expected velocities field using basic the Bando's car following model (Wen-Xing and Li-Dong, 2018). The parameters of the proposed car following model were calibrated along with the stability control based on the lateral driving behaviors of automated vehicle flows. Hence, this study proposes a car following model to

represent automated braking feature for CVLLA based on the recent study by Wen-Xing et al., (Wen-Xing and Li-Dong, 2018) which was developed and validated for acceleration choice of automated vehicles. Nevertheless, the lane keeping assistance feature for CVLLA was implemented by changing the lateral behavior of VISSIM default in a sense that the vehicle would be positioned in the middle of the occupying lane representing lane centering with steering assist. To be more specific, the automated braking feature would help CVLLA vehicles by maintaining the distance between the leading and following vehicles, while lane keeping assistance would provide steering assist by centering the vehicles within the lane. The aforementioned car following and lateral behavior of CVLLA was applied as Dynamic Link Library (DLL) plug-in using C++ programming interface which overrides the VISSIM default driving behavior in order to approximate the decision processes of CVLLA. However, CVLLA allows only two control functions such as automated braking and lane keeping ability so that other controls must be done by human (i.e., lane changing). Therefore, the proposed driving behavior model performed two control functions (i.e., automated braking and lane keeping assistance) of CVLLA vehicle while lane changing behavior was utilized by VISSIM default lane changing model to represent the human behavior control in the real-world.

The first feature of CVLLA was considered automated braking control which would be governed by a realistic car following model of automated vehicles. Like CV, CVLLA also has two cases of the car following model implementation on an arterial section (1) vehicle to vehicle (2) signal to vehicle. The illustration of car following model for CVLLA vehicles on an arterial section under the CV environment is presented in Figure 15. The first case Figure 15 (a) describes the V2V communication with a stream of N CVLLA vehicles. The connected vehicle part collects the status

information of each CVLLA vehicle such as the real-time position, velocity, and acceleration. Based on these information, CVLLA vehicles would use automated braking control by utilizing realistic car following model proposed by Wen-Xing et al., (Wen-Xing and Li-Dong, 2018). This car following behavior is based on the Bando's basic car following model which is given in Equation 26 in which $\ddot{x}_j(t)$ and $\dot{x}_j(t)$ denote the acceleration and velocity, respectively, of the jth vehicle at time t (M Bando, K Hasebe, a Nakayama, a Shibata, 1995).

$$\ddot{x}_j(t) = \alpha[V\left(\Delta x_j(t)\right) - \dot{x}_j(t)] \tag{26}$$

Where, α representing the drivers sensitivity. $\Delta x_j(t) = x_{j+1}(t) - x_j(t)$ denotes the headway between j^{th} vehicle and $(j+1)^{th}$ vehicle [see Figure 15(a)]. $V\left(\Delta x_j(t)\right)$ is the optimal velocity function of the jth vehicle which is given in Equation 27 based on the previous literature (Helbing and Tilch, 1998; Zhu and Zhang, 2014).

$$V\left(\Delta x_j(t)\right) = \frac{v_{max}}{2}[\tanh\left(0.13\left(\Delta x_j(t) - L_j\right)\right) - 1.57 + \tanh(0.13L_j + 1.57)] \tag{27}$$

Where, v_{max} represents the maximum velocity and L_j denotes the length of the jth vehicle.

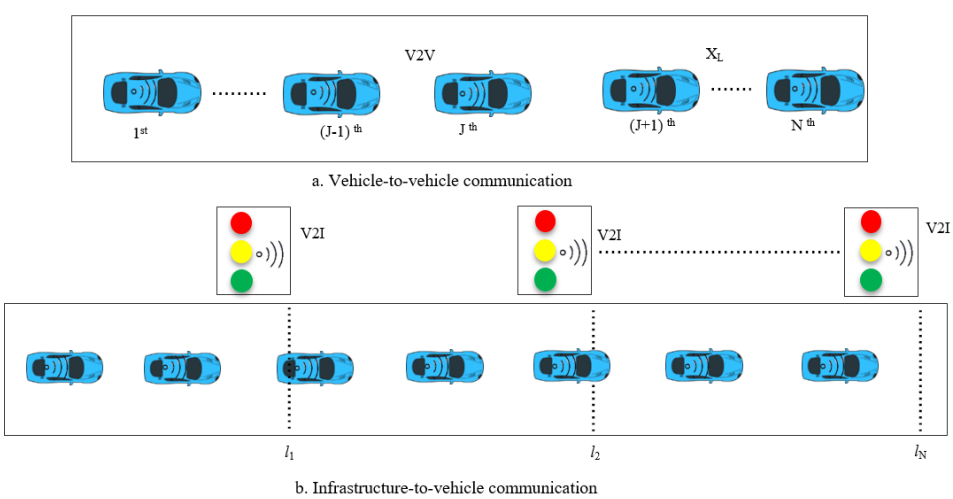

Figure 15 Illustration of the CVLLA implementation on an arterial section.

It is worth noting that Bando's basic model is widely accepted car following model to represent the human driving behavior. Nevertheless, CVLLA are equipped with V2V communication so that real-time position, velocity, and acceleration can be timely collected. Therefore, the CVLLA vehicles move forward according to the forward traffic states. Based on Bando's model, Wen-Xing et al., (Wen-Xing and Li-Dong, 2018) proposed a new car following model which added an extra term in Bando's model to replicate the automated car following behavior but did not focus on lane changing behavior. The proposed car following model is shown in Equation 28 and 29.

$$\ddot{x}_j(t) = \alpha[V\left(\Delta x_j(t)\right) + \beta\Delta V(\Delta x_j(t)) - \dot{x}_j(t)] \tag{28}$$

$$\Delta V(\Delta x_j(t)) = V\left(\Delta x_{j+1}(t)\right) - V\left(\Delta x_j(t)\right)] \tag{29}$$

The extra added term in Bando's model $\beta\Delta V(\Delta x_j\ (t))$ was used to model the automated behavior in which β is a constant named strength factor. The strength factor should be less than 0.5 which make sure that the optimal velocity $V(\Delta x_j\ (t))$ plays the dominant role in the base car following model. This proposed model can infer that if the leading vehicle's optimal velocity is greater than the following (i.e. $\Delta V\ (\Delta x_j(t)) > 0$) then the following vehicle will move with a higher velocity. If the leading vehicle's optimal velocity is less than the following vehicle (i.e. $\Delta V\ (\Delta x_j(t)) < 0$) then the following vehicle will move with a lower velocity. If the leading vehicle's optimal velocity equals to the following vehicle i.e. $\Delta V\ (\Delta x_j(t)) = 0$ then the following vehicle will move with same velocity (Wen-Xing and Li-Dong, 2018).

The proposed car following behavior of CVLLA vehicles mentioned above is accurate for freeway traffic because of the absence of signals. However, CVLLA vehicles follow exactly the same car following model in Equations 9 and10 when the signal is green on an arterial section. In contrast,

when the signal becomes red, the nearest moving vehicle to the stop line would stop at the stop line. Therefore, CVLLA vehicle near the stop line in a red phase does not satisfy the car following model described Equations 9 and 10. This behavior is also modeled from the basic Bando's car following model (Zhu and Zhang, 2014). The latter case in Figure 15 (b) describes the vehicle to signal with a stream of n CVLLA vehicles having N signals under I2V communications. The CVLLA vehicle can collect the signal status with signal timing information's using I2V communications. The car following behavior of the nearest CVLLA vehicle approaching the red signal is formulated as follows in Equation 11 in which $\ddot{x}_j(t)$ and $\dot{x}_j(t)$ denote the acceleration and velocity of the ith vehicle at time t. In contrast with Equation 9, there is no extra term in Equation 30 as there is only one vehicle which is supposed to be stop near the stop line in red signal phase.

$$\ddot{x}_i(t) = \alpha[V\big(l_n - x_{i,n}(t)\big) - \dot{x}_{i,n}(t)] \tag{30}$$

Where, α representing the drivers' sensitivity as mentioned above. $\dot{x}_{i,n}(t)$ is the position of *i*th vehicle and l_n is the position of the nth signal at the nth stop line. $V\big(l_n - x_{i,n}(t)\big)$ is the optimal velocity function of the ith vehicle and the idea is that the *i*th vehicle moving with an expected velocity closes to the Nth stop line and finally stops at the stop line which is given in Equation 31 (Zhu and Zhang, 2014).

$$V\left(l_n - x_{i_{i,n}}(t)\right) = \frac{v_{max}}{2}\left[\tanh\left(0.13\left(l_n - x_{i,n}(t) - L_i\right)\right) - 1.57 + \tanh(0.13L_i + 1.57)\right] \tag{31}$$

Where, v_{max} represents the maximum velocity and L_i denotes the length of the *i*th vehicle. The parameters of the α and β are considered 2 and 0.4, respectively based on the stability of the proposed car following model for automated vehicles (Wen-Xing and Li-Dong, 2018).

The second feature of CVLLA was considered lane keeping assistance which would be governed by a lateral behavior model in VISSIM. There are three lateral position for addressing the lateral behavior in VISSIM-0: at the right lane edge, 0.5: middle of the lane, and 1: at the left lane edge (VISSIM, 2017). However, there are four lateral position options in PTV VISSIM which defines the desired lateral position of a vehicle within the lane. The options are: "Left of lane", Middle of lane, Right of lane, and Any. The options "Any" means that the vehicle can occupy either middle of lane or left of lane or right of lane. In the base scenario, the authors selected the "Any" option as default lateral driving behavior model in VISSIM to replicate the behavior of conventional vehicle. The default lateral behavior model in VISSIM was considered to keep the vehicles at any of those three cases which represent the lateral driving behavior of conventional vehicles in the real-world. It is worth mentioning that the "Any" options would approximate the lateral driving behaviors in the real-world as the conventional vehicles do not have the lane centering assists so that the vehicle would not be positioned middle of the lane all the time. However, to approximate the behavior of CVLLA, a car following model is required for the automated braking feature in the form of acceleration choice while lateral behavior model would represent the lane keeping assistance feature. Toward that end, for the lateral driving behavior of CVLLA, we coded lateral position to be equal to 0.5 (middle of lane) which means that the vehicle would be positioned in the middle of the occupying lane representing lane centering with steering assist. To be more specific, the lateral behavior of VISSIM for conventional vehicles ensure that the vehicle would occupy in any of the occupying lane but not only the middle of the lane all the time, while CVLLA ensures that the vehicle will occupy always the middle of the lane representing lane keeping assistance. The above logic of this lateral behavior model was coded in C++ programming language which overrides the VISSIM default lateral driving behavior model in order to

approximate the behavior lane centering along with the car following model within CVLLA. Therefore, two features such as automated braking and lane keeping assistance are implemented within CVLLA vehicle to approximate the lower level automated vehicle behavior under connected vehicle environment.

In a nutshell, several car following models have been introduced to capture the human drivers' longitudinal driving behavior such as Wiedemann model, Intelligent Driver Model, Gazis-Herman-Rothery model, Gipps model etc. Nevertheless, the car following models are prerequisite for any traffic simulation software. It is worth mentioning that the commercially available software's are using previously developed car following models. For example, VISSIM and AIMSUN are using Wiedemann and Gipps car following models, respectively in order to regulate the traffic in the simulation. Most of the car-following models have their own set of parameters. However, the parameters of the car following models for CV and CVLLA vehicles were not calibrated because of unavailability of those vehicles in the corresponding studied section. It is unfortunate that the availability of connected and automated vehicles might not be accomplished in the immediate future. Nevertheless, some deployment of CV's has been carried out in very limited segments and the parameters of the car following models were calibrated based on the available connected and automated vehicle in some studies (Kesting et al., 2010b; Li et al., 2017a, 2017b; Milanés and Shladover, 2014). This study adopted these parameters in the corresponding car following model such as IDM (Kesting et al., 2010b; Li et al., 2017a, 2017b; Milanés and Shladover, 2014) and modified Bando's (Wen-Xing and Li-Dong, 2018) in order to test the effectiveness of CV and CVLLA in the studied arterial segments.

5.4 Surrogate Measures of Safety

Surrogate safety measures are a widely used technique to assess the crash risk of a road network because crashes are rare events. Nevertheless, microsimulation software is modeled with crash free car following algorithm. Therefore, surrogate measures of safety can be used to evaluate the crash risk from the VISSIM vehicle trajectory data. This study divided two major parts of the road network to evaluate the surrogate measures of safety to identify the crash risk on an arterial section: (1) segments' crash risk and (2) intersections' crash risk.

5.4.1 Segment Crash Risk

Two types of surrogate measures of safety indicators are used in measuring the segment crash risk in the studied sections. The first type represents the time proximity-based indicator (i.e., time-to-collision, post encroachment time). The second type represents evasive action–based indicators (i.e., yaw rate and jerk). In our study, four-time proximity-based surrogate measures of safety were used to estimate the segment crash risk for both CV and CVLLA technologies. Time-to-Collison (TTC) is the most commonly used time proximity-based surrogate measure of safety in the burgeoning traffic safety literature. The TTC is the time required for a collision to occur between the leading and following vehicles if the speed difference is unchanged (Hayward, 1972). To be more specific, the TTC represents the time required for two successive vehicles, occupying the same lane, to collide if they continue at their present speed when the following vehicle (n) moves faster than the leading vehicle (n-1). The TTC notion can be expressed as in equation 32:

$$TTC_n(t) = \begin{cases} \dfrac{x_{n-1}(t) - x_n(t) - L_{n-1}}{v_n(t) - v_{n-1}(t)}, & if\ v_n(t) > v_{n-1}(t) \\ \infty, & if\ v_n(t) \leq v_{n-1}(t) \end{cases} \tag{32}$$

where $TTC_n(t)$ = the TTC value of following vehicle *n* at time *t*, x = the positions of vehicles, v=

the velocities of vehicles, L_{n-1}= Length of leading vehicle.

Furthermore, two distinct types of TTC are usually considered in traffic safety analysis: TTC1 and TTC2. TTC1 assumes that the preceding vehicle maintains its speed, while TTC2 describes situations when the preceding vehicle stops suddenly, which is also called TTC at braking (Peng et al., 2017). For the segment crash risk analysis, traffic data were collected at eighteen detectors in the mid segments among the intersections in the VISSIM network, and few small TTC1 values were observed during the simulation. Thus, TTC at braking (TTC2) is employed in this study to evaluate traffic safety for segment crash risk from VISSIM data collection points. The definition of the TTC at braking (TTC_{brake}) is as follows (Peng et al., 2017):

$$TTC_{brake}(t) = \frac{x_{n-1}(t) - x_n(t) - L_{n-1}}{v_n(t)} \tag{33}$$

The smaller TTC_{brake} value indicates the lager risk at a certain time instant. Two surrogate safety measures, derived from TTC, denoted as Time Exposed Time-to-Collision (TET) and Time Integrated Time-to-Collision (TIT), are utilized to evaluate the effect of both CV and CVLLA technologies. The TET refers to the total time spent under dangerous traffic conditions, determined by TTC value below the threshold value of TTC (TTC^*)(Minderhoud and Bovy, 2001).

$$TET\ (t) = \sum_{n=1}^{N} \delta_t \times \Delta t, \quad \delta_t = \begin{cases} 1, & 0 < TTC_{brake}\ (t) \leq TTC^* \\ 0, & otherwise \end{cases} \tag{34}$$

$$TET = \sum_{t=1}^{Time} TET(t) \tag{35}$$

where t = the time ID, n = the vehicle ID, N = the total number of vehicles, δ = the switching variable, Δt = the time step, which was 0.1 s in simulation, Time = the simulation period, and TTC^*

= the threshold of TTC. The TTC* is used to differentiate the unsafe car following conditions from the ones that are considered safe.

The TIT is referred to as the entity of the TTC lower than the TTC threshold. The reciprocal transformation was made considering that a lower TTC means a higher collision risk:

$$TIT(t) = \sum_{n=1}^{N} \left[\frac{1}{TTC_{brake}(t)} - \frac{1}{TTC^*}\right] . \Delta t, 0 < TTC_{brake}(t) \leq TTC^* \tag{36}$$

$$TIT = \sum_{t=1}^{Time} TIT(t) \tag{37}$$

The third time proximity-based surrogate measure of safety utilized for the segment crash risk, derived from the rear-end crash risk index (RCRI), is Time Exposed Rear-end Crash Risk Index (TERCRI) which was proposed by first author (M. S. Rahman et al., 2019d; Rahman et al., 2018b; Rahman and Abdel-Aty, 2018). A rear-end crash can happen if the leading vehicle stops suddenly while the following vehicle does not decelerate timely to avoid a collision. So, the principal cause of a rear end crash is maintaining insufficient stopping distance between the leading and the following vehicles. To avoid rear-end crashes, the stopping distance of the following vehicle should be smaller than the leading vehicle. Oh et al., (Oh et al., 2006) proposed rear-end crash risk index (RCRI) in which the dangerous condition can be mathematically expressed as follows:

$$SD_F > SD_L \tag{38}$$

$$SD_L = v_L \times h + \frac{v_L^2}{2 \times a_L} + l_L \tag{39}$$

$$SD_F = v_F \times PRT + \frac{v_F^2}{2 \times a_F} \tag{40}$$

Where SD_L and SD_F are the stopping distance of the leading and the following vehicles, respectively. l_L the length of the leading vehicle, v_L the speed of the leading vehicle, v_F the speed of the following vehicle, PRT is the perception-reaction time, h the time headway, a_L the deceleration rate of the leading vehicle. and a_F is the deceleration rate of the following vehicle. As mentioned earlier, we used two types of vehicles PC and HGV in VISSIM simulation. Therefore, different maximum deceleration rate of PC and HGV were selected to estimate the reliable safety distance of leading and following vehicles using Equations 39 and 40. The deceleration rates of PC and HGV were selected as 3.42 m/s^2 and 2.42 m/s^2, respectively, while the PRT was used as 1.5 s, these values are generally accepted by AASHTO (American Association of State Highway and Transportation Officials (AASHTO), 2004).The proposed TERCRI was governed by the following equations:

$$TERCRI\ (t) = \sum_{n=1}^{N} RCRI_n(t) \times \Delta t, \quad RCRI_n\ (t) = \begin{cases} 1, & SDF_F > SD_L \\ 0, & Otherwise \end{cases} \tag{41}$$

$$TERCRI = \sum_{t=1}^{Time} TERCRI(t) \tag{42}$$

Therefore, the TERCRI refers to the total time spent under rear-end crash risk, determined by stopping distance of the leading and the following vehicles.

Additionally, lane changing crashes are among the most common type of crashes in multilane arterials. The fourth and final time proximity based surrogate measures for segment crash risk considered in our study is lane changing conflicts (LCC). The Surrogate Safety Assessment Model (SSAM), developed by the Federal Highway Administration, was applied to analyze the LCC which can be related to the surrogate measures of the lane changing or angle or sideswipe crashes. The experimental VISSIM model generated several groups of traffic trajectory data files. The

vehicle conflicts' data were stored in these trajectory data files which contains the conflict locations' coordinates, conflict time, time-to-conflict, post-encroachment-time etc. Hence, the SSAM was applied to analyze these conflict data in order to compare the LCC among the three scenarios.

This study also considered the evasive action-based indicator in our study. Several studies have shown the usefulness of evasive action-based indicators in measuring the severity of conflicts (Tageldin et al., 2015; Tageldin and Sayed, 2016; Zaki et al., 2014). Several traffic conflict indicators based on detecting evasive actions such as deceleration, jerk, and yaw-rate are recommended to better measure traffic conflicts in less organized traffic environments (China) with a high mix of road user (Guo et al., 2018; Tageldin et al., 2015). This chapter also considered jerk as evasive action-based indicator to calculate the safety critical driving behavior in order to compare the three scenarios. Jerk represents the derivative of the acceleration. It is used for braking behavior that varies as a reaction to the environment. The evasive action involving powerful braking or sudden acceleration can be reflected in the jerk profile. The acceleration is the derivative of speed, which can be calculated by Equation 43. The jerk can be calculated using Equation 44, as follows:

$$A(t) = \dot{V}_t = (\ddot{x}_t, \ddot{y}_t) \tag{43}$$

$$\text{Jerk (t)} = \dot{A}_t \tag{44}$$

Where, $A(t)$ is the acceleration of vehicle at instant t; (x_t, y_t) is the position of vehicle at instant t; and Jerk (t) is the jerk of vehicle at instant t.

Bagdadi and Várhelyi (Bagdadi and Várhelyi, 2011) argue that jerks may be a better way of relating

acceleration behavior to crashes. In their study, a regression model was developed using the sample of 166 drivers with 33 crash-involved in order to test the relationship between the number of critical or dangerous jerks (defined as critical jerks that are equal to or below than -9.9 m/s^3) and self-reported crashes. The regression results showed that the number of accidents increased by 1.13 times for each additional critical jerk over a three-year period. Hence, jerkiness in driving may be an indication of a riskier driving style and a higher probability of accident involvement. In our study, I collected the trajectory data containing acceleration values for all vehicles from Fritzing Part File (.FZP) in VISSIM. Therefore, this study calculated the number of critical jerk (NCJ) from the Fritzing Part File for each of three scenarios. A threshold level of -9.9 m/s^3 is used for the jerks as an indicator of safety-critical driving behavior based on previous studies (Bagdadi and Várhelyi, 2011; Nygård, 1999). This study calculated the NCJ from all jerk values that are equal to or below the threshold value of -9.9 m/s^3.

5.4.2 Intersection Crash Risk

One of the most dominant type of crashes on an arterial section is intersections' crash. However, rear-end crash is the most prevalent type of crash in a segment. Angle and sideswipe crash along with rear-end crashes are common at intersections. Therefore, it is necessary to evaluate the segment and intersection crash risks separately for CV and CVLLA technologies. The surrogate measure of intersection crashes can be obtained using Surrogate Safety Assessment Model (SSAM) developed by the Federal Highway Administration. SSAM conflict analysis can offer rational conflict estimations of signalized intersections which can be considered as surrogate measure of intersection crash risk. SSAM uses several parameters to measure the conflicts and describe the conflict locations, and characteristics. The main conflict measure parameters

considered in SSAM are Time-to-collision (TTC), Post encroachment time (PET), Maximum speed (MaxS), Speed difference (DeltaS), the second vehicle's initial deceleration rate (DR), the second vehicle's maximum deceleration (MaxD), and the maximum speed difference value among the two-crashed vehicle (MaxDeltaV) (see Gettman et al., (Gettman et al., 2008)for detailed review). A conflict is recorded in SSAM when the minimum TTC and PET values exceed the predetermined threshold values, and the conflict type associated with each conflict is identified according to the lane and link information or the angle between the two converging vehicles (Fan et al., 2013). This study uses the default maximum TTC threshold and PET threshold value 1.50 and 5.00 seconds, respectively, in order to calculate the conflicts from the VISSIM trajectory file. To identify the potential conflicts at intersections, the influence area of the intersection was defined as within 250 ft. along any leg of the intersection from the center of the intersection. From recognition of this chosen value, in several studies conducted in the state of Florida (Abdel-Aty and Wang, 2006a, 2006b; Wang et al., 2018; Wang and Abdel-Aty, 2006; Yuan et al., 2019b, 2018a, 2018b; Yuan and Mohamed Abdel-Aty, 2018), the default value of 250 ft. was used to identify the intersection related crashes. Hence, the nine studied intersections in our VISSIM network were analyzed to compare the effectiveness CV and CVLLA technologies of each MPR over non-CV scenarios. Furthermore, binary logistic regression was employed to evaluate the intersection crash risk since the dependent variable Y can only take on two values: Y = 1 for conflicts, and Y = 0 for non-conflicts. The probability that a conflict will occur in the studied intersections is modeled as logistic distribution in Equation 45 for three scenarios with different MPRs.

$$\pi(x) = \frac{e^{g(x)}}{1 + e^{g(x)}} \tag{45}$$

The logit of the multiple logistic regression model (Link Function) is given by Equation 46.

$$g(x) = \ln\left[\frac{\pi(x)}{1-\pi(x)}\right] = \beta_0 + \beta_1 x_1 + \beta_2 x_2 + \ \ldots\ldots\ldots\ldots\ \beta_{nx_n} \tag{46}$$

where π(x) is conditional probability of conflicts (surrogate measure of crashes), which is equal to the number of conflicts divided by the total number of observations (sum of conflicts and non-conflicts). x_n are independent variables (scenarios with different MPR: base, CV, and CVLLA). β_n are model coefficients, which directly determines odds ratio involved in the number of conflicts. The odds of an event are defined as the probability of the outcome event (conflicts) occurring divided by the probability of the event not occurring (non-conflicts). The odds ratio that is equal to $exp(\beta_n)$ tells the relative amount by which the odds of the outcome increase (OR greater than 1.0) or decrease (OR less than 1.0) when the value of the predictor value is increased by 1.0 unit (quantitative variables) or one category (categorical variables) compared to the base category (Yan et al., 2005).

5.5 Results and Discussion

As mentioned earlier, the CV and CVLLA technologies were applied on an urban arterial section to evaluate the segment and intersection crash risks separately.

5.5.1 Segment Crash Risk

To evaluate the safety performance of segment crash risk for both CV and CVLLA technologies on an arterial section, five surrogate measures of safety were considered: TET, TIT, and TERCRI, LCC, and NCJ. To have a better understanding, I implemented CV and CVLLA with varying market penetration rates and then the two technologies were compared with the base scenario (non-CV scenario) in order to observe the segment crash risks of those technologies. Each scenario (base

scenario, CV, CVLLA) was repeatedly simulated for 30 times with MPRs of 30%, 40%, 60%, 80%, and 100% (CV and CVLLA) in order to consider random effects of simulation. To calculate the TET and TIT from VISSIM data collection points utilizing the segments of the network, TTC threshold was considered 2 seconds for the preliminary analysis and then a sensitivity analysis is conducted for different TTC thresholds from 1 to 3 seconds. In SSAM, the potential lane changing conflicts (LCC) are considered if the TTC and the PET values are lower than 1.5 sec and 5.0 sec, respectively (Gettman et al., 2008). The descriptive statistics of TET, TIT, TERCRI, LCC, and NCJ in three scenarios (Base, CV, and CVLLA) are presented in Table 10 with 5 selected MPRs (30%, 40%, 60%, 80%, and 100%) for CV and CVLLA technologies. The results of the table showed that, non-CV scenario has the largest mean value of each TET (1755.97), TIT (443.10), TERCRI (388.83), LCC (519), and NCJ (804) while the lower TET, TIT, TERCRI, LCC, and NCJ were obtained in CV and CVLLA compared to the base scenario for each MPRs. For each MPR, CVLLA has lower segment crash risk compared to CV in terms of TET, TIT, TERCRI, LCC, and NCJ. Looking at the 40% MPR, the mean values of the five surrogate indicators of CVLLA scenario were lower with TET (1685.77), TIT (398.83), TERCRI (371.34), LCC (484), and NCJ (767), respectively, compared to CV scenario of TET (1703.33), TIT (407.70), TERCRI (376.39), LCC (493), and NCJ (781), respectively. Therefore, the scenario with CVLLA for each MPRs has the lowest segment crash risks compared to CV scenario, while the scenario with base condition (non-CV) has the highest segment crash risks.

Table 10 Summary Statistics of TET, TIT, TERCRI, LCC, and NCJ with Different MPRs

Scenario	MPR	SSM	TET (s)	TIT (s)	TERCRI (s)	LCC (#)	NCJ (#)
Base	0%	Mean	1755.97	443.1	388.83	519	804
		Std deviation	47.09	27.23	9.22	52.49	23.14
		Minimum	1651	406	370	433	769
		Maximum	1842	513	405	618	889
CV	30%	Mean	1720.83	425.43	386.5	499	790
		Std deviation	46.08	26.12	9.17	52.63	22.96
		Minimum	1618	390	368	413	757
		Maximum	1805	492	403	598	875
	40%	Mean	1703.33	407.7	376.39	493	781
		Std deviation	45.71	25.06	9.39	52.49	23.49
		Minimum	1601	374	359	407	746
		Maximum	1787	472	393	592	868
	60 %	Mean	1650.6	385.43	361.67	485	762
		Std deviation	44.15	23.67	8.59	52.93	23.45
		Minimum	1552	353	344	399	720
		Maximum	1731	446	377	548	847
	80 %	Mean	1562.8	367.6	342.2	473	729
		Std deviation	41.98	22.67	8.1	52.47	22.72
		Minimum	1469	337	326	387	699
		Maximum	1639	426	356	572	814
	100 %	Mean	1457.4	345.7	308.03	458	708
		Std deviation	39.09	21.25	14.91	52.49	23.14
		Minimum	1370	317	251	372	673
		Maximum	1529	400	324	557	793
CVLLA	30%	Mean	1712.07	420.9	384.56	491	779
		Std deviation	45.88	25.78	9.12	53.37	22.87
		Minimum	1610	386	366	401	744
		Maximum	1796	487	401	590	862
	40%	Mean	1685.77	398.83	371.34	484	767
		Std deviation	45.21	24.58	8.81	52.48	22.95
		Minimum	1585	365	353	398	734
		Maximum	1768	462	387	583	852
	60 %	Mean	1606.7	367.6	342.2	464	726
		Std deviation	43.01	22.67	8.1	52.48	22.87
		Minimum	1511	337	326	378	691
		Maximum	1685	426	356	563	809
	80 %	Mean	1492.7	341.23	311.1	435	676
		Std deviation	40.16	20.95	7.41	52.49	23.60
		Minimum	1403	313	296	349	641
		Maximum	1566	395	324	534	761
	100 %	Mean	1369.6	314.6	263.67	407	622
		Std deviation	36.85	19.37	13.12	52.48	23.15
		Minimum	1288	288	248	321	584
		Maximum	1437	364	316	506	707

This study applies Analysis of Variance (ANOVA) to compare the differences between several

group means and their associated variations, which provides a statistical test of comparing means of more than two groups. Since conducting multiple two-sample t-tests is not convenient and would result in an increased chance of errors (Peng et al., 2017), ANOVA is applied to analyze the five surrogate measures of safety under three driving scenarios (Base, CV, and CVLLA) with different MPRs of CV and CVLLA. Table 11 shows the results of one-way ANOVA test for comparing five surrogate measures of safety between the base and CV scenarios. In summary, the results of Table 11 illustrate the significant reduction of the five surrogate measures of safety, (i.e., TET, TIT, TERCRI, LCC, and NCJ) with the implementation of CV and CVLLA technologies. Compared to the base scenario, the TET, TIT, TERCRI, LCC, and NCJ decreased significantly in both CV and CVLLA technologies. Model performances were evaluated for three different condition sets (Base, CV and CVLLA) and CV scenarios each under five different MPRs (30%, 40%, 60%, 80%, and 100%). To find out the segment crash risks of the applied technologies, the mean values of the surrogate safety measures were compared with the base condition. The results revealed that the applied CV technologies enhanced traffic safety by decreasing the surrogate measures of safety for segment crash risks on an arterial section. The maximum significant safety improvement of arterial segment was found at 100 % MPR, while the improvement below 30% MPRs was insignificant for TET, TIT, and NCJ value at 5% level of significance. For TERCRI and LCC, the minimum significant reduction was found equal to or more than 40% MPR. For each of the 15 scenarios listed in Table 11, the mean differences of TET, TIT, TERCRI, LCC, and NCJ were higher for CV compared to CVLLA. It was also found that the CVLLA achieved significant reductions in TET, TIT, TERCRI, LCC, and NCJ compared to CV when the MPRs were equal or greater than 60%. Thereby, CVLLA clearly outperformed CV in terms of segment crash risks on the arterial section.

Table 11 Comparisons of Measure of Effectiveness by Conducting One-way ANOVA

MPR	Comparisons	Surrogate Safety Measures														
		Time Proximity-Based												Evasive Action-Based		
		TET (s)			TIT (s)			TERCRI (s)			LCC (#)			NCJ (#)		
		Mean difference	95% Confidence Interval		Mean difference	95% Confidence Interval		Mean difference	95% Confidence Interval		Mean difference	95% Confidence Interval		Mean difference	95% Confidence Interval	
30%	Base-CV	35.1	5.9	64.3	17.6	1.0	34.2	2.3#	-3.4	8.1	20.0*	-13.0	53.0	14.0*	-1.0	28.0
	Base-CVLLA	43.9	14.7	73.1	22.2	5.5	38.8	4.2#	-1.5	10.1	28.0*	-5.3	61.2	25.0	10.0	39.0
	CV-CVLLA	8.8#	-20.5	37.9	4.5#	-12.1	21.1	1.9#	-7.7	3.8	8.0*	-25.0	41.0	11.0*	-3.0	25.0
40%	Base-CV	52.6	23.6	81.6	35.4	19.2	51.5	12.4	6.6	18.2	26.0*	-7.0	59.0	23.0	8.0	38.0
	Base-CVLLA	70.2	41.2	99.2	44.2	28.1	60.4	17.5	11.7	23.2	35.0	2.0	68.0	37.0	22.0	52.0
	CV-CVLLA	17.6#	-11.4	46.5	8.8#	-7.3	25.0	5.0#	-0.7	10.8	9.0*	-24.0	42.0	14.0*	-1.0	29.0
60 %	Base-CV	105.3	77.1	133.5	57.6	42.2	73.1	27.1	21.7	32.6	34.0	1.0	67.0	42.0	27.0	56.0
	Base-CVLLA	149.2	121.0	177.4	75.5	59.9	91.0	46.6	41.1	52.0	55.0	22.0	88.0	78.0	63.0	92.0
	CV-CVLLA	43.9	15.7	72.1	17.8	2.3	33.3	19.4	14.0	24.9	21.0*	-12.0	54.0	36.0	21.0	51.0
80 %	Base-CV	193.2	165.9	220.3	75.5	60.5	90.4	46.6	41.4	51.8	46.0	13.0	79.0	75.0	60.0	90.0
	Base-CVLLA	263.3	236.1	290.4	101.8	86.8	116.8	77.7	72.5	82.9	84.0	51.0	117.0	128.0	113.0	143.0
	CV-CVLLA	70.1	42.9	97.3	26.3	11.3	41.3	31.1	25.8	36.3	38.0	5.0	71.0	53.0	38.0	68.0
100 %	Base-CV	298.5	272.6	324.5	97.4	82.9	111.8	80.8	72.8	88.7	61.0	28.0	94.0	96.0	81.0	111.0
	Base-CVLLA	386.3	360.4	412.3	128.5	114.1	142.9	125.1	117.2	133.1	112.0	79.0	145.0	182.0	167.0	197.0
	CV-CVLLA	87.8	61.8	113.8	31.1	16.6	45.5	44.3	36.4	52.3	51.0	18.0	84.0	86.0	71.0	101.0

#Difference is insignificant at 5% level

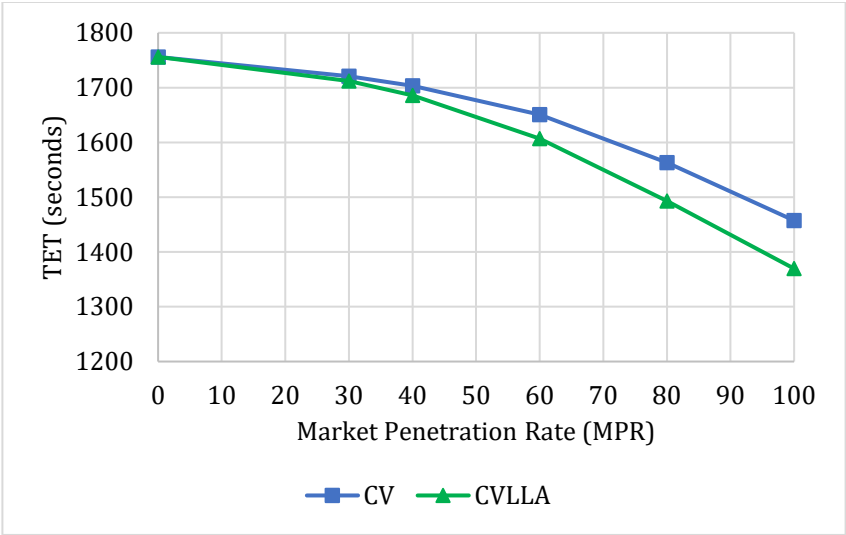

(a) TET

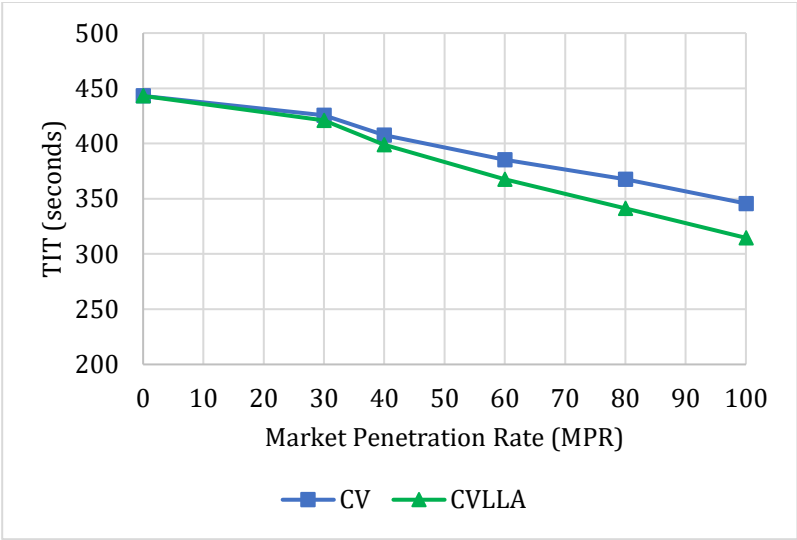

(a) TIT

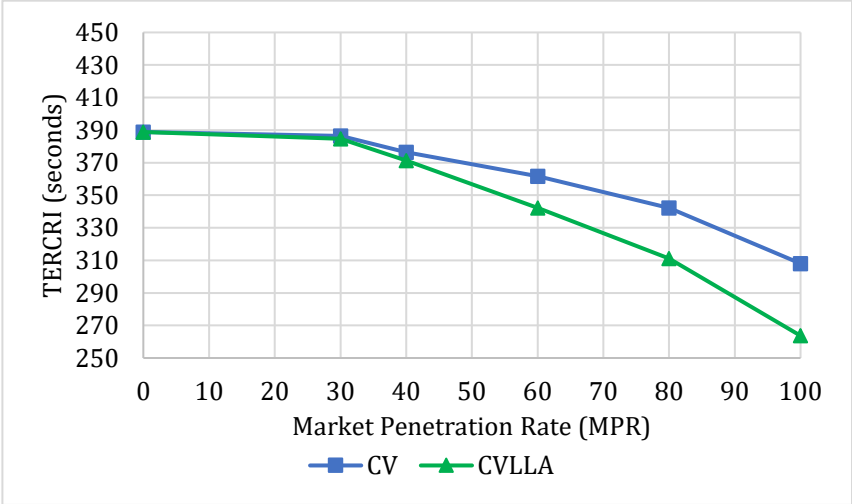

(c) TERCRI

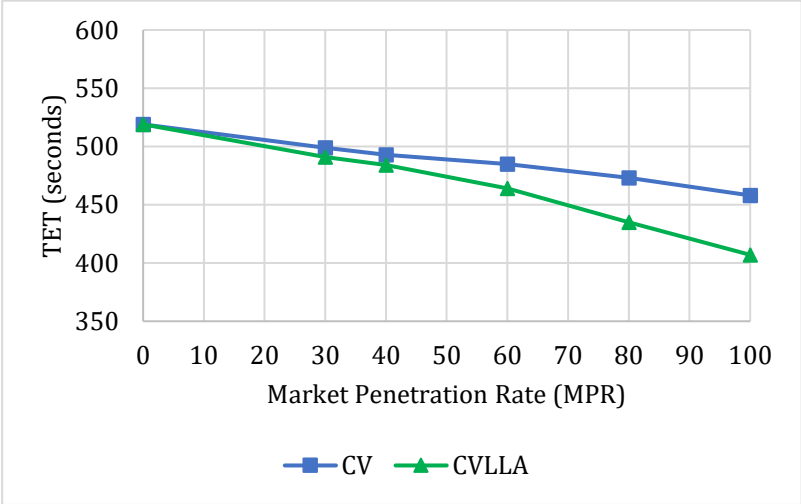

(c) LCC

Figure 16 Reduction of surrogate measures of safety with different MPRs.

Figure 16 shows the decreasing trend of TET, TIT, TERCRI, and LCC for CV and CVLLA scenarios with increasing MPRs. As seen from the figures, the higher the percentage of the CV and CVLLA implemented, the lower were the TET, TIT, TERCRI, and LCC therefore the higher were the safety benefits achieved. Moreover, the TET, TIT, TERCRI, and LCC were lowest in the CVLLA scenario compared to the CV scenario for each MPR.

In the aforementioned results, this study have selected 2 seconds as the TTC threshold in order to test the statistical significance of TET and TIT values between the base and CV scenarios with different market penetration rate based on the previous research (Li et al., 2017a, 2017b, 2016b, 2014; Rahman and Abdel-Aty, 2018). However, the validation of the TTC threshold is not undertaken in the safety literature. Therefore, a sensitivity analysis of how the safety comparison between base and CV scenarios vary with a range of TTC threshold value was conducted. Sensitivity analysis of TTC threshold is worthwhile as different researchers used different values of TTC thresholds ranging from 1 to 3 seconds. Towards that end, I calculated TET and TIT values based on different TTC thresholds ranging from 1 to 3 seconds. The different values TTC thresholds provide similar results of segment crash risks in the studied urban arterial section. Table 12 shows the similar results of segment crash risks considering five different values of TTC thresholds ranging from 1 to 3 seconds at 100% MPR of CV and CVLLA. For different values of TTC thresholds, all TET (TIT) values were decreased within 16% to 19% (20% to 23%) for CV technologies compared to base scenario, while TET (TIT) values are all reduced within 21% to 23% (27% to 29%) of CVLLA compared with that of base condition. For example, at TTC value of 2.5 seconds, TIT value of base scenario is 661.07 while the CV scenario is 509.02 which is 23% less than the base scenario. And, for the TTC value of 3 seconds, TIT values of both base and CV

scenarios are 844.07 and 661.49, respectively. Therefore, the CV scenario is 22% lesser than the base scenario which showed almost similar result using TTC threshold 2.5 seconds. So, the TET and TIT values of the corresponding CV and CVLLA scenarios are compared with the base scenario for each TTC threshold of 1.0, 1.5, 2.0, 2.5, and 3.0 seconds and obtained almost similar results.

Table 12 Sensitivity Analysis of Different Values of TTC Threshold for 100% MPR

TTC* (s)	Scenarios	Base condition		CV		CVLLA	
	Measures	TET	TIT	TET	TIT	TET	TIT
1.0	Average	159.73	141.20	130.97	112.96	122.99	103.08
	% of change	-	-	18%	20%	23%	27%
1.5	Average	688.06	245.43	577.97	191.43	543.57	179.16
	% of change	-	-	16%	22%	21%	27%
2.0	Average	1755.97	443.10	1457.40	345.70	1369.60	314.60
	% of change	-	-	17%	22%	22%	29%
2.5	Average	2584.03	661.07	2170.58	509.02	2015.54	475.97
	% of change	-	-	16%	23%	22%	28%
3.0	Average	3086.47	848.07	2500.04	661.49	2438.31	619.09
	% of change	-	-	19%	22%	21%	27%

For better visual representation, Figure 17 shows the results of TET and TIT values for three scenarios including base, CV at 100% MPR, and CVLLA at 100% MPR in terms of different TTC thresholds (1 to 3 seconds). For each TTC threshold in base, 100% MPR of CV and CVLLA scenarios, TET and TIT values were lowest in the CVLLA scenario. In the CV scenario, the values of TET and TIT for every TTC threshold are smaller than the base scenario but larger than the CVLLA scenario. Therefore, irrespective of TTC thresholds, both CV approaches have higher safety benefits and CVLLA clearly outperformed CV technologies in terms of the segment's crash

risk.

In a nutshell, the deployment of CV and CVLLA have significantly decreased the TET, TIT, TERCRI, LCC, and NCJ; thereby might decrease the probability of segment crashes on an arterial segment. However, it is clearly seen that lower level automation features with CV technology significantly outperformed CV scenario with no automation.

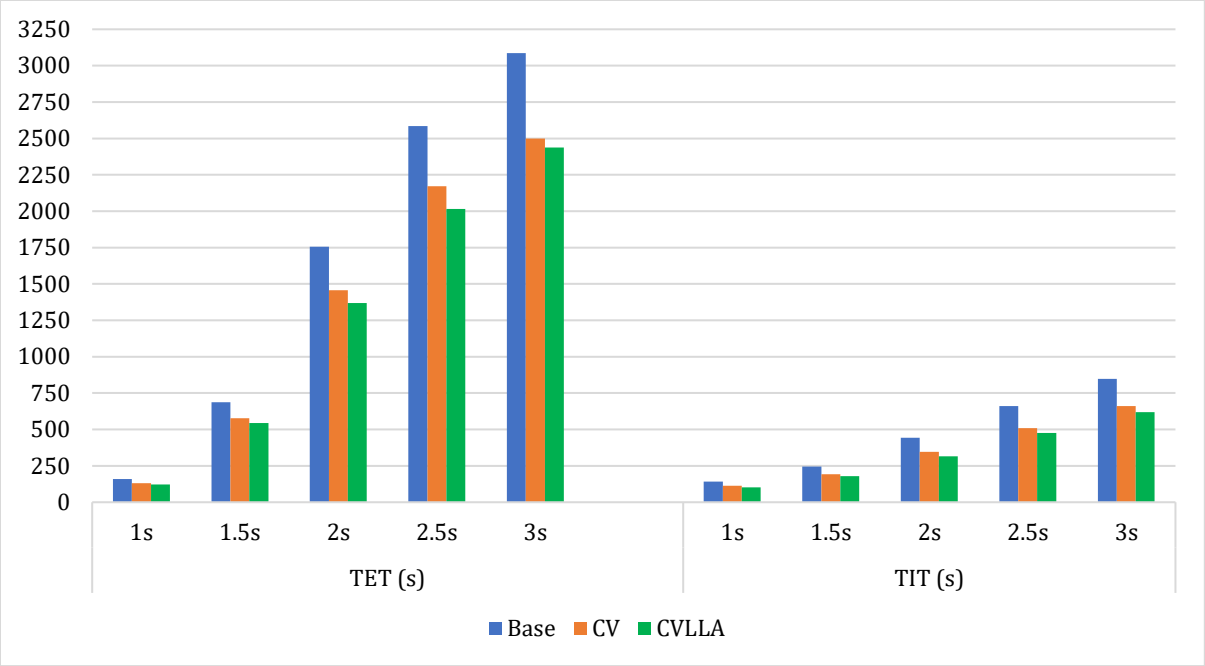

Figure 17 Sensitivity analysis of TTC thresholds.

5.5.2 Intersection Crash Risk

As indicated earlier, SSAM software was used to analyze the number of conflicts within the nine studied intersections influence area each of 250 feet for three scenarios (i.e., Base, CV, and CVLLA) with different MPRs of CV and CVLLA. The potential conflicts are considered if the TTC and the PET values are lower than 1.5 sec and 5.0 sec, respectively (Gettman et al., 2008). The descriptive statistics of total number of conflicts for the three scenarios are presented in Table 6 with 30%, 40%, 60%, 80%, and 100% MPRs of CV scenarios. From Table 13, the non-CV

scenario has the largest mean value of total number of conflicts 1702 resulting from 30 simulation runs. Lower number of conflicts were found in both CV and CVLLA scenarios compared to non-CV scenario for each MPR. Furthermore, the result clearly inferred that CVLLA has lower intersection related crash risk compared to CV in terms of total number of conflicts for each corresponding MPRs. At 100% MPR, the mean value of total number of conflicts was found to be 1125 in CVLLA scenario while total number of conflicts of CV scenario was 1302. Therefore, the scenario with CVLLA for each MPR has the lowest intersection crash risk compared to the corresponding CV scenario, while the scenario with base condition (non-CV) has the highest intersection crash risk.

Table 13 Summary Statistics of Conflicts with Different MPR

Scenario	MPR	Number of Runs	Mean	Standard Deviation	Minimum	Maximum
Base	0%	30	1702	57.71	1598	1837
CV	30%	30	1645	57.30	1491	1769
	40%	30	1584	56.31	1445	1691
	60 %	30	1532	54.23	1390	1627
	80 %	30	1488	51.30	1311	1535
	100 %	30	1302	48.77	1208	1452
CVLLA	30%	30	1621	57.28	1553	1728
	40%	30	1546	55.45	1408	1684
	60 %	30	1422	52.52	1288	1545
	80 %	30	1276	48.49	1122	1386
	100 %	30	1125	44.80	1056	1305

A logistic regression model was also developed to test the significance of binary outcome (conflict or non-conflict) variable and the different scenarios with different MPRs. There are 11 scenarios with three different condition sets (Base, CV and CVLLA) for which each CV and CVLLA has five different MPRs (30%, 40%, 60%, 80%, and 100%). Table 14 lists the model estimation results

and odds ratios of conflicts in different scenarios compared to the base scenario. The parameter estimates of all the CV scenarios (both CV and CVLLA with different MPRs) are significant at 5% significance level compared to base scenario except at 30% MPR of CV and CVLLA. The odds ratio of conflicts was also not significant at 5% significance level for the CV scenarios ($CV_{30\%}$ and $CVLLA_{30\%}$) compared to the base scenario at 30% MPR. Moreover, the odds ratios of conflicts in CVLLA scenarios compared to CV scenarios were also calculated to evaluate the effectiveness of those technologies for each MPR and the model results showed that odds ratios of conflicts in CVLLA scenarios compared to CV scenarios were significant when the MPRs is equal or greater than 60%.

Table 14 Model Estimation and Odds Ratios of Different Scenarios

Parameter	Coefficient estimate (p value)	Odds ratio (One relative to other)	Odds ratio	95% Wald confidence limit	
				Lower Limit	Upper Limit
Intercept	-2.060 (<0.001)	-	-	-	
Scenarios	-	-	-	-	
Base	Reference	-	-	-	
$CV_{30\%}$	-0.038 (0.296) #	$CV_{30\%}$ vs Base	0.962#	0.896	1.034
$CVLLA_{30\%}$	-0.055 (0.136) #	$CVLLA_{30\%}$ vs Base	0.947#	0.881	1.017
-	-	$CVLLA_{30\%}$ vs $CV_{30\%}$	0.984#	0.915	1.058
$CV_{40\%}$	-0.081 (0.029)	$CV_{40\%}$ vs Base	0.922	0.858	0.992
$CVLLA_{40\%}$	-0.108 (0.004)	$CVLLA_{40\%}$ vs Base	0.898	0.835	0.966
-	-	$CVLLA_{40\%}$ vs $CV_{40\%}$	0.973#	0.904	1.048
$CV_{60\%}$	-0.119 (0.002)	$CV_{60\%}$ vs Base	0.888	0.826	0.955
$CVLLA_{60\%}$	-0.199 (<0.001)	$CVLLA_{60\%}$ vs Base	0.819	0.761	0.882
-	-	$CVLLA_{60\%}$ vs $CV_{60\%}$	0.922	0.855	0.995
$CV_{80\%}$	-0.177 (<0.001)	$CV_{80\%}$ vs Base	0.838	0.778	0.902
$CVLLA_{80\%}$	-0.309 (<0.001)	$CVLLA_{80\%}$ vs Base	0.734	0.680	0.793
-	-	$CVLLA_{80\%}$ vs $CV_{80\%}$	0.876	0.810	0.948
$CV_{100\%}$	-0.291 (<0.001)	$CV_{100\%}$ vs Base	0.747	0.693	0.807
$CVLLA_{100\%}$	-0.450 (<0.001)	$CVLLA_{100\%}$ vs Base	0.638	0.589	0.690
-	-	$CVLLA_{100\%}$ vs $CV_{100\%}$	0.853	0.785	0.927

#Difference is insignificant at 5% level

Looking at the 100% MPR, the odds of having conflicts in CVLLA scenario is about 36% lower than the same odds of having conflicts in the base scenario, while the odds of having conflicts in CV scenario is about 25% lower than the same odds of having conflicts in the base scenario. Moreover, the odds of having conflicts in CVLLA scenario at 100% MPR is about 15% lower than the same odds of having conflicts in CV scenario at 100% MPR.

The aforementioned results of odds ratio between base and CV scenarios are obtained from considering TTC and PET thresholds of 1.5 and 5.0 seconds, respectively. However, it is possible to accept lower TTC and PET values to calculate the total number of conflicts in connected and automated vehicle technologies. Therefore, the study also considered different sets of TTC and PET values to calculate conflicts and found similar results in a sense that CVLLA scenario outperformed other two scenarios, while non-CV scenario has the highest crash risk in terms of intersection crash risk. The authors added another sensitivity analysis including different sets of TTC and PET values in order to see the effectiveness of CV and CVLLA over non-CV scenario. Table 15 shows the results of intersection crash risks considering five different sets of TTC and PET thresholds at 100% MPR of CV and CVLLA. For different values of TTC and PET thresholds, the total number of conflicts were decreased by 21% to 24% for CV technologies compared to base scenario, while total number of conflicts are all reduced by 31% to 34% of CVLLA compared with that of base condition.

Table 15 Sensitivity Analysis of Different Values of TTC and PET Threshold for 100% MPR

TTC* (s)	PET* (s)	Scenarios	Base	CV	CVLLA
		Measures	**Total Number of Conflicts**	**Total Number of Conflicts**	**Total Number of Conflicts**
0.5	1.0	Average	759	592	523
		% of change	-	22%	31%
0.8	2.0	Average	1119	884	750
		% of change	-	21%	33%
1.0	3.0	Average	1490	1148	1013
		% of change	-	23%	32%
1.2	4.0	Average	1648	1286	1087
		% of change	-	22%	34%
1.5	5.0	Average	1702	1302	1125
		% of change	-	24%	34%

Like segment crash risks, the application of both CV and CVLLA technologies improved safety significantly in terms of conflict frequency in the intersections' influence area. It is worth noting that, CVLLA technology significantly outperformed CV scenario with no automation features in terms of safety improvement of intersections.

5.6 Summary

This chapter investigated the safety impact of connected vehicles (CV) and connected vehicle lower level automation (CVLLA) utilizing both vehicle to vehicle (V2V) and infrastructure-to-vehicle (I2V) communications on an urban arterial using microsimulation. Two automated feature such as automated braking and lane keeping assistance were considered to model the lower level automated vehicle under V2V and I2V communication technologies. Safety performance of both CV technologies were tested in terms of segment and intersection crash risks using surrogate safety

assessment modeling techniques. The driving behaviors of both CV and CVLLA were applied in VISSIM through C++ programming language. Five surrogate measures of safety including the TET, TIT, TERCRI, LCC, and NCJ were considered as segment crash risks indicators, while the intersection crash risks were evaluated using Surrogate Safety Assessment Model (SSAM). The safety benefits were observed under different MPRs for both CV technologies. In general, both CV and CVLLA technologies reduce segment crash risks by providing significant reductions of TET, TIT, and TERCRI. For intersection crash risks, logistic regression model results showed significant reduction of conflict frequency for CV scenarios compared to base scenario. For both segment and the intersection crash risks, it was found that the higher the MPRs of CV implemented the higher were the safety benefits achieved. Maximum improvement was found to be at 100% MPR for both CV and CVLLA technologies. For segment crash risks, a minimum of 30% MPR was needed to observe significant safety benefits of both CV and CVLLA technologies in terms of TET, TIT, and NCJ compared to the base scenario. However, it was found that at least 40% MPR is needed to achieve the safety benefits of intersection crash risks. Hence, taking both segment and the intersection crash risks into consideration, the CV and CVLLA technologies performed better than non-CV scenario. Finally, the results showed that the CVLLA significantly outperformed CV in terms of both segment and intersection crash risks. It was also found that at least 60% MPR was needed to achieve the safety benefits of segment and intersection crash risks of CVLLA compared to CV technologies.

The chapter highlighted simulation-based approach that might be a viable tool to evaluate both segment and intersection crash risks concurrently under CV and CVLLA technologies, while there has been limited empirical data on safety performance of those technologies. To be sure, there are

no research without limitations. First, the ability of the proposed driving behaviors of CV and CVLLA technologies as the parameter of those behaviors are not calibrated within a real-world road network due to the fact that those technologies are still being developed. The full market penetration of those CV technologies might not be accomplished in the immediate future. Therefore, traffic flow will likely be composed of a mixture of conventional vehicles and CVs. With this regard, the interaction between CV technologies and the conventional vehicles are largely unknown. However, this study modeled CV and CVLLA behaviors by changing VISSIM's default car-following model in accordance with the recent literature, there is a clear scope to develop a more realistic car-following model for CVs and would calibrate it with real-world data.

CHAPTER 6: TRAFFIC SAFETY AND OPERATIONAL BENEFITS OF CONNECTED AND AUTOMATED VEHICLE ON EXPRESSWAYS: APPLICATION OF REAL-WORLD VALIDATED CAV DATA

6.1 Introduction

Connected and automated vehicle (CAV) technologies have been regarded as a promising solution for improving safety and mobility performance of the roadway network. By leveraging vehicle-to-vehicle (V2V) and vehicle-to-infrastructure (V2I) communications, CAV is expected to provide cooperative movements and thus increase freeway/expressway traffic safety and operations (Kockelman et al., 2016; Papadoulis et al., 2019; M. S. Rahman et al., 2019d; Rahman and Abdel-Aty, 2018). The combination of the two types of technologies (i.e. connected vehicle technologies, automated vehicle technologies) has generated high expectations regarding traffic safety by minimizing drivers' errors, which is a major cause solely or in combination with other factors for more than 94% of traffic crashes (Singh, 2015; Yue et al., 2018). Nevertheless, the evaluation of their safety and mobility benefits are still ambiguous because of the unattainability of real-world CAV data. Based on this disadvantage, few previous studies have implemented the simulation techniques to evaluate the potential safety and mobility benefits of CAVs. However, none of the studies has considered validated car following and lane changing models based on real-world CAV data. The interactions between the CAV and conventional vehicles are largely unknown in their chosen CAV models. Moreover, the optimal market penetration rates (MPRs) of both peak and off-peak hours have not been evaluated based on both traffic safety and operational characteristics.

This study considers the traffic safety and operational benefits of CAV on expressway segments. Microscopic traffic simulation was used to achieve the objectives of the study. The simulated area

consisted of a twenty-two miles network of SR-408 in Central Florida. The two-baseline simulation model were built, calibrated, and validated using real-word minute level detector data considering both peak and off-peak hours traffic. The CAV applications were tested in the studied simulated network using PTV VISSIM 11, which has the capability to model CAVs with validated driving behavior models based on real-world CAV data. Afterward, the numbers of CAV scenarios were tested including different MPRs (0% to 100%, for every 10% interval) and the traffic condition (peak hour vs non-peak hour). The safety and operation performance for various scenarios were evaluated using different measures of effectiveness. Operational measures included average travel time and average delay, while the safety measures considered both time proximity (i.e., conflicts) based and evasive action based (i.e., jerk) surrogate measures of safety. To achieve balanced mobility and safety benefits from mixed traffic environment, optimal CAV MPR could be determined at varying traffic conditions.

6.2 Methodology

The overall architecture of the proposed simulation framework is presented in Figure 18. First of all, a real-world simulation network was developed in order to replicate the baseline scenarios. The calibration and the validation of the simulation network must be conducted with the help of real-world traffic data. In this study, the traffic volume and speed data were collected from Microwave Vehicle Detection System (MVDS) detectors for every 20 seconds. Then, the CAV models in the simulation network were selected based on the validated car following and lane changing models in VISSIM using real world CAV data. Finally, the trajectory files were exported from the VISSIM simulation scenarios including both traffic operation (.rsr file) and safety (.trj file) measures. For traffic safety measures, the Surrogate Safety Assessment Model (SSAM) were

used to process the vehicle trajectory data.

The driving behaviors of CAV is the prerequisite to better assess the impact of CAV in traffic simulation. The driving behaviors of CAVs and conventional vehicles should have significant differences in terms of car following and lane changing models. Most of the previous studies replicate the CAV behavior by adopting the calibrated Intelligent Driver Model (IDM) which is the simplest complete car following (Li et al., 2016a; Rahman et al., 2018a; Rahman and Abdel-Aty, 2018; Wu et al., 2019a). However, the lane changing models were not considered in CAV modelling which is one of the most important limitations of these research. Moreover, the interactions between the CAV and the conventional vehicles (passenger cars, trucks) is still a great constraint to CAV MPRs. To address these important issues, VISSIM 11 provides the validated car following and lane changing models using real-world CAV data as a part of the project CoEXist (PTV Group, 2019). It is worth mentioning that CoEXist is a European project (May 2017-April 2020) which aims at preparing for the transition phase during which CAV and conventional vehicles will coexist on cities' roads. To the best authors' knowledge, this is the first application of CAV behavior embedded in commercially available software based on real word data from public test track with connected and automated vehicles.

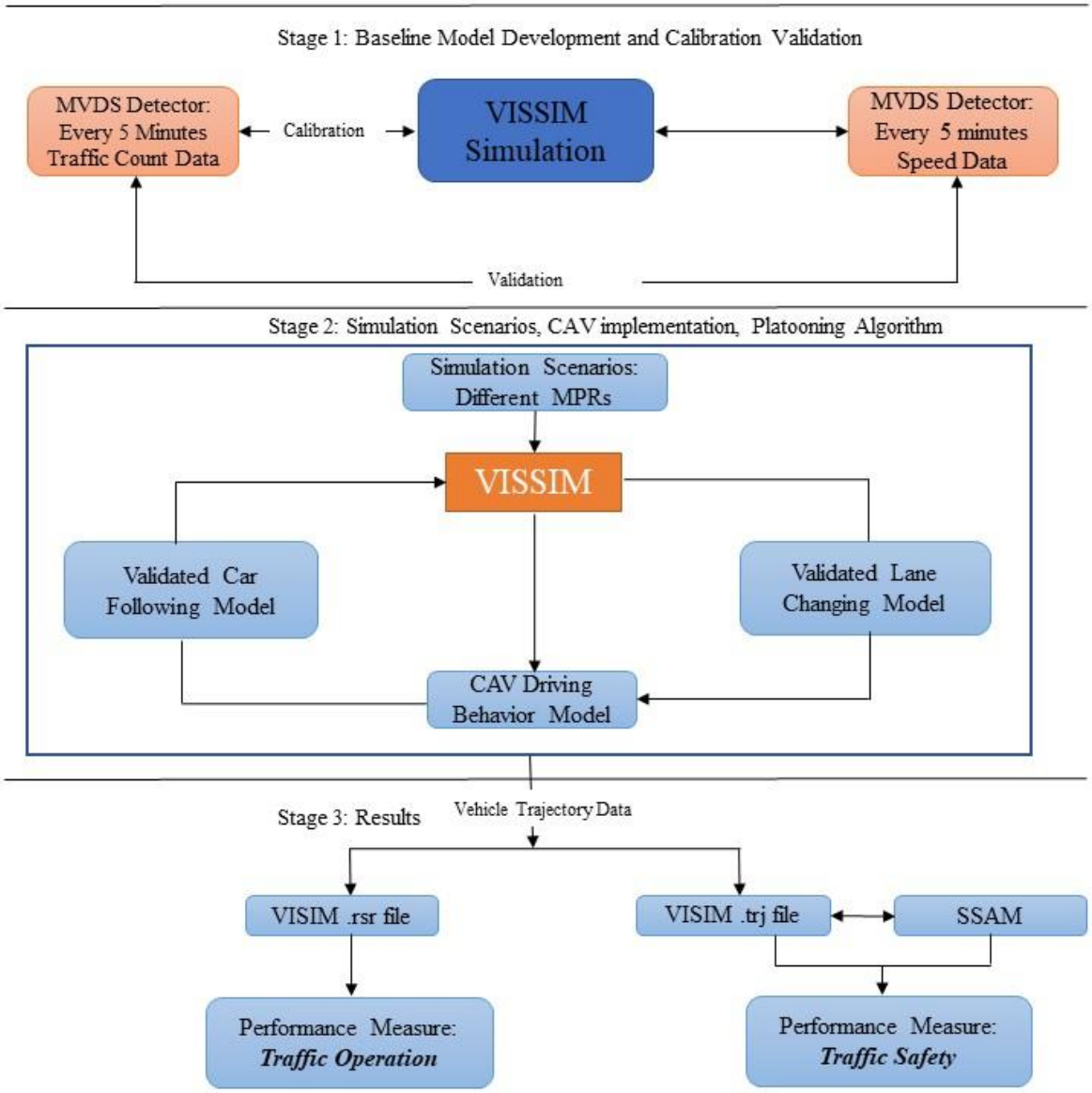

Figure 18 Architecture of the simulation framework.

Three types of connected and/or automated vehicles behavior are designed in VISSIM (version 11.0) including cautious, normal, and all-knowing driving logic. In the cautious driving logic, vehicles always respect the road code and safe behavior. Regarding the normal driving logic, the vehicles follow the existing average driver. The all-knowing driver logic predicts all other road users' behavior with the help of communication (V2V and/or V2I) technologies (PTV Group, 2019). Figure 19 shows the different vehicles' gaps between different driving logics.

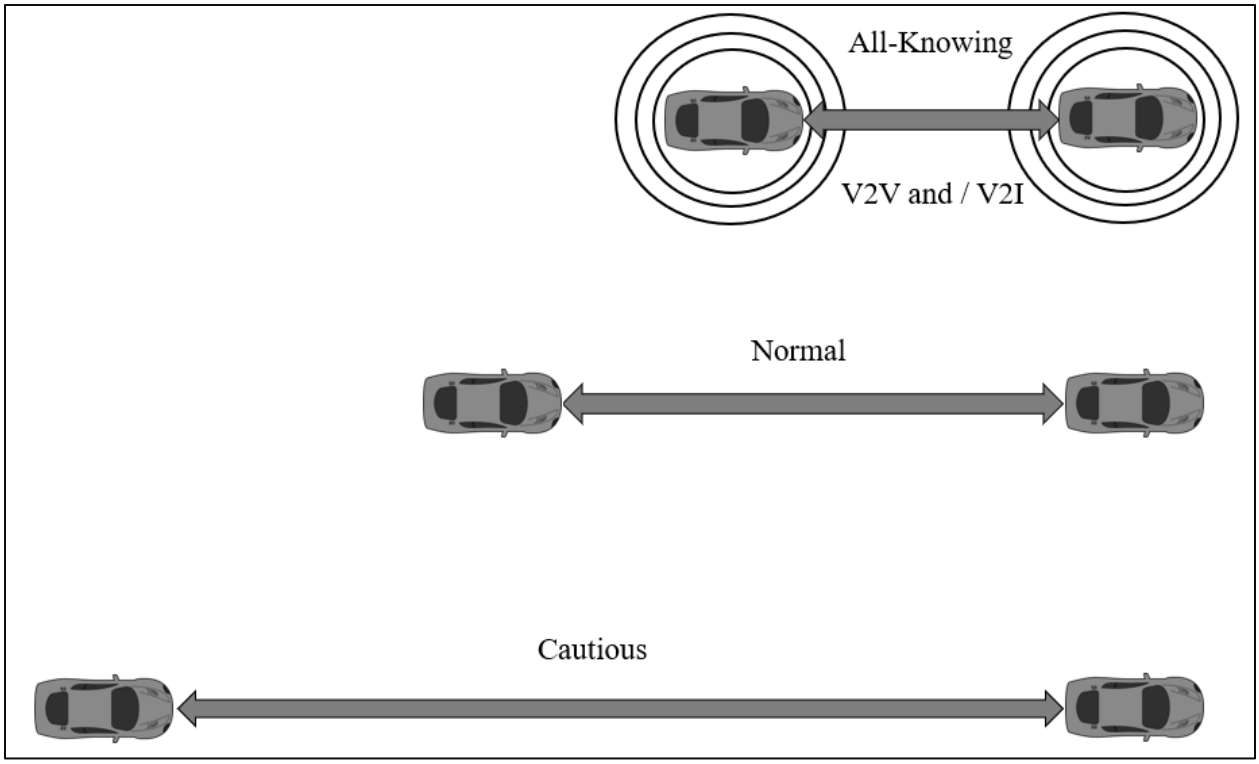

Figure 19 Gap between the vehicles for different CAV models in VISSIM.

From Figure 19, the cautious driving logic has the largest gaps compared to other driving logics. The normal driving logic has gaps similar to human drivers but with higher safety in terms of other added attributes in the corresponding driving behavior model. The all-knowing driving logic has smaller gaps with the help of connectivity which replicate the behavior of CAV. Hence, the all-knowing driving logic provided by VISSIM 11 is used to investigate the effects of CAV in the studied network. The following paragraph of the method section is focused on the all-knowing/CAV driving behaviors utilizing the validated parameters for both car following and lane changing models using real-world CAV data.

6.2.1 Driving behaviors of CAV in simulation

As mentioned earlier, the all-knowing driving behavior model of PTV VISSIM 11.0 were implemented to approximate the behavior of CAVs in the studied expressway section. The car following and lane changing models' parameters were calibrated based on the real-world CAV

projects named CoEXits. Moreover, multiple additional attributes are available in the driving behavior dialogs in VISSIM for modelling CAVs. One of the important new features of this CAV model is enforce absolute braking distance which will always make sure that CAV could brake without a collision, even if the leading vehicle comes to an immediate stop. This condition applies (1) lane changes for the vehicle itself on the adjacent lane and for the trailing vehicle on the new lane (2) conflict areas for the following vehicle on the major road and (3) car following, lane changing and gap acceptance at the freeway and/or intersections. In this case, I checked the enforce absolute braking distance which would be reasonable for the automated features of CAVs. The second important added attribute is the number of interaction objects and vehicles. Figure 20 shows the absolute braking and the number of interaction objects and vehicle (red marking) in the driving behavior dialogue box of the CAV model.

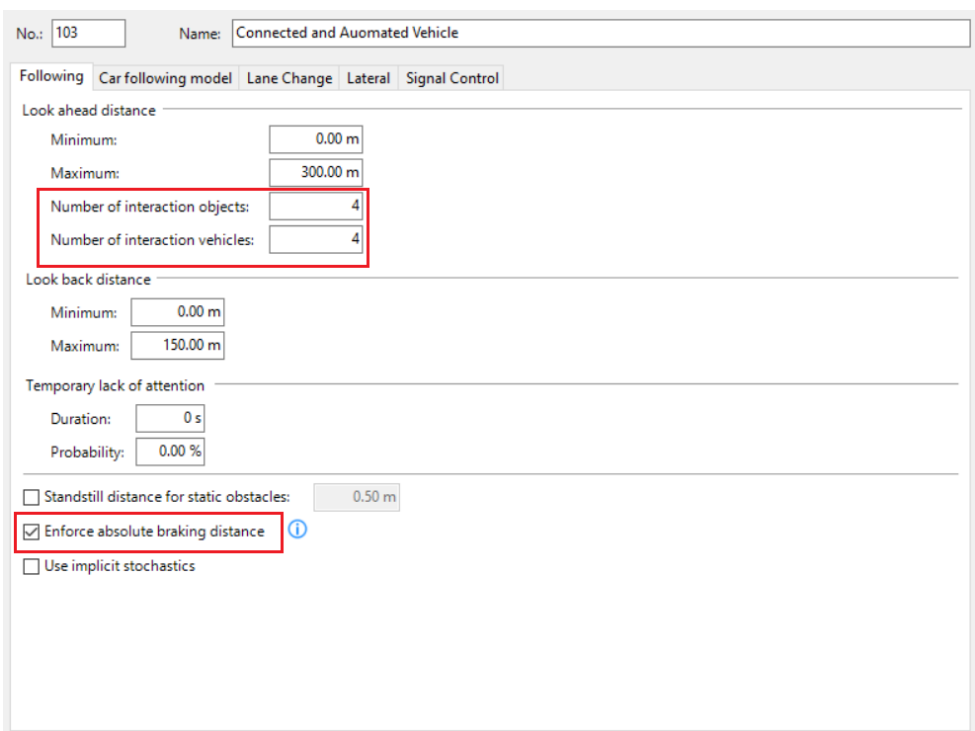

Figure 20 Driving behavior window with the new attributes to model CAV in VISSIM.

From Figure 20, the attribute of observed vehicles from the previous versions of VISSIM (Version

less or equal 10.0) has been split into two features: (1) number of interaction objects refers to vehicles and internal objects (reduced speed areas, stop signs, priority rules, red signal head) (2) number of interaction vehicles refers only to real vehicles. The number of interaction vehicles defines an upper limit for the observed leading vehicles, therefore, for example, this could be set to 1 for CAV that cannot see through the leading vehicle. A red signal downstream of the leading vehicle would still be observed, but not the second real vehicle downstream. Figure 21 shows an example of number of interaction objects=3 (First three objects are visible to the red car) and number of interaction vehicles=1 (only one vehicle is visible for red car). This study assumed number of interaction objects=4 and number of interaction vehicles=3 which is consistent with the results of CoEXits project because of choosing the all-knowing/CAV driving logics. Therefore, the red car is communicating with at most 3 vehicles in the front with the help of V2V communications.

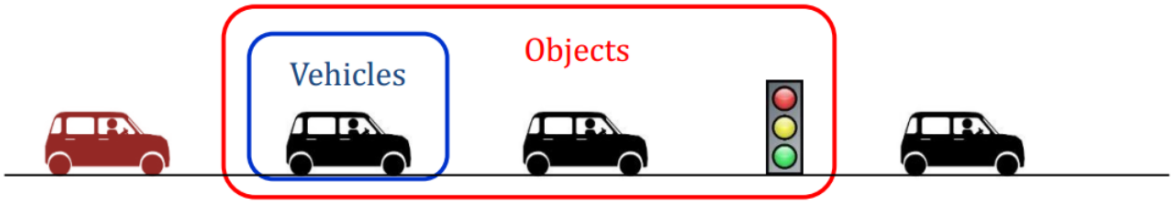

Figure 21 Number of interaction objects and number of interaction vehicle concept.

On the new tab in car following, some of the parameter values affecting the desired safety distance can be specified per vehicle class of the leading vehicle in addition to the value for all other vehicles. To be specific, the headway distance between the CAV and the conventional vehicles are obtained based on the public test track CAV data. From the results of CAV data, it was found a smaller safety distance when following another CAV but a larger safety distance when following a human driver. We selected the headway between the CAVs to be 0.6 second; the CAV and the

human driver is 0.9 seconds based on the results of the CoExists project. This is very important attribute in this CAV modelling which was ignored in the previous CAV studies. Therefore, the interaction between CAV and the conventional vehicles would be better assessed in terms of market penetration rates of CAV.

The car following CC parameters of Weidmann 99 model were validated using real-world public test track CAV data. The CC parameters of the conventional vehicle and the CAV in the Weidmann car following model are presented in Table 16.

Table 16 Car Following CC Parameters of CAV Compared to Standard Vehicle

Car following parameter	Description	Units	Human Driver Parameter	CAV Driving Logic
CC0	The average standstill distance	meter	1.50	1.00
CC1	The headway time	seconds	0.90	0.60
CC2	The distance difference in the oscillation condition	meter	4.00	0
CC3	Controls the deceleration process	N/A	-8.00	-6.00
CC4	Defines negative speed difference	N/A	-0.35	-0.1
CC5	Defines positive speed difference	N/A	0.35	0.1
CC6	The distance influence on speed oscillation	N/A	11.44	0
CC7	The acceleration at the oscillation condition	m/s^2	0.25	0.1
CC8	The desired standstill acceleration	m/s^2	3.50	4
CC9	The desired acceleration at 50 mph	m/s^2	1.50	2

The lane changing behavior are also validated based on the real-world CAV data. Table 17 shows the validated lane changing model which is the first application in CAV modelling based on real-world CAV data in terms of lateral movement. The aforementioned car following and lane changing models are the main factors to approximate the driving behaviors of CAVs in the VISSIM simulation software.

Table 17 Lane Changing Parameters of CAV Compared to Standard Vehicle

Lane Changing Model	Units	Human Driving Logic		CAV Driving Logic	
		Own	Trailing Vehicle	Own	Trailing Vehicle
Maximum Deceleration	m/s2	-4.00	-3.00	-4.00	-4.00
-1 m/s per distance	meter	200	200	100	100
Accepted deceleration	m/s2	-1.00	-0.50	-1.00	-1.50
Waiting time per diffusion	seconds	60.00		60.00	
Min. net headway (front to rear)	meter	0.50		0.50	
Safety distance reduction factor	N/A	0.60		0.75	
Maximum deceleration for cooperative braking	m/s2	-3.00		-6.00	

6.3 Network of Interest

A freeways section of Holland East-West Expressway (SR408), Orlando, Florida was selected as a test bed of this study. This test bed is approximately 22-miles section of SR408 having 17 weaving segments from West Colonial Drive, Orlando to Challenger Parkway, Orlando. The simulation model used in this study was VISSIM latest version 11.0. Both peak and off-peak hour were considered in the simulation model. The peak period was defined from 7:00 a.m. to 9:00 a.m. and the off-peak period from 10:00 a.m. to 12:00 p.m. The field traffic data (i.e. flow) were aggregated into 5-minute traffic counts and the speed data were also collected on the same day to use in the validation of the VISSIM baseline simulation model. Traffic counts and speed data were collected from the Microwave Vehicle Detection System (MVDS) detector system. Moreover, further traffic information for building the simulation network including passenger car (PC) and heavy goods vehicle (HGV) percentages, and desired speed distribution were also calculated for input in the VISSIM model. The simulation time was set from 6:30 A.M. to 9:30 A.M and 9:30 A.M. to 12:30 P.M. for peak and off-peak period, respectively. After excluding the first 30 minutes of VISSIM warm up time and the last 30 minutes of cool-down time, 120 minutes VISSIM data

was used for model calibration and validation.

6.3.1 Network calibration and validation

The most important part of any simulation model is calibrating the model by defining or fine-tuning the values of the parameters so that the difference between observed and simulated traffic measurement (i.e., traffic counts, speed, travel time etc.) is minimum. In this regard, calibration criteria are formulated by the general optimization framework as follows.

$$\min f\left(M^{obs}, M^{sim}\right) \tag{1}$$

Which is subjected to the constraints:

$$l_{\theta_i} \leq \theta_i \leq u_{\theta_i}, \quad i = 1,2, \dots, n \tag{2}$$

Where,

θ_i=the vectors of continuous variable (i.e. model parameters to be calibrated)

$f(.)$ =Objective function (or fitness function).

M^{obs}, M^{sim}=Observed and simulated traffic measurements.

$l_{\theta_i}, u_{\theta_i}$=the respective lower and upper bounds of model parameter

n = number of parameters.

In this study, we used Geoffrey E. Heavers (GEH) as objective function (fitness function) using traffic counts. The specification of minimizing GEH is given as follows:

$$GEH = \sum_{j=1}^{N} \sqrt{\frac{2 \times (M_{obs}(n) - M_{sim}(n))^2}{(M_{obs}(n) + M_{sim}(n)}} \tag{3}$$

$M_{obs}(n)$=actual traffic counts for a given time interval j.

$M_{sim}(n)$=simulated traffic counts for a given time interval j.

N =total number of observations.

The base calibration parameters for VISSIM that have been considered in this research are the driver behavior parameters of Wiedmann-99 as the test bed was selected in a freeway section. A sensitivity analysis was conducted on VISSIM driver behavior parameters based on their allowable minimum and maximum values in the simulation model. For each parameter, a range of values between the minimum and maximum (include default value) were chosen to run VISSIM model and the corresponding values of objective function GEH were calculated. It is worth mentioning that each parameter value was run ten times with different random seeds and averaged it to calculate the simulated traffic measurement which captures the random effects of the simulation. For each parameter, the minimum value of GEH is the corresponding calibrated value for that parameter. Based on the literature review, six parameters were chosen for VISSIM calibration and validation for weaving segments (Jolovic and Stevanovic, 2012; Koppula, 2002; Woody, 2006; Wu et al., 2005). They were DLCD (desired lane change distance), CC0 (standstill distance), CC1 (headway time), CC2 (following variation), waiting time per diffusion, and safety distance reduction factor. A total of 490 simulation runs [(1 base-models + 6×8 car-following parameters) times 10 random seeds] were conducted. The sensitivity analysis results showed that three most important parameters were vital to reflect the safety in weaving segment. These include DLCD, CC1, and safety distance reduction factor. The default value of DLCD, CC_1, and safety distance reduction factor in VISSIM were 200 meters, 0.9 seconds, and 0.60, respectively whereas the calibrated values were found to be 400 meters, 0.8 seconds, and 0.50, respectively. The simulated volume would precisely reflect the field volume if more than 85% of the measurement locations GEH values are less than five (Wang et al., 2017; Yu and Abdel-Aty, 2014) and the criteria was met with minimizing the objective function.

For the validation of the VISSIM model, the two-sample t-test was used to test the hypothesis that whether the distribution of the simulated and the observed speeds are statistically identical or not. The two-sample test is a parametric technique which can be used to prove that difference between the two population's means are equal. Let $X_1, \ldots, X_m$ be the field speed and $Y_1, \ldots, Y_n$ be the simulated speed from the VISSIM simulation averaging 10 runs (different random seeds). The null hypothesis is the difference between the two population's means is equal to some constant as follows:

$$T = \frac{\bar{Y} - \bar{X}}{\frac{s_1^2}{N_1} + \frac{s_2^2}{N_2}} \tag{4}$$

The hypothesis is rejected if the test statistic, T, is greater than the critical value obtained from t-table considering level of significance. The speed data for vehicles are recorded from VISSIM data collection point and compared with field observations by two sample t-test . From the t-test result, it is found that the T is less than the critical value with 5% significance level. Hence, the distribution of the simulated and the observed speeds are statistically identical which confirmed the good validation results of the VISSIM model.

6.4 Measure of Effectiveness

Both traffic operation and safety measures were utilized in order to assess the benefits of CAV application in expressway segments. Two measures of effectiveness (MOE) were considered to assess the mobility performances of CAV with different market penetration rate: Average Travel Time (ATT), and Average Delay (AD). Ten similar travel time measurements location were selected in the VISSIM network for both base and CAV scenarios. A travel time measurement section consists of a "From Section" and a "To Section". The mean travel time and delay from traversing the "From Section" up to the traversing of the "To Section", including the waiting time

and/or holding time, is calculated. For these ten measurement locations, the average travel time and average delay for each vehicle were extracted from the vehicle travel time raw data as .rsr file in VISSIM. The data contains both travel time and delay information of each individual vehicle for every second.

In terms of safety performance, surrogate safety assessment techniques were used to assess the crash risk in the studied expressway segments. Surrogate safety measures are a widely used technique to assess the crash risk of a road network due to the rare events of crashes. In this study, two types of surrogate measures of safety indicators were considered. The first type represents the time proximity-based indicator (i.e., time-to-collision, post-encroachment time). The second type represents evasive action–based indicators (i.e., yaw rate and jerk). In our study, two surrogate safety measures (i.e. time proximity based, evasive action based) were used to estimate the crash risks in the studied section. For time proximity-based indicator, the Surrogate Safety Assessment model (SSAM) was used to offer rational conflict estimations of expressway segments. SSAM uses several parameters to measure the conflicts and describe the conflict locations, and characteristics. The main conflict measure parameters considered in SSAM are Time-to-collision (TTC) and Post-encroachment time (PET) (See (Gettman et al., 2008) for detailed review). A conflict is recorded in SSAM when the two time proximity based indicators such as TTC and PET values exceed the predetermined threshold values, and the conflict type associated with each conflict is identified according to the lane and link information or the angle between the two converging vehicles (Fan et al., 2013). This study uses the default maximum TTC threshold and PET threshold values 1.50 and 5.00 seconds, respectively, in order to calculate the total number of conflicts (TNC) from the VISSIM trajectory file.

Furthermore, we also considered jerk as evasive action-based indicator to calculate the safety critical driving behavior in order to compare the corresponding scenarios. Jerk represents the derivative of the acceleration. It is used for braking behavior that varies as a reaction to the environment. The evasive action involving powerful braking or sudden acceleration can be reflected in the jerk profile. The acceleration is the derivative of speed, which can be calculated by Equation 5. The jerk can be calculated using Equation 6, as follows:

$$A(t) = \dot{V}_t = (\ddot{x}_t, \ddot{y}_t) \tag{5}$$

$$\text{Jerk (t)} = \dot{A}_t \tag{6}$$

Where, $A(t)$ is the acceleration of vehicle at instant t; (x_t, y_t) is the position of vehicle at instant t; and Jerk (t) is the jerk of vehicle at instant t.

In the beginning, Bagdadi and Várhelyi (Bagdadi and Várhelyi, 2011) pointed out that jerks would have a better surrogate measure which consider the deceleration behavior to crashes. In their study, 33 crashes involving 166 drivers' behaviors were analyzed using regression model in terms of the number of critical or dangerous jerks (defined as critical jerks that are equal to or below than -9.9 m/s^3) and self-reported crashes. The regression results found that the number of accidents increased by 1.13 times for each additional critical jerk over a three-year period. Hence, jerkiness in driving may be an indication of a riskier driving style and a higher probability of accident involvement. This study collected the trajectory data containing acceleration values for all vehicles from Fritzing Part File (.FZP) in VISSIM. Therefore, the study calculated the total number of critical jerk (TNCJ) from the Fritzing Part File for each of three scenarios. A threshold level of -9.9 m/s^3 is used for the jerks as an indicator of safety-critical driving behavior based on previous studies (Bagdadi and

Várhelyi, 2011; Nygård, 1999). This study calculated the TNCJ from all jerk values that are equal to or below the threshold value of −9.9 m/s^3.

6.5 Results

6.5.1 Operation analysis

Traffic operation measurements were analyzed to assess the operational impact of CAV in the studied section. As indicated earlier, the performance measures for traffic operation included ATT and AD. ATT and AD for every vehicle were obtained from the VISSIM trajectory data. Performance measures of CAV scenarios with different MPRs ranging 10% to 100% (with 10% increment) were compared with the baseline scenario (0% CAV) to quantify the mobility benefits. Both peak and off-peak period were considered, hence, a total of 22 scenarios (including baseline) were build and tested using microsimulation. All the scenarios were repeatedly simulated for 30 times to consider random effects of simulation. Table 18 shows the studied scenarios with the descriptive statistics of ATT and AD. The results in the table showed that, baseline (0% CAV) scenario had the largest mean values of both ATT and AD, while lower ATT and AD were obtained in CAV scenarios for each MPRs. For instance, 100% MPR of peak period, the mean values of the ATT and AD for CAV scenario were lower with ATT (145.80 s) and AD (16.50 s), compared to non-CV scenario of ATT (176.20 s), and AD (21.03 s). In terms of 100% MPR in off-peak period, the mean values of the ATT and AD for the CAV scenario were lower with ATT (97.24 s) and AD (8.32 s), compared to non-CV scenario of ATT (138.50 s), and AD (12.59 s). Therefore, the CAV for each MPRs has higher mobility benefits for both peak and off-peak period compared to the baseline condition.

Table 18 Descriptive Statistics of Traffic Operations Performance Measures in Every 5 Minutes

Scenarios	Time of Day	MOE	Minimum (seconds)	Maximum (seconds)	Mean (seconds)	Standard Deviation (seconds)
Base (0% CAV)	Peak	ATT (s)	167.60	182.30	176.20	3.54
		AD (s)	16.60	25.13	21.03	2.49
	Off-peak	ATT (s)	130.80	145.40	138.5	3.17
		AD (s)	9.90	15.76	12.59	1.49
CAV Scenario (10% MPR)	Peak	ATT (s)	165.90	179.30	174.50	3.36
		AD (s)	16.19	24.34	20.38	2.36
	Off-peak	ATT (s)	128.20	145.40	135.80	3.10
		AD (s)	9.31	14.80	11.84	1.41
CAV Scenario (20% MPR)	Peak	ATT (s)	161.70	176.70	171.60	2.73
		AD (s)	15.73	23.81	19.92	2.36
	Off-peak	ATT (s)	125.50	139.60	132.90	3.04
		AD (s)	9.08	14.45	11.55	1.37
CAV Scenario (30% MPR)	Peak	ATT (s)	157.20	178.60	165.30	3.32
		AD (s)	15.16	22.94	19.19	2.27
	Off-peak	ATT (s)	121.2	134.8	128.4	2.93
		AD (s)	8.78	13.98	11.17	1.32
CAV Scenario (40% MPR)	Peak	ATT (s)	153.3	166.8	161.2	3.24
		AD (s)	14.69	22.24	18.61	2.21
	Off-peak	ATT (s)	116.40	129.40	123.3	2.81
		AD (s)	8.45	13.46	10.75	1.28
CAV Scenario (50% MPR)	Peak	ATT (s)	150.30	163.50	158.0	3.18
		AD (s)	14.46	21.89	18.31	2.16
	Off-peak	ATT (s)	112.10	124.60	118.70	2.71
		AD (s)	8.03	12.78	10.21	1.21
CAV Scenario (60% MPR)	Peak	ATT (s)	147.3	160.2	154.9	3.11
		AD (s)	14.19	21.49	17.98	2.13
	Off-peak	ATT (s)	107.90	120.00	114.30	2.61
		AD (s)	7.80	12.41	9.92	1.18
CAV Scenario (70% MPR)	Peak	ATT (s)	144.5	157.1	151.9	3.05
		AD (s)	13.89	21.03	17.59	2.08
	Off-peak	ATT (s)	104.90	116.60	111.10	2.54
		AD (s)	7.46	11.80	9.49	1.13
CAV Scenario (80% MPR)	Peak	ATT (s)	142.8	155.3	150.1	3.02
		AD (s)	13.50	20.43	17.09	2.02
	Off-peak	ATT (s)	101.6	113.00	107.60	2.46
		AD (s)	7.04	11.20	8.95	1.06
CAV Scenario (90% MPR)	Peak	ATT (s)	140.90	153.3	148.20	2.98
		AD (s)	13.30	20.13	16.84	1.99
	Off-peak	ATT (s)	95.58	106.30	101.20	2.31
		AD (s)	6.90	1098	8.78	1.04
CAV Scenario (100% MPR)	Peak	ATT (s)	138.8	150.90	145.80	2.66
		AD (s)	13.03	19.72	16.50	1.95
	Off-peak	ATT (s)	91.80	102.10	97.24	2.25
		AD (s)	6.54	10.41	8.32	0.99

Moreover, Table 19 illustrates the summary of two sample t-test at 95% confidence level for

comparing the ATT and AD between CAV and baseline scenarios. Compared to the base scenario, ATT and AD decreased significantly in the CAV scenarios. For both peak and off-peak period, simulation model performances were evaluated for two different condition sets (Base and CAV) each under 10 different MPRs (10% to 100%, 10% increment) of CAV scenarios. To find out the mobility impact of the CAV technologies, the mean values of the mobility measures were compared with the baseline scenario. From Table 19, it was found that the maximum significant improvement resulted at 100 % MPR for both peak and off-peak hours. For example, in the peak period of 100% MPR, the ATT and AD were found to be reduced by 17.22% and 21.50%, respectively, in CAV case compared to base condition.

Table 19 Summary of Measure of Effectiveness in Terms of Traffic Operation

MPR	Comparisons	Traffic Condition	ATT in 5 minutes (s)		AD in 5 minutes (s)	
			Mean difference (P-value)	% Reduction	Mean difference (P-value)	% Reduction
10 %	Base – CAV	Peak	1.68 (0.100) #	0.95	0.65 (0.360) #	3.09
		Off-Peak	2.77 (0.0037)	2.01	0.76 (0.078) #	6.03
20%	Base – CAV	Peak	4.46 (<0.0001)	2.59	1.10 (0.122) #	5.23
		Off-Peak	5.59 (<0.0001)	4.04	1.04 (0.015)	8.26
30 %	Base – CAV	Peak	11.06 (<0.0001)	6.27	1.83 (0.0001)	8.70
		Off-Peak	10.14 (0.0001)	7.32	1.43 (0.0011)	11.35
40 %	Base – CAV	Peak	14.97 (<0.001)	8.49	2.41 (<0.0001)	11.41
		Off-Peak	15.26 (<0.0001)	11.02	1.84 (<0.0001)	14.61
50 %	Base – CAV	Peak	18.15 (<0.0001)	10.30	2.71 (<0.0001)	12.88
		Off-Peak	19.84 (<0.0001)	14.32	2.38 (<0.0001)	18.90
60 %	Base – CAV	Peak	21.32 (<0.0001)	12.09	3.05 (<0.0001)	14.50
		Off-Peak	24.27 (<0.0001)	17.52	2.67 (<0.0001)	21.20
70 %	Base – CAV	Peak	24.31 (<0.0001)	13.79	3.43 (<0.0001)	16.26
		Off-Peak	27.47 (<0.0001)	19.83	3.10 (<0.0001)	24.62
80 %	Base – CAV	Peak	26.07 (<0.0001)	14.80	3.93 (<0.0001)	18.69
		Off-Peak	30.92 (<0.0001)	22.32	3.64 (<0.0001)	28.91
90%	Base – CAV	Peak	28.01 (<0.0001)	15.89	4.18 (<0.0001)	19.87
		Off-Peak	37.29 (<0.0001)	26.92	3.82 (<0.0001)	30.34
100 %	Base – CAV	Peak	30.35 (<0.0001)	17.22	4.52 (<0.0001)	21.50
		Off-Peak	41.30 (<0.0001)	29.82	4.27 (<0.0001)	33.92

#Difference is insignificant at 5% level

On the other hand, in off-peak hours, the reductions were found to be 29.82% and 33.92%, respectively. The results revealed that the applied CAV technologies enhanced operations by

decreasing the traffic operational measures (ATT and AD) in the studied section. It is interesting to note that the mobility improvement for off-peak and peak hours were found to be insignificant below 20% and 30% MPRs, respectively in considering both AD and ATT. So, it is concluded that off-peak period has more improvement compared to the peak period in terms of CAV scenarios in the studied section of expressway.

Furthermore, statistical model was applied to better asses the effects of traffic operational characteristic (i.e., ATT and AD) on CAV effectiveness for different MPRs and traffic condition. Tobit model was used for identifying the different MPRs and traffic condition that maximize the traffic operational performance at the studied section. In the Tobit model, different scenario variables of various MPRs (0% to 100%) and traffic conditions (peak and off-peak) were included. The statistical analysis software (SAS 9.4) was used for generating the model results. The model formulation takes the following form:

$$y_i = \begin{cases} y_i^* & if y_i^* > 0 \\ 0, & if\ \ y_i^* \leq 0 \end{cases} \tag{2}$$

$$y_i^* = \beta_0 + \beta_z X + \varepsilon_i \tag{3}$$

Where, y_i is the response variable (ATT or AD in expressway segment i) and y_i^* is a latent variable. The observable variable y_i becomes equal to y_i^* when the latent variable is above zero and becomes zero otherwise. β_0 is the intercept, β_z represents the coefficients of the independent variables (i.e., different MPRs and traffic condition); ε_i is a normally distributed error term with a mean equal to zero and a variance (α^2); z represents the different scenarios of various MPRs and traffic condition of all studied cases; X is the different scenarios in all cases. The results of the models are shown in Table 20. In our model settings, we considered 0% MPR (baseline scenario) and peak period as

reference category.

Table 20 Tobit Model Results for Traffic Operation Analysis

Parameter	Average Travel Time (ATT)		Average Delay (AD)	
	Estimate	P-value	Estimate	p-value
Intercept	177.74	<0.0001	20.89	<0.0001
MPR 0%	Reference			
MPR 10%	-2.20	0.2270	-0.70	<0.0001
MPR 20%	-5.10	0.0051	-1.08	<0.0001
MPR 30%	-10.50	<0.0001	-1.63	<0.0001
MPR 40%	-15.10	<0.0001	-2.13	<0.0001
MPR 50%	-19.00	<0.0001	-2.55	<0.0001
MRP 60%	-22.75	<0.0001	-2.86	<0.0001
MPR 70%	-25.85	<0.0001	-3.27	<0.0001
MPR 80%	-28.50	<0.0001	-3.79	<0.0001
MPR 90%	-32.65	<0.0001	-4.00	<0.0001
MPR 100%	-35.83	<0.0001	-4.40	<0.0001
Off-peak (vs Peak)	-40.78	<0.0001	-8.17	<0.0001
Log Likelihood (Convergence)	-44.4016		20.3955	
AIC	114.8033		-14.79	

From Table 20, the parameter estimates for MPRs indicate that the ATT and AD decreases with increasing MPRs of CAV. It is worth mentioning that the higher the percentage of the CAV implemented, the higher were the operational benefits achieved. Regarding the traffic condition, the off-peak period had a significantly lower ATT and AD compared with the peak period.

Apart from statistical significance, Figure 22(a) and 22(b) compares the profile of average travel time between the baseline and CAV scenarios in 100 % MPR for both peak and off-peak period. For every 5-minute time interval which is denoted in the x axis, the ATT (denoted in y axis) were calculated.

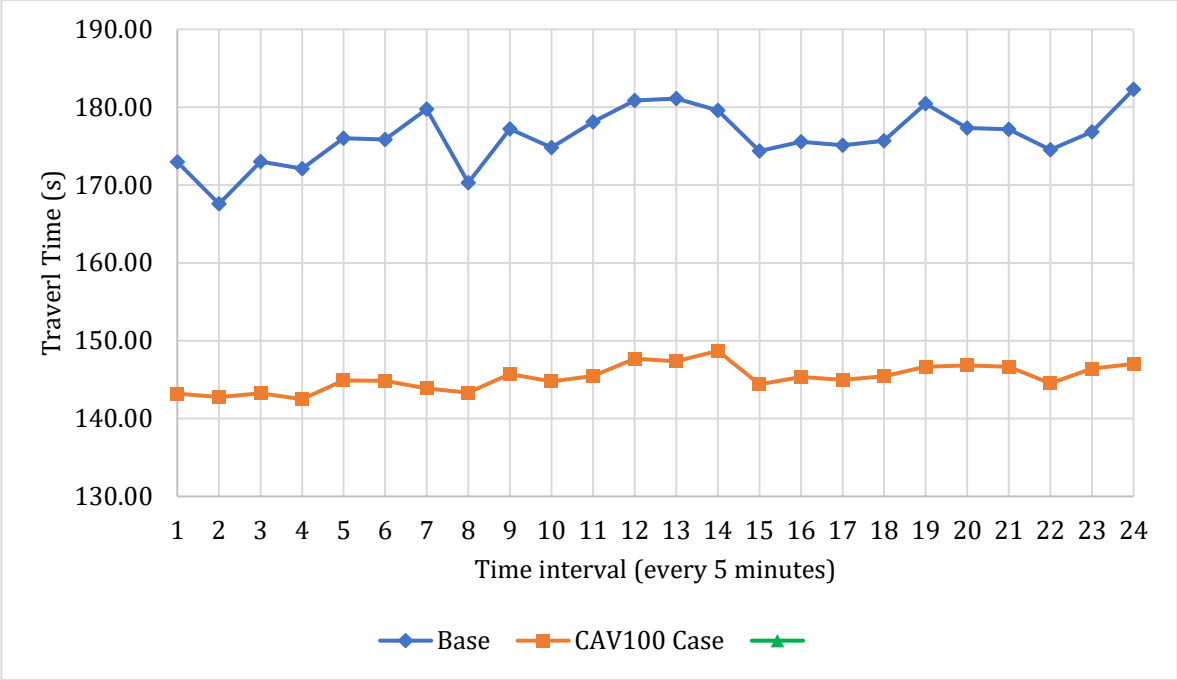

(a) Peak Period

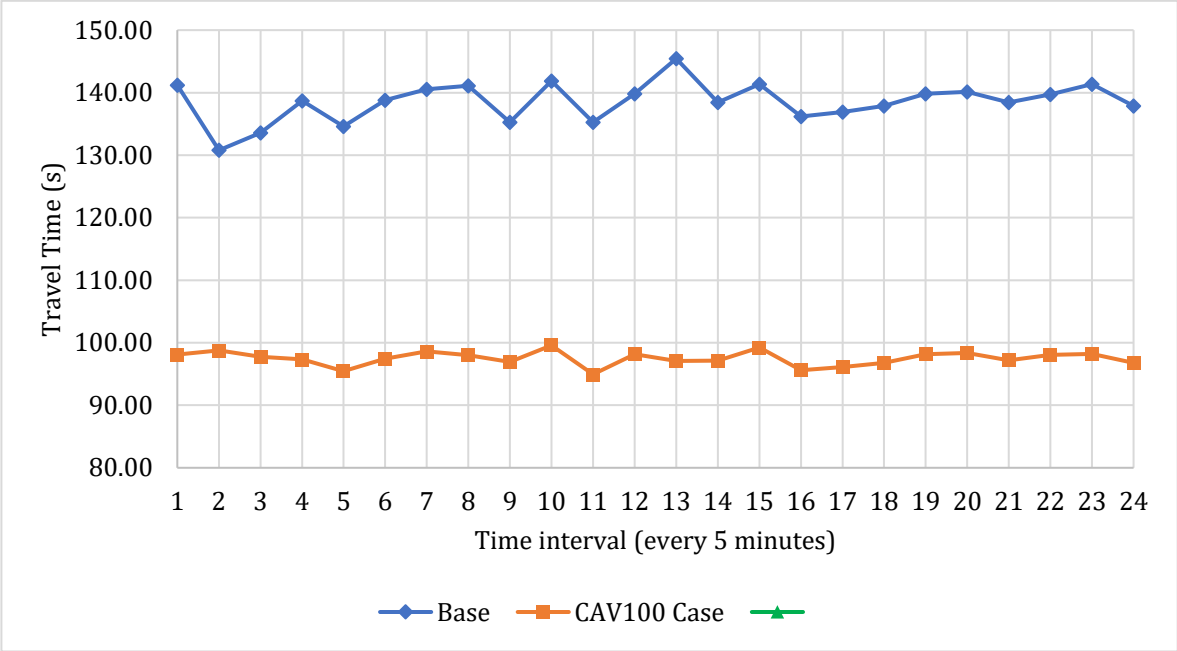

(b) Off-peak period

Figure 22 Stabilized profile of travel time at 100% MPR.

Figure 22 (a) and 22 (b) illustrates that CAV technologies not only reduced the travel time but were able also to stabilize the profile. With lower variances in travel time of CAV technologies are expected to increase the travel time reliability of the studied network. In a nutshell, the deployment

of CAV in the studied expressway segment would significantly decrease ATT and AD, and thereby significantly increase the mobility performance of the road network.

6.5.2 Traffic Safety

As mentioned earlier, this study considered both time proximity based and the evasive action-based surrogate measures as traffic safety indicators. The total number of conflicts (TNC) extracted from SSAM was considered as time proximity-based measures, while the total number of critical jerk (TNCJ) considered as the evasive action-based measures. Afterwards, the CAV scenarios were compared with the base scenario to quantify the crash risk in term of surrogate measures of safety with different MPRs ranging from 10% to 100% with the increment of 10%. As previously explained, both scenarios (baseline and CAV) were repeatedly simulated for 30 times to consider random effects of simulation. The descriptive statistics of traffic safety performance measures are shown in Table 21. The results of the table showed that the non-CAV scenario has the largest mean value of TNC and TNCJ, while the lower TNC and TNCJ were obtained in CAV scenario for each MPR. Hence, CAV scenarios have higher safety benefit compared to base scenario in terms of both surrogate measures of safety. Looking at the 100% MPR in peak condition, the mean values of the surrogate measures of safety for CAV scenarios were lower with TNC (1011) and TNCJ (609) , compared to non-CV scenario of TNC (1618) and TNCJ (952). In terms of 100% MPR in off-peak period, the mean values of the TNC and TNCJ for CAV scenarios were lower with TNC (309) and TNCJ (207), compared to non-CV scenario of TNC (736), and TNCJ (504). Therefore, the scenarios with CAV for each MPRs has the higher safety benefits compared to the baseline condition.

Table 21 Descriptive Statistics of Traffic Safety Measures

Scenarios	Time of Day	Surrogate Measures	Minimum	Maximum	Mean	Standard Deviation
Base (0% CAV)	Peak	TNC	1271	2157	1618	215.50
		TNCJ	856	1038	952	58.76
	Off-peak	TNC	664	866	736	47.17
		TNCJ	425	589	504	36.24
CAV Platooning (10% MPR)	Peak	TNC	1207	2049	1538	204.80
		TNCJ	834	1012	928	57.30
	Off-peak	TNC	644	840	714	45.73
		TNCJ	412	571	489	35.14
CAV Platooning (20% MPR)	Peak	TNC	1195	2028	1521	202.60
		TNCJ	830	1007	924	56.96
	Off-peak	TNC	604	788	669	42.91
		TNCJ	383	530	454	32.59
CAV Platooning (30% MPR)	Peak	TNC	1169	1984	1489	198.30
		TNCJ	805	976	895	55.27
	Off-peak	TNC	571	745	633	40.59
		TNCJ	353	489	419	29.97
CAV Platooning (40% MPR)	Peak	TNC	1118	1898	1425	189.70
		TNCJ	779	945	867	53.48
	Off-peak	TNC	498	650	552	35.39
		TNCJ	315	436	373	26.76
CAV Platooning (50% MPR)	Peak	TNC	1055	1790	1344	178.90
		TNCJ	745	903	828	51.14
	Off-peak	TNC	458	598	508	32.57
		TNCJ	285	395	338	24.33
CAV Platooning (60% MPR)	Peak	TNC	991	1682	1263	168.10
		TNCJ	702	851	781	48.15
	Off-peak	TNC	405	528	449	28.71
		TNCJ	264	365	313	22.37
CAV Platooning (70% MPR)	Peak	TNC	941	1596	1184	154.50
		TNCJ	659	799	733	45.19
	Off-peak	TNC	365	476	405	25.91
		TNCJ	225	312	267	19.28
CAV Platooning (80% MPR)	Peak	TNC	864	1467	1101	146.60
		TNCJ	633	768	705	43.56
	Off-peak	TNC	332	433	368	23.58
		TNCJ	208	289	247	17.68
CAV Platooning (90% MPR)	Peak	TNC	813	1380	1036	138.00
		TNCJ	574	695	638	39.29
	Off-peak	TNC	305	398	339	21.65
		TNCJ	187	259	222	15.99
CAV Platooning (100% MPR)	Peak	TNC	796	1345	1011	133.70
		TNCJ	548	664	609	37.62
	Off-peak	TNC	279	364	309	19.85
		TNCJ	174	241	207	14.75

To address the statistical significance, Table 22 illustrates the summary of two sample t-test for two surrogate measures of safety, (i.e., TNC and TNCJ) between the scenarios for both peak and of-peak period condition. Compared to the base scenario, TNC and TNCJ were decreased significantly within CAV technologies. The safety performances were evaluated for base and CAV settings each under 10 different MPRs (10% to 100%, with 10% increment). To find out the safety impacts of CAV technologies, the mean values of the surrogate safety measures of each CAV scenarios were compared with the base condition. From Table 22, it was found that the maximum significant improvement happened at 100 % MPR for both peak and off-peak conditions. For example, in 100% MPR of peak condition, TNC and TNCJ found to be reduced by 37.55% and 36.03%, respectively, in CAV case compared to baseline case. On the other hand, in off-peak hours, the reductions of TNC and TNCJ were found to be 58.02% and 59.13%, respectively. The results revealed that CAVs can enhance traffic safety by decreasing both evasive action-based and time proximity based surrogate measures. It is interesting to note that the safety improvement for off-peak and peak hours were found to be insignificant below 20% and 30% MPRs which is consistent results in terms of traffic operation benefits. It is worth noting that the off-peak period had more traffic safety improvement compared to the peak period in terms of CAV MPRs.

Table 22 Summary of Measure of Effectiveness in Terms of Traffic Safety

MPR	Comparisons	Traffic Condition	TNC		TNCJ	
			Mean difference (P-value)	Percentages %	Mean difference (P-value)	Percentages %
10 %	Base – CAV	Peak	80 (0.141) #	4.94	24 (0.118) #	2.52
		Off-Peak	22 (0.071) #	2.98	15 (0.105) #	2.97
20%	Base – CAV	Peak	97 (0.080) #	5.99	29 (0.060) #	3.05
		Off-Peak	66 (0.001)	8.96	50 (0.001)	9.92
30 %	Base – CAV	Peak	130 (0.019)	8.03	57 (0.0003)	5.98
		Off-Peak	103 (0.001)	13.99	85 (0.001)	16.86
40 %	Base – CAV	Peak	194 (0.001)	11.99	86 (0.001)	9.03
		Off-Peak	184 (0.001)	25.00	131 (0.001)	25.99
50 %	Base – CAV	Peak	275 (0.001)	17.00	124 (0.001)	13.02
		Off-Peak	228 (0.001)	30.97	166 (0.001)	32.94
60 %	Base – CAV	Peak	356 (0.001)	22.00	171 (0.001)	17.96
		Off-Peak	287 (0.001)	38.99	192 (0.001)	38.09
70 %	Base – CAV	Peak	434 (0.001)	26.82	219 (0.001)	23.00
		Off-Peak	331 (0.001)	42.65	237 (0.001)	47.02
80 %	Base – CAV	Peak	518 (0.001)	32.01	248 (0.001)	26.05
		Off-Peak	368 (0.001)	47.42	257 (0.001)	50.99
90%	Base – CAV	Peak	582 (0.001)	35.97	314 (0.001)	32.98
		Off-Peak	398 (0.001)	54.07	283 (0.001)	56.15
100 %	Base – CAV	Peak	607 (0.001)	37.55	343 (0.001)	36.03
		Off-Peak	427 (0.001)	58.02%	298 (0.001)	59.13

#Difference is insignificant at 5% level

Furthermore, the negative binomial model was also developed for the two surrogate safety measures (i.e., TNC and NCJ) in order to quantify the effect of safety benefits in terms of MPRs and traffic conditions. The results of the models are shown in Table 23. Based on the results of negative binomial models, I found that the higher MPRs had significant lower number of conflicts and critical jerk compared to the baseline condition. It is worth mentioning that the higher the percentage of the CAV implemented, the higher were the safety benefits achieved in terms of surrogate safety measures. Regarding the traffic conditions, the off-peak period had significantly smaller number of conflicts and jerk value compared with the peak period.

Table 23 Negative Binomial Model Results for Traffic Safety Analysis

Parameter	TNC		TNCJ	
	Estimate	Wald Chi Square (P-value)	Estimate	Wald Chi Square (P-value)
Intercept	7.469	24220.70 (<0.0001)	6.963	15657.90 (<0.0001)
MPR 0%	Reference			
MPR 10%	-0.041	0.40 (0.527)	-0.028	0.14 (0.708)
MPR 20%	-0.079	1.46 (0.227)	-0.067	0.79 (0.374)
MPR 30%	-0.116	3.18 (0.075)	-0.122	2.60 (0.1066)
MPR 40%	-0.202	9.55 (0.002)	-0.192	6.39 (0.0115)
MPR 50%	-0.272	17.03 (<0.0001)	-0.260	11.65 (0.0006)
MRP 60%	-0.359	29.40 (<0.0001)	-0.326	18.11 (<0.0001)
MPR 70%	-0.439	43.32 (<0.0001)	-0.428	30.45 (<0.0001)
MPR 80%	-0.520	59.96 (<0.0001)	-0.481	38.08 (<0.0001)
MPR 90%	-0.589	75.80 (<0.0001)	-0.582	54.72 (<0.0001)
MPR 100%	-0.638	87.89 (<0.0001)	-0.637	64.63 (<0.0001)
Off-peak (vs Peak)	-0.959	1091.21 (<0.0001)	-0.859	649.26 (<0.0001)
Log Likelihood (Convergence)	-119.3390		-112.7880	
AIC	264.6779		251.5760	

For better visual representation, Figure 23 shows the decreasing trend of TNC and TNCJ for CAV scenarios with increasing MPRs.

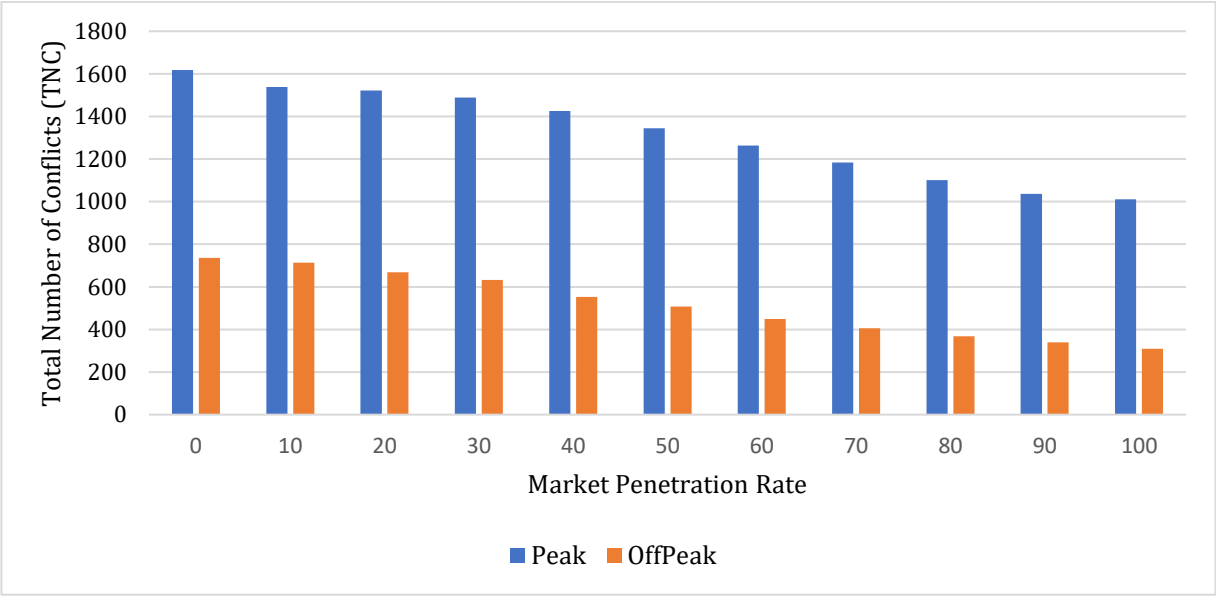

(a) Total Number of Conflicts (TNC)

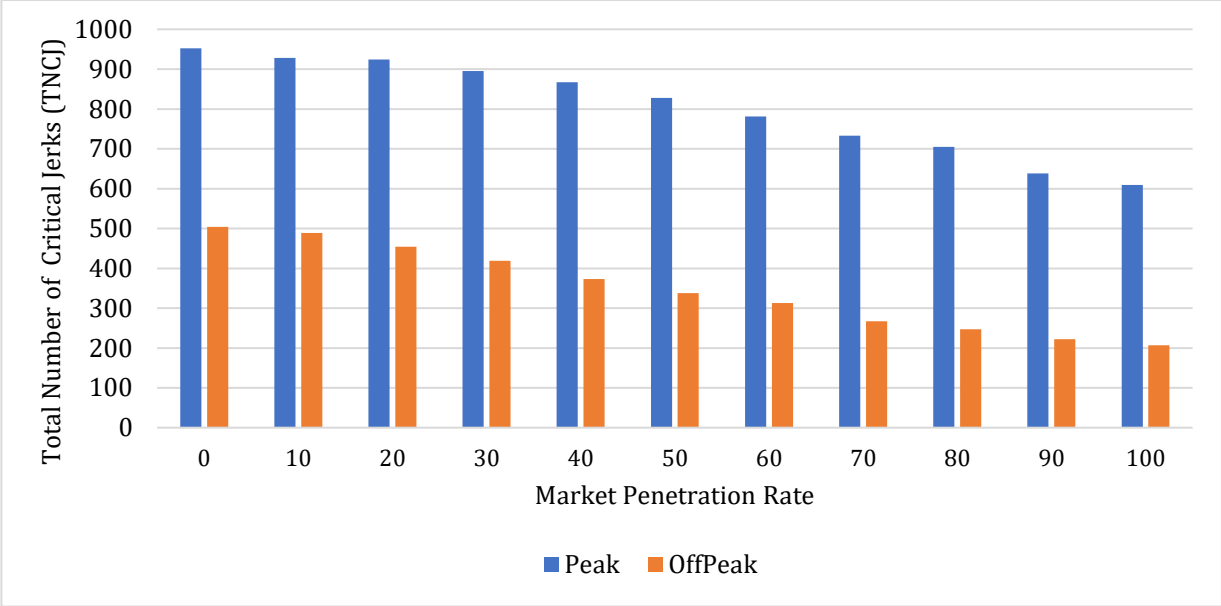

(b) Total Number of Critical Jerk (TNCJ)

Figure 23 Reduction of surrogate measures of safety with different MPRs.

As seen from the figures, the higher CAV implementation, the lower TNC and TNCJ values, and therefore the higher were the safety benefits achieved. Overall, the deployment of CAV technologies in the studied expressway would significantly decrease conflicts and jerk, and thereby increase the safety performance of the road network.

6.6 Summary and Conclusions

The primary objective of this study was to evaluate both traffic operation and safety benefits under connected and automated vehicle (CAV) technologies. The simulation experiments were designed in VISSIM and the baseline condition was calibrated and validated for both peak and of-peak period utilizing real-time detectors data. The driving behaviors of CAV were validated in VISSIM to approximate the decision process of CAV in simulation. Both traffic operation and safety measures were considered to evaluate the CAV technologies under different market penetration rates (MPRs). Average travel time (ATT) and the average delay (AD) were considered as traffic

mobility indicators, while total number of conflicts (TNC) (time proximity based surrogate measures) and total number of critical jerk (TNCJ) (evasive action –based surrogate measures) were considered as traffic safety indicators.

In general, CAV technologies improved the mobility and safety performances in expressway segments by providing significant reductions in ATT, AD, TNC, and TNCJ. Two sample t-test were conducted to evaluate the significance of CAV effectiveness for different MPRs over baseline scenario. From the results it is found that the higher percentages of CAV technologies implemented, higher were the mobility and safety benefits achieved. However, at least 30% and 20% MPR was needed to achieve both the safety and operational benefits of peak and off-peak hour, respectively. This chapter also found the lower variances in travel time and delay of CAV technologies for every 5 minutes interval which are expected to increase the travel time reliability of studied network. Tobit and negative binomial models were successfully developed to investigate the impacts of MPRs of CAV and traffic condition for traffic operation and safety effectiveness, respectively. Analysis of both operation and safety characteristics suggested that higher MPR increase both mobility and safety benefits and off-peak periods had better safety and operational performance (e.g., lower travel time, lower conflicts) compared to peak periods. Hence, the study has major implications for improving expressway facilities by recommending optimal market penetration of the CAV technologies considering both peak and off-peak periods.

The results of this particular study could provide useful insights to the decision maker or traffic operators about the optimized CAV MPR with considering both traffic operation and safety perspective including both peak and off-peak periods. The CAV technologies could be integrated

into a traffic microsimulation platform to simulate CAVs at a corridor-level in a mixed traffic stream and under different infrastructure and vehicle-based scenarios.

CHAPTER 7: CONCLUSIONS

7.1 Summary

This dissertation concentrates on different types of CAV effectiveness in both traffic safety and operation characteristics for different roadways, traffic, and weather conditions. The traffic safety and the mobility benefits were explored by utilizing different types of CAV technologies including CV, AV, and CV platooning. In this study, simulation modelling techniques were performed to analyze the effectiveness of CAV due to the lack of high-resolution CAV data. The baseline scenarios of the simulation model were built, calibrated, and validated by utilizing multiple detectors including traffic count, speed, and travel time. Meanwhile, the driving behavior of different types of CAV were modelled using C++ programming language in order to approximate the behavior of CAVs. Then, different MPR of CAVs were analyzed as the MPR is among the most critical issues in the near future. Furthermore, different scenarios of CAVs with different MPRs were compared with the baseline scenario. Different types of statistical tests (Two sample t-test, ANOVA) and modelling techniques were utilized (i.e., Logistic regression, Negative binomial, Tobit) to evaluate the effectiveness of market penetration rates and the traffic condition. Finally, the optimal market penetration rates of CAVs were identified to obtain the significant benefits for different types of traffic (i.e., peak and off-peak hour), roadway (i.e., freeway, expressway, arterial, managed lane), and weather condition (i.e., clear, reduced visibility).

In Chapter 3, two CV strategies were applied in dense fog condition in microsimulation. The strategies include connected vehicle without platooning (CVWPL) and connected vehicle with platooning (CVPL) technology. The car following model was proposed for both technologies with an assumption that the CVs will follow this car following behavior in fog condition. Additionally,

surrogate measures of safety including the standard deviation of speed, the standard deviation of headway, and read-end crash risk index (RCRI) were considered as proximal safety indicator in this study. Different MPRs were tested to observe the safety benefit under CV environment. In general, both CV technologies were improved safety in fog condition by providing significant reduction of standard deviation speed, headway, and RCRI. It was found that the higher MPRs of CV implemented, the higher safety benefit achieved. It is worth mentioning that maximum improvement was found to be significant at 100 % MPR while the improvement also achieved at 20% MPR but the result was not significant. A minimum of 30% MPR was needed to observe benefits from safety perspective compared to base scenario. The result showed that the connected vehicle with platooning technology significantly outperformed the one without platooning technology in terms of three surrogate measure of safety mentioned above. It was also found that at least 50 % market penetration rates were needed to achieve the benefit of safety for the CV with platooning technology compared to CV without platooning technology. Additionally, stabilize profile of both standard deviation of speed and headway also demonstrated that crash risk would decrease by implementing both CV technologies. On the other hand, simulation results asserted that speed was higher in both CV technologies compared to base scenario. Therefore, both CV technologies not only improved the traffic safety but also traffic operation. However, the average speed was larger in CV with platooning technology compared to CV without platooning technology. Hence, taking both traffic safety and operation into consideration, the CV with platooning technology outperformed CV without platooning technology. Overall, the traffic safety in fog condition was improved by the implementation of CV technologies. Additionally, the CVPL technology outperformed the CVWPL technology from a safety and operation perspective.

In Chapter 4, the primary objective of this study was to evaluate longitudinal safety of managed-lane CV platoons on expressways based on simulation results. The simulation experiments were firstly designed, including deployment of managed-lane CV platoons and all lanes CV platoons on a congested expressway. Then, a vehicle behavior model for CV platoon was used based on the IDM model and four surrogate safety measures, standard deviation of speed, TET, TIT, and TERCRI were utilized as indicators for safety evaluations. Sensitivity analysis were also conducted for different TTC thresholds to compare the results among the three scenarios. The distribution of four surrogate measures of safety approximately follow the normal distribution because of the stochastic nature of simulation. The values of standard deviation of speed, TET, TIT, and TERCRI of base scenario was largest. The results showed that both CV platoons scenarios improved safety significantly over non-CV scenario. However, managed-lane CV platoons showed the smaller value of those surrogate measures of safety compared to all lanes CV platoons. Hence, the scenario with managed-lane CV platoons has the lower longitudinal crash risks compared to all lanes CV platoons. Moreover, the result of one-way ANOVA analysis showed that the significant differences among the three tested scenarios and inferred that managed-lane CV platoons significantly outperformed all lanes CV platoons. And, the results of sensitivity analysis indicated that the TTC threshold ranging from 1 to 3 seconds have almost same results. Hence, the different TTC thresholds did not affect the simulation results.

In Chapter 5, we investigated the safety impact of connected vehicles (CV) and connected vehicle lower level automation (CVLLA) utilizing both vehicle to vehicle (V2V) and infrastructure-to-vehicle (I2V) communications on an urban arterial using microsimulation. Two automated feature such as automated braking and lane keeping assistance were considered to model the lower level

automated vehicle under V2V and I2V communication technologies. Safety performance of both CV technologies were tested in terms of segment and intersection crash risks using surrogate safety assessment modeling techniques. The driving behaviors of both CV and CVLLA were applied in VISSIM through C++ programming language. Five surrogate measures of safety including the TET, TIT, TERCRI, LCC, and NCJ were considered as segment crash risks indicators, while the intersection crash risks were evaluated using Surrogate Safety Assessment Model (SSAM). The safety benefits were observed under different MPRs for both CV technologies. In general, both CV and CVLLA technologies reduce segment crash risks by providing significant reductions of TET, TIT, and TERCRI. For intersection crash risks, logistic regression model results showed significant reduction of conflict frequency for CV scenarios compared to base scenario. For both segment and the intersection crash risks, it was found that the higher the MPRs of CV implemented the higher were the safety benefits achieved. Maximum improvement was found to be at 100% MPR for both CV and CVLLA technologies. For segment crash risks, a minimum of 30% MPR was needed to observe significant safety benefits of both CV and CVLLA technologies in terms of TET, TIT, and NCJ compared to the base scenario. However, it was found that at least 40% MPR is needed to achieve the safety benefits of intersection crash risks. Hence, taking both segment and the intersection crash risks into consideration, the CV and CVLLA technologies performed better than non-CV scenario. Finally, the results showed that the CVLLA significantly outperformed CV in terms of both segment and intersection crash risks. It was also found that at least 60% MPR was needed to achieve the safety benefits of segment and intersection crash risks of CVLLA compared to CV technologies.

In Chapter 6, the primary objective was to evaluate the traffic operation and safety benefits under CAV technologies. The simulation experiments were designed in VISSIM and the baseline condition was calibrated and validated for both peak and of-peak period utilizing real-time detectors data. The driving behaviors of CAV were validated in VISSIM to approximate the decision process of CAV in simulation. Both traffic operation and safety measures were considered to evaluate the CAV technologies under different market penetration rates (MPRs). Average travel time (ATT) and the average delay (AD) were considered as traffic mobility indicators, while total number of conflicts (TNC) (time proximity based surrogate measures) and total number of critical jerk (TNCJ) (evasive action –based surrogate measures) were considered as traffic safety indicators. In general, CAV technologies improved the mobility and safety performances in expressway segments by providing significant reductions in ATT, AD, TNC, and TNCJ. Two sample t-test were conducted to evaluate the significance of CAV effectiveness for different MPRs over baseline scenario. From the results it is found that the higher percentages of CAV technologies implemented, higher were the mobility and safety benefits achieved. However, at least 30% and 20% MPR was needed to achieve both the safety and operational benefits of peak and off-peak hour, respectively. We also found the lower variances in travel time and delay of CAV technologies for every 5 minutes interval which are expected to increase the travel time reliability of studied network. Tobit and negative binomial models were successfully developed to investigate the impacts of MPRs of CAV and traffic condition for traffic operation and safety effectiveness, respectively. Analysis of both operation and safety characteristics suggested that higher market penetration rate increase both mobility and safety benefits and off-peak periods had better safety and operational performance (e.g., lower travel time, lower conflicts) compared to peak periods.

Hence, the study has major implications for improving expressway facilities by recommending optimal market penetration of the CAV technologies considering both peak and off-peak periods.

7.2 Implications

Chapter 3 evaluated the traffic safety and operational benefits of different CV technologies (i.e., CVPL, CVWPL) in reduced visibility conditions. From the simulation model results, both CVPL and CVWPL significantly outperformed the baseline condition when the MPRs were at least 30%. Meanwhile, the model results also found that the CVPL significantly outperformed CVWPL for the MPRs of 50% or higher in reduced visibility (i.e., fog) conditions. These findings imply that driving behaviors of CV would have significant impacts on both traffic safety and operations under inclement weather. It is recommended that at least 30% MPR of CV technologies could reduce significant number of traffic conflicts (surrogate of traffic crashes) and enhance traffic mobilities in fog conditions compared to clear weather conditions. Hence, if engineers intend to decrease fog related crashes, the CV technologies would be a viable option to improve both the traffic safety and operational characteristics.

Chapter 4 have already proved that the usage of CV managed-lane would reduce the significant number of conflicts for the studied congested expressways. As the full MPRs of CV may not be available in the foreseeable future, the decision maker can operate the CVs in the managed-lane to obtain the significant safety benefits. Meanwhile, the interaction between CVs and conventional vehicles might not have great issues if CVs are implemented as managed lane concept. Therefore, it is suggested that CV managed-lane could be useful strategies in the CV transition period.

Chapter 5 provides some important implications for CAV practitioners for arterial traffic. CV and CVLLA can reduce both intersection and segment crash risk considering both evasive action-based and time-proximity based surrogates measures. Meanwhile, for segment crash risks, a minimum of 30% MPR was needed to observe significant safety benefits of CAVs in terms surrogate safety measures. However, it was found that at least 40% MPR is needed to achieve the safety benefits of intersection crash risks. This finding implies that studying the connected and lower level automated vehicle in arterials might be a worthwhile endeavor in the transition period of lower level to full automation.

Chapter 6 utilized CAV model validated by real-world CAV data to observe both traffic safety and operation benefits under different traffic conditions (i.e., peak and off-peak hours). Meanwhile, the interaction between the CAVs and conventional vehicles were evaluated correctly in terms of real-world validated CAV data. The optimal market penetration rates of CAV for both peak and off-peak period were evaluated. From both traffic safety and operation perspective, at least 20% and 30% MPR is needed to achieve significant safety and operational benefits for off-peak and peak hour, respectively. Therefore, the finding of this study has major implications for improving expressway facilities by recommending optimal MPR of CAV to achieve balanced mobility and safety benefits with varying traffic conditions.

REFERENCES

Abdel-Aty, M.A., Oloufa, A., Peng, Y., Shen, T., Yang, X., Lee, J., 2014. Real time monitoring and prediction of reduced visibility events on florida's highways. Report, BDV24 962–1.

Abdel-Aty, M., Ahmed, M.M., Lee, J., Shi, Q., Abuzwidah, M., 2012. Synthesis of Visibility Detection Systems. Univ. Cent. Florida, Orlando, FL, USA, Final Rep.

Abdel-Aty, M., Dilmore, J., Dhindsa, A., 2006. Evaluation of variable speed limits for real-time freeway safety improvement. Accid. Anal. Prev. 38 2 , 335–345. doi:10.1016/j.aap.2005.10.010

Abdel-Aty, M., Ekram, A.A., Huang, H., Choi, K., 2011. A study on crashes related to visibility obstruction due to fog and smoke. Accid. Anal. Prev. 43 5 , 1730–1737. doi:10.1016/j.aap.2011.04.003

Abdel-Aty, M., Haleem, K., Cunningham, R., Gayah, V., 2009. Application of variable speed limits and ramp metering to improve safety and efficiency of freeways., in: 2nd International Symposium on Freeway and Tollway Operations. pp. 1–13.

Abdel-Aty, M., Lee, J., Wang, L., Cai, Q., Saad, M., Yuan, J., 2017. Phase II : Operational and Safety-Based Analyses of Varied Toll Lane Configurations. SAFER-SIM Univ. Transp. Center, Iowa City, IA.

Abdel-Aty, M., Wang, X., 2006a. Crash Estimation at Signalized Intersections Along Corridors: Analyzing Spatial Effect and Identifying Significant Factors. Transp. Res. Rec. 1953 1953 , 98–111. doi:10.3141/1953-12

Abdel-Aty, M., Wang, X., 2006b. Crash Estimation at Signalized Intersections Along Corridors: Analyzing Spatial Effect and Identifying Significant Factors. Transp. Res. Rec. 1953, 98–111. doi:10.3141/1953-12

Abdelfatah, A., Marzouk, M., Garib, A., Hussain, A.-H., 2013. Effect of fog on freeway performance : initial results. 13th World Conf. Transp. Res. Janeiro, Brazil 1–11.

Al-Ghamdi, A.S., 2007. Experimental evaluation of fog warning system. Accid. Anal. Prev. 39 6 , 1065–1072. doi:10.1016/j.aap.2005.05.007

American Association of State Highway and Transportation Officials (AASHTO), 2004. A policy on geometric design of highways and streets. Washington, D.C.

Arvin, R., Kamrani, M., Khattak, A.J., 2019. How instantaneous driving behavior contributes to crashes at intersections : Extracting useful information from connected vehicle message data. Accid. Anal. Prev. 127 January , 118–133. doi:10.1016/j.aap.2019.01.014

Atkins, 2016. Research on the Impacts of Connected and Autonomous Vehicles (CAVs) on Traffic Flow. Dep. Transp.

Bagdadi, O., Várhelyi, A., 2011. Jerky driving - An indicator of accident proneness? Accid. Anal. Prev. 43 4 , 1359–1363. doi:10.1016/j.aap.2011.02.009

Brackstone, M., McDonald, M., 1999. Car-following: A historical review. Transp. Res. Part F Traffic Psychol. Behav. 2 4 , 181–196. doi:10.1016/S1369-8478(00)00005-X

Brooks, J.O., Crisler, M.C., Klein, N., Goodenough, R., Beeco, R.W., Guirl, C., Tyler, P.J., Hilpert, A., Miller, Y., Grygier, J., Burroughs, B., Martin, A., Ray, R., Palmer, C., Beck, C., 2011. Speed choice and driving performance in simulated foggy conditions. Accid. Anal. Prev. 43 3 , 698–705. doi:10.1016/j.aap.2010.10.014

Broughton, K.L.M., Switzer, F., Scott, D., 2007. Car following decisions under three visibility conditions and two speeds tested with a driving simulator. Accid. Anal. Prev. 39 1 , 106–116. doi:10.1016/j.aap.2006.06.009

Cai, Q., Saad, M., Abdel-Aty, M., Yuan, J., Lee, J., 2018. Safety Impact of Weaving Distance on

Freeway Facilities with Managed Lanes using Both Microscopic Traffic and Driving Simulations. Transp. Res. Rec. doi:10.1177/0361198118780884

Caro, S., Cavallo, V., Marendaz, C., Boer, E.R., Vienne, F., 2009. Can headway reduction in fog be explained by impaired perception of relative motion? Hum. Factors 51 3 , 378–392. doi:10.1177/0018720809339621

Derbel, O., Mourllion, B., Basset, M., 2012. Safety assessment of mixed traffic based on accident scenario, IFAC Proceedings Volumes (IFAC-PapersOnline). IFAC. doi:10.3182/20120912-3-BG-2031.00025

Duell, M., Saxena, N., Chand, S., Amini, N., Grzybowska, H., Waller, S.T., 2016. Deployment and Calibration Considerations for Large-Scale Regional Dynamic Traffic Assignment. Transp. Res. Rec. J. Transp. Res. Board 2567, 78–86.

Fagnant, D.J., Kockelman, K., 2015. Preparing a nation for autonomous vehicles : opportunities , barriers and policy recommendations. Transp. Res. Part A 77, 167–181. doi:10.1016/j.tra.2015.04.003

Fan, R., Wang, W., Liu, P., Yu, H., 2013. Using VISSIM simulation model and Surrogate Safety Assessment Model for estimating field measured traffic conflicts at freeway merge areas. IET Intell. Transp. Syst. 7 1 , 68–77. doi:10.1049/iet-its.2011.0232

Fernandes, P., Nunes, U., 2010. Platooning of autonomous vehicles with intervehicle communications in SUMO traffic simulator. IEEE Conf. Intell. Transp. Syst. Proceedings, ITSC 1313–1318. doi:10.1109/ITSC.2010.5625277

FHWA, 2012. Traffic Analysis Toolbox Volume XIV: Guidebook on the Utilization of Dynamic Traffic Assignment in Modeling. U.S. Dep. Transp. Report No. FHWA-HOP-13-015, Washington, D.C .

Fyfe, M., Sayed, T., 2017. Safety Evaluation of Connected Vehicles for a Cumulative Travel Time Adaptive Signal Control Microsimulation Using the Surrogate Safety Assessment Model. Transp. Res. Board 96th Annu. Meet. 17–01651 .

Genders, W., Razavi, S.N., 2016. Impact of Connected Vehicle on Work Zone Network Safety through Dynamic Route Guidance. J. Comput. Civ. Eng. 30 2 . doi:10.1061/(ASCE)CP.1943-5487.0000490

Gettman, D., Head, L., 2003. Surrogate safety measures from traffic simulation models. Transp. Res. Rec. J. Transp. Res. Board 1840, 104–115.

Gettman, D., Pu, L., Sayed, T., Shelby, S.G., 2008. Surrogate safety assessment model and validation. Fed. Highw. Adm. Off. Saf. Res. Dev. FHWA-HRT-08-051 .

Glad, R.W., 2001. Weave Analysis and performance: The Washington State case study. (No:WA-RD 515.1) .

Golob, T.F., Recker, W.W., Alvarez, V.M., 2004. Safety aspects of freeway weaving sections. Transp. Res. Part A Policy Pract. 38 (1) , 35–51.

Gong, Y., Abdel-Aty, M., Cai, Q., Rahman, M.S., 2019. A Decentralized Network Level Adaptive Signal Control Algorithm by Deep Reinforcement Learning, in: Transportation Research Board 98th Annual Meeting.

Guériau, M., Billot, R., El Faouzi, N.E., Monteil, J., Armetta, F., Hassas, S., 2016. How to assess the benefits of connected vehicles? A simulation framework for the design of cooperative traffic management strategies. Transp. Res. Part C Emerg. Technol. 67, 266–279. doi:10.1016/j.trc.2016.01.020

Guo, Y., Ph, D., Sayed, T., Ph, D., Eng, P., Zaki, M.H., Ph, D., 2018. Exploring Evasive Action – Based Indicators for PTW Conflicts in Shared Traffic Facility Environments. J. Transp. Eng.

Part A Syst. 144 11 , 1–10. doi:10.1061/JTEPBS.0000190.

Habtemichael, F., Picado-Santos, L., 2013. Sensitivity analysis of VISSIM driver behavior parameters on safety of simulated vehicles and their interaction with operations of simulated traffic, in: 92nd Annual Meeting of the Transportation Research Board. Washington, DC.

Hadi, M., Xiao, Y., Wang, T., Iqbal, M.S., Massahi, A., Jia, J., Chen, X., Fartash, H., 2015. Decision Support Systems for Transportation System Management and Operations. Florida Dep. Transp.

Hadi, M., Xiao, Y., Wang, T., Qom, S.F., Azizi, L., Iqbal, M.S., Jia, J., Massahi, A., 2016. Framework for Multi-Resolution Analyses of Advanced Traffic Management Strategies FDOT Project BDV29-977-19. Tech. Report. Florida Int. Univ.

Hassan, H., Abdel-Aty, M., Oloufa, A., 2011. Effect of warning messages and variable speeds in different visibility conditions. Transp. Res. Board 90th Annu. Meet. 11–0354 .

Hassan, H.M., Abdel-Aty, M.A., Choi, K., Algadhi, S.A., 2012. Driver behavior and preferences for changeable message signs and variable speed limits in reduced visibility conditions. J. Intell. Transp. Syst. 16 3 , 132–146. doi:10.1080/15472450.2012.691842

Hayward, J.C., 1972. Near-miss determination through use of a scale of danger. Highw. Res. Board. Washington, D.C.

Helbing, D., Tilch, B., 1998. Generalized Force Model of Traffic Dynamics. Phys. Rev. E 58 1 , 133–138. doi:10.1103/PhysRevE.58.133

Hellinga, B., Mandelzys, M., 2011. Impact of driver compliance on the safety and operational impacts of freeway variable speed limit systems. J. Transp. Eng. 137 4 , 260–268. doi:10.1061/(ASCE)TE.1943-5436.0000214.

Ilgin Guler, S., Menendez, M., Meier, L., 2014. Using connected vehicle technology to improve

the efficiency of intersections. Transp. Res. Part C Emerg. Technol. 46, 121–131. doi:10.1016/j.trc.2014.05.008

Jin, Q., Wu, G., Boriboonsomsin, K., Barth, M., 2014. Improving traffic operations using real-time optimal lane selection with connected vehicle technology. IEEE Intell. Veh. Symp. Proc. 70–75. doi:10.1109/IVS.2014.6856515

Jin, Q., Wu, G., Boriboonsomsin, K., Barth, M., 2013. Platoon-based multi-agent intersection management for connected vehicle. IEEE Conf. Intell. Transp. Syst. Proceedings, ITSC 1462–1467. doi:10.1109/ITSC.2013.6728436

Jolovic, D., Stevanovic, A., 2012. Evaluation of vissim and freeval to assess an oversaturated freeway weaving segmen, in: TRB Annual Meeting.

Kamrani, M., Arvin, R., Khattak, A.J., 2018. Extracting useful information from connected vehicle data: an empirical study of driving volatility measures and crash frequency at intersections, in: 97th Annual Meeting of theTransportation Research Board.

Kamrani, M., Khattak, A.J., Wali, B., 2017. Can data generated by connected vehicles enhance safety? Proactive approach to intersection safety manageme, in: 96th Annual Meeting of the Transportation Research Board.

Kesting, A., Treiber, M., 2013. Traffic flow dynamics: data, models and simulation. Springer Berlin Heidelberg, Berlin, Heidelb.

Kesting, A., Treiber, M., Helbing, D., 2010a. Enhanced intelligent driver model to access the impact of driving strategies on traffic capacity. Philos. Trans. R. Soc. London A Math. Phys. Eng. Sci. 368 1928 , 4585–4605. doi:10.1098/rsta.2010.0084

Kesting, A., Treiber, M., Helbing, D., 2010b. Enhanced intelligent driver model to access the impact of driving strategies on traffic capacity. Philos. Trans. A. Math. Phys. Eng. Sci. 368

(1928) , 4585–4605.

Kesting, A., Treiber, M., Schönhof, M., Helbing, D., 2008. Adaptive cruise control design for active congestion avoidance. Transp. Res. Part C Emerg. Technol. 16 (6) , 668–683.

Khondaker, B., Kattan, L., 2015. Variable speed limit: A microscopic analysis in a connected vehicle environment. Transp. Res. Part C Emerg. Technol. 58, 146–159.

Kim, K., Park, B.-J., 2016. Safety features of freeway weaving segments with buffer-separated high-occupancy-vehicle (hov) lane, in: Transportation Research Board 95th Annual Meeting (No:16-3055).

Kim, K., Yook, D., Ko, Y., Kim, D., 2015. An analysis of expected effects of the autonomous vehicles on transport and land use in Korea.

Kim, S.-J., Kim, W., Rilett, L.R., 2005. Calibration of microsimulation models using nonparametric statistical techniques. Transp. Res. Rec. 1935, 111–119. doi:10.3141/1935-13

Kockelman, K., Avery, P., Bansal, P., Boyles, S.D., Bujanovic, P., Choudhary, T., Clements, L., Domnenko, G., Fagnant, D., Helsel, J., Hutchinson, R., Levin, M., Li, J., Li, T., Loftus-Otway, L., Nichols, A., Simoni, M., Stewart, D., 2016. Implications of connected and automated vehicles on the safety and operations of roadway networks: A final report 7 FHWA/TX-16/0-6849-1, 0-6849-1 . doi:FHWA/TX-16/0-6849-1

Koppula, N., 2002. A comparative analysis of weaving areas in hcm, transims, corsim, vissim and integration. Thesis, Virginia Polytech. Institute.

Lee, C., Hellinga, B., Saccomanno, F., 2006. Evaluation of variable speed limits to improve traffic safety. Transp. Res. Part C Emerg. Technol. 14 3 , 213–228. doi:10.1016/j.trc.2006.06.002

Lee, J., Abdel-Aty, M., Rahman, M., 2018. Enhancing School Zone and School Bus Safety. SAFER-SIM Univ. Transp. Center, Iowa City, IA.

Lee, J., Park, B., 2012. Development and evaluation of a cooperative vehicle intersection control algorithm under the connected vehicles environment. IEEE Trans. Intell. Transp. Syst. 13 1 , 81–90. doi:10.1109/TITS.2011.2178836

Letter, C., Elefteriadou, L., 2017. Efficient control of fully automated connected vehicles at freeway merge segments. Transp. Res. Part C Emerg. Technol. 80, 190–205. doi:10.1016/j.trc.2017.04.015

Li, Y., Li, Z., Wang, H., Wang, W., Xing, L., 2017a. Evaluating the safety impact of adaptive cruise control in traffic oscillations on freeways. Accid. Anal. Prev. 104, 137–145.

Li, Y., Wang, H., Wang, W., Liu, S., Xiang, Y., 2016a. Reducing the risk of rear-end collisions with infrastructure-to-vehicle (I2V) integration of variable speed limit control and adaptive cruise control system. Traffic Inj. Prev. 17 (6) , 597–603.

Li, Y., Wang, H., Wang, W., Liu, S., Xiang, Y., 2016b. Reducing the risk of rear-end collisions with infrastructure-to-vehicle (I2V) integration of variable speed limit control and adaptive cruise control system. Traffic Inj. Prev. 17 6 , 597–603. doi:10.1080/15389588.2015.1121384

Li, Y., Wang, H., Wang, W., Xing, L., Liu, S., Wei, X., 2017b. Evaluation of the impacts of cooperative adaptive cruise control on reducing rear-end collision risks on freeways. Accid. Anal. Prev. 98, 87–95.

Li, Z., Chitturi, M., Zheng, D., Bill, A., Noyce, D., 2013. Modeling Reservation-Based Autonomous Intersection Control in VISSIM. Transp. Res. Rec. J. Transp. Res. Board 2381, 81–90. doi:10.3141/2381-10

Li, Z., Li, Y., Liu, P., Wang, W., Xu, C., 2014. Development of a variable speed limit strategy to reduce secondary collision risks during inclement weathers. Accid. Anal. Prev. 72, 134–145.

Liu, J., Khattak, A.J., 2018. Mapping location-based driving volatility for connected and

automated vehicles, in: 97th Annual Meeting of theTransportation Research Board.

Liu, J., Khattak, A.J., 2016. Delivering improved alerts , warnings , and control assistance using basic safety messages transmitted between connected vehicles q. Transp. Res. PART C 68, 83–100. doi:10.1016/j.trc.2016.03.009

Lownes, N., Machemehl, R., 2006. Sensitivity of simulated capacity to modification of VISSIM driver behavior parameters. Transp. Res. Rec. J. Transp. Res. Board 1988, 102–110. doi:10.3141/1988-15

Luo, L., Joshua, S., 2011. Examination of Traffic Incident Management Strategies via Multi-Resolution Modeling with Dynamic Traffic Assignment. Transp. Res. Board 90th Annu. Meet.

Lyles, R.W., Taylor, W.C., Lavansiri, D., Grossklaus, J., 2004. Field test of variable speed limits in work zones. 83rd Annu. Meet. Transp. Res. Board, Washington, D.C.

M Bando, K Hasebe, a Nakayama, a Shibata, Y.S., 1995. Dynamical model of traffic congestion and numerical simulation. Phys. Rev. E. Stat. Phys. Plasmas. Fluids. Relat. Interdiscip. Topics 51 2 , 1035–1042. doi:10.1371/journal.pcbi.1002329

Milanés, V., Shladover, S.E., 2014. Modeling cooperative and autonomous adaptive cruise control dynamic responses using experimental data. Transp. Res. Part C Emerg. Technol. 48, 285–300.

Minderhoud, M.M., Bovy, P.H.L., 2001. Extended time-to-collision measures for road traffic safety assessment. Accid. Anal. Prev. 33 (1) , 89–97.

Mirheli, A., Hajibabai, L., Hajbabaie, A., 2018. Development of a signal-head-free intersection control logic in a fully connected and autonomous vehicle environment. Transp. Res. Part C Emerg. Technol. 92, 412–425.

Morando, M.M., Tian, Q., Truong, L.T., Vu, H.L., 2018. Studying the Safety Impact of Autonomous Vehicles Using Simulation-Based Surrogate Safety Measures. J. Adv. Transp. doi:10.1155/2018/6135183

National Highway Traffic Safety Administration, 2016. Vehcile-to-vehicle communication technology for light vehicles. Washingt. DC US Dep. Transp. FMVSS 150 .

Nezamuddin, N., Jiang, N., Zhang, T., Waller, S.T., 2011. Traffic operations and safety benefits of active traffic strategies on txdot freeways Publication Number: FHWA. TX-12/0-6576-1, USA. .

Nygård, M., 1999. A Method for Analysing Traffic Safety with Help of Speed Profiles. Tampere University of Technology. Tampere Univ. Technol.

Oh, C., Park, S., Ritchie, S.G., 2006. A method for identifying rear-end collision risks using inductive loop detectors. Accid. Anal. Prev. 38 (2) , 295–301.

Olia, A., Abdelgawad, H., Abdulhai, B., Razavi, S.N., 2016. Assessing the potential impacts of connected vehicles: mobility, environmental, and safety perspectives. J. Intell. Transp. Syst. 20 3 , 229–243. doi:10.1080/15472450.2015.1062728

Paikari, E., Tahmasseby, S., Far, B., 2014. A simulation-based benefit analysis of deploying connected vehicles using dedicated short range communication, in: Intelligent Vehicles Symposium Proceedings, IEEE. pp. 980–985.

Pang, M.B., Zheng, S.S., Cai, Z.H., 2015. Simulation of three lanes one-way freeway in low visibility weather by possible traffic accidents. Phys. A Stat. Mech. its Appl. 433, 161–170. doi:10.1016/j.physa.2015.03.066

Papadoulis, A., Quddus, M., Imprialou, M., 2019. Evaluating the safety impact of connected and autonomous vehicles on motorways. Accid. Anal. Prev. 124 January , 12–22.

doi:10.1016/j.aap.2018.12.019

Peng, Y., Abdel-Aty, M., Shi, Q., Yu, R., 2017. Assessing the impact of reduced visibility on traffic crash risk using microscopic data and surrogate safety measures. Transp. Res. Part C Emerg. Technol. 74, 295–305.

Perrin, J., Martin, P.T., Coleman, B., 2002. Testing the adverse visibility information system evaluation (ADVISE): Safer driving in fog. Transp. Res. Board 81st Annu. Meet.

Plattner, B., Karnik, N., Jo, B., Hall, R.E., Schallauer, A., Carrion, V., Feucht, M., Steiner, H., 2007. State and trait emotions in delinquent adolescents. Child Psychiatry Hum. Dev. 38 2 , 155–169. doi:10.1016/j.aap.2017.11.036

Poczter, S.L., 2014. The Google Car : Driving Toward A Better Future ? J. Bus. Case Stud. 10 1 , 7–14.

Pourabdollah, M., Bjarkvik, E., Furer, F., Lindenberg, B., Burgdorf, K., 2018. Calibration and evaluation of car following models using real-world driving data. IEEE Conf. Intell. Transp. Syst. Proceedings, ITSC 2018–March June 2018 , 1–6. doi:10.1109/ITSC.2017.8317836

Pravinvongvuth, S., Loudon, W.R., 2011. Development and Application of the First Large-Scale Hybrid Meso-Microsimulation Model in Practice. Transp. Res. Board 90th Annu. Meet.

PTV Group, 2019. PTV Group. (2014). Ptv vissim 11.0 user manual.

Pulugurtha, S.S., Bhatt, J., 2010. Evaluating the role of weaving section characteristics and traffic on crashes in weaving areas. Traffic Inj. Prev. 11 (1) , 104–13.

Qian, X., Gregoire, J., Moutarde, F., Fortelle, A.D. La, 2014. Priority-based coordination of autonomous and legacy vehicles at intersection. IEEE Conf. Intell. Transp. Syst. Proceedings, ITSC 1166–1171.

Rahman, M.H., Abdel-Aty, M., Lee, J., Rahman, M.S., 2019. Enhancing Traffic Safety at School

Zones by Operation and Engineering Countermeasures: A Microscopic Simulation Approach. Simul. Model. Pract. Theory.

Rahman, M.S., 2018. Applying Machine Learning Techniques to Analyze the Pedestrian and Bicycle Crashes at the Macroscopic Level. Electron. Theses Diss.

Rahman, M.S., Abdel-Aty, M., 2018. Longitudinal safety evaluation of connected vehicles' platooning on expressways. Accid. Anal. Prev. 117, 381–391.

Rahman, M.S., Abdel-Aty, M., Hasan, S., Cai, Q., 2019a. Applying machine learning approaches to analyze the vulnerable road- users' crashes at statewide traffic analysis zones. J. Safety Res. doi:10.1016/j.jsr.2019.04.008

Rahman, M.S., Abdel-Aty, M., Hasan, S., Cai, Q., 2019b. Applying Data Mining Techniques to Analyze the Pedestrian and Bicycle Crashes at the Macroscopic Level, in: Transportation Research Board 98th Annual MeetingTransportation Research Board.

Rahman, M.S., Abdel-aty, M., Lee, J., Rahman, H., 2019c. Understanding the Safety Benefits of Connected and Automated Vehicles on Arterials' Intersections and Segments, in: Transportation Research Board 98th Annual Meeting.

Rahman, M.S., Abdel-Aty, M., Lee, J., Rahman, H., 2019d. Safety benefits of arterials ' crash risk under connected and automated vehicles 1. Transp. Res. Part C 100 July 2018 , 354–371. doi:10.1016/j.trc.2019.01.029

Rahman, M.S., Abdel-Aty, M., Wang, L., Lee, J., 2018a. Understanding the Highway Safety Benefits of Different Approaches of Connected Vehicles in Reduced Visibility Conditions. Transp. Res. Rec. J. Transp. Res. Board.

Rahman, M.S., Abdel-Aty, M., Wang, L., Lee, J., 2018b. Understanding the Highway Safety Benefits of Different Approaches of Connected Vehicles in Reduced-Visibility Conditions.

Transp. Res. Rec. J. Transp. Res. Board.

Rämä, P., 1999. Effects of weather-controlled variable speed limits and warning signs on driver behavior. Transp. Res. Rec. J. Transp. Res. Board 1689, 53–59.

Saad, M., Abdel-Aty, M., Cai, Q., Lee, J., 2019a. Bicycle Safety Analysis at Intersections from Crowdsourced Data. Transp. Res. Rec. J. Transp. Res. Board.

Saad, M., Abdel-aty, M., Lee, J., 2019b. Analysis of driving behavior at expressway toll plazas. Transp. Res. Part F Psychol. Behav. 61, 163–177. doi:10.1016/j.trf.2017.12.008

Saad, M., Abdel-aty, M., Lee, J., Wang, L., 2019c. Integrated Safety and Operational Analysis of the Access Design of Managed Toll Lanes. Transp. Res. Rec. doi:10.1177/0361198118823502

Saad, M., Abdel-aty, M., Lee, J., Wang, L., 2018a. Determining the optimal access design of managed lanes considering dynamic pricing, in: 18th International Conference Road Safety on Five Continents.

Saad, M., Abdel-Aty, M., Lee, J., Wang, L., 2018b. Safety Analysis of Access Zone Design for Managed Toll Lanes on Freeways. J. Transp. Eng. Part A Syst. 144 11 , 1–13. doi:10.1061/JTEPBS.0000191.

Saad, M., Abdel-Aty, M., Lee, J., Wang, L., 2018. Access Design Safety Analysis for Managed Lanes Including Accessibility Level and Weaving Length. Transp. Res. Board 97th Annu. Meet. Res. Board.

Shafiei, S., Gu, Z., Sarvi, M., Saberi, M., Board, T.R., 2017. Deployment and Calibration of Large-Scale Mesoscopic Dynamic Traffic Assignment Model of Melbourne, Australia. Transp. Res. Board 96th Annu. Meet. Annu. Meet.

Singh, S., 2015. Critical Reasons for Crashes Investigated in the National motor Vehicle Crash

Causation Survey. Natl. Cent. Stat. Anal. DOT HS 812 115 .

Sultan, B., Brackstone, M., McDonald, M., 2002. Parameter analysis for collision avoidance systems, in: 9th World Congress on Intelligent Transport Systems.

Tageldin, A., Sayed, T., 2016. Developing evasive action-based indicators for identifying pedestrian conflicts in less organized traffic environments Ahmed. Turkish Online J. Educ. Technol. 2016 july , 248–254. doi:10.1002/atr

Tageldin, A., Sayed, T., Wang, X., 2015. Can Time Proximity Measures Be Used as Safety Indicators in All Driving Cultures? Transp. Res. Rec. J. Transp. Res. Board 2520 January , 165–174. doi:10.3141/2520-19

Tajalli, M., Hajbabaie, A., 2018. Collision mitigation at signalized intersection using connected vehicles. 97th Annu. Meet. Transp. Res. Board.

Talebpour, A., Mahmassani, H., 2015. Influence of Autonomous and Connected Vehicles on Stability of Traffic Flow. Transp. Res. Board 94th Annu. Meet.

Talebpour, A., Mahmassani, H.S., 2016a. Influence of connected and autonomous vehicles on traffic flow stability and throughput. Transp. Res. Part C Emerg. Technol. 71, 143–163.

Talebpour, A., Mahmassani, H.S., 2016b. Influence of connected and autonomous vehicles on traffic flow stability and throughput. Transp. Res. Part C Emerg. Technol. 71, 143–163.

Talebpour, A., Mahmassani, H.S., Elfar, A., 2017. Investigating the effects of reserved lanes for autonomous vehicles on congestion and travel time reliability. Transp. Res. Rec. J. Transp. Res. Board 2622, 1–12.

Talebpour, A., Mahmassani, H.S., Hamdar, S.H., 2015. Modeling Lane-Changing Behavior in a Connected Environment: A Game Theory Approach. Transp. Res. Procedia 7, 420–440.

Teukolsky, W. H., S., Vetterling, W., Flannery, B., 2002. Numerical Recipes in C: The Art of

Scientific Computing. Cambridge Univ. Press.

Tian, D., Zhou, J., Wang, Y., Sheng, Z., Xia, H., Yi, Z., 2016. Modeling chain collisions in vehicular networks with variable penetration rates. Transp. Res. Part C Emerg. Technol. 69, 36–59.

Tokishi, J., Chiu, Y.-C., 2013. Evaluation and Improvement of Consistency of Hybrid and Multi-Resolution Traffic Simulation Models. Transp. Res. Board 92nd Annu. Meet.

Treiber, M., Hennecke, A., Helbing, D., 2000. Congested traffic states in empirical observations and microscopic simulations. Phys. Rev. E 62 (2) , 1805–1824.

Treiber, M., Kesting, A., Helbing, D., 2007. Influence of reaction times and anticipation on stability of vehicular traffic flow. Transp. Res. Rec. J. Transp. Res. Board 1999, 23–29. doi:10.3141/1999-03

VISSIM, P.T.V., 2017. 10.0 User Manual. Karlsruhe, Niemcy.

Wan, N., Vahidi, A., Luckow, A., 2016. Optimal speed advisory for connected vehicles in arterial roads and the impact on mixed traffic. Transp. Res. Part C Emerg. Technol. 69, 548–563. doi:10.1016/j.trc.2016.01.011

Wang, L., Abdel-Aty, M., Lee, J., 2017. Implementation of active traffic management strategies for safety of a congested expressway weaving segment. Transp. Res. Rec. J. Transp. Res. Board 2635, 28–35.

Wang, X., Abdel-Aty, M., 2006. Temporal and spatial analyses of rear-end crashes at signalized intersections. Accid. Anal. Prev. 38 6 , 1137–1150. doi:10.1016/j.aap.2006.04.022

Wang, X., Yuan, J., Schultz, G.G., Fang, S., 2018. Investigating the safety impact of roadway network features of suburban arterials in Shanghai. Accid. Anal. Prev. 113 January , 137–148. doi:10.1016/j.aap.2018.01.029

Wen-Xing, Z., Li-Dong, Z., 2018. A new car-following model for autonomous vehicles flow with mean expected velocity field. Phys. A Stat. Mech. its Appl. 492, 2154–2165. doi:10.1016/j.physa.2017.11.133

Woody, T., 2006. Calibrating freeway simulation models in vissim. Univ. Washingt. Seattle CEE, 416, 580.

Wu, W., Li, P.K., Zhang, Y., 2015. Modelling and Simulation of Vehicle Speed Guidance in Connected Vehicle Environment. Int. J. Simul. Model. 14 1 , 145–157. doi:10.2507/IJSIMM14(1)CO3

Wu, Y., Abdel-Aty, M., Wang, L., Rahman, M.S., 2019a. Improving Flow and Safety in Low Visibility Conditions by Applying Connected Vehicles and Variable Speed Limits Technologies, in: Transportation Research Board 98th Annual Meeting.

Wu, Y., Abdel-aty, M., Wang, L., Rahman, S., 2019b. Combined connected vehicles and variable speed limit strategies to reduce rear-end crash risk under fog conditions. J. Intell. Transp. Syst. 1–20. doi:10.1080/15472450.2019.1634560

Wu, Z., Sun, J., Yang, X., 2005. Calibration of VISSIM for shanghai expressway using genetic algorithm, in: Simulation Conference, 2005 Proceedings of the Winter. IEEE. p. 4–pp.

Xie, K., Yang, D., Ozbay, K., Yang, H., 2019. Use of real-world connected vehicle data in identifying high-risk locations based on a new surrogate safety measure. Accid. Anal. Prev. 125 May 2018 , 311–319. doi:10.1016/j.aap.2018.07.002

Yan, X., Radwan, E., Abdel-Aty, M., 2005. Characteristics of rear-end accidents at signalized intersections using multiple logistic regression model. Accid. Anal. Prev. 37 6 , 983–995. doi:10.1016/j.aap.2005.05.001

Yu, R., Abdel-Aty, M., 2014. An optimal variable speed limits system to ameliorate traffic safety

risk. Transp. Res. Part C Emerg. Technol. 46, 235–246.

Yuan, J., Abdel-Aty, M., Cai, Q., Lee, J., 2019a. Investigating drivers' mandatory lane change behavior on the weaving section of freeway with managed lanes: A driving simulator study. Transp. Res. Part F Traffic Psychol. Behav. 62, 11–32.

Yuan, J., Abdel-Aty, M., Gong, Y., Cai, Q., 2019b. Real-Time Crash Risk Prediction using Long Short-Term Memory Recurrent Neural Network. Transp. Res. Rec.

Yuan, J., Abdel-Aty, M., Wang, L., Lee, J., Wang, X., Yu, R., 2018a. Real-Time Crash Risk Analysis of Urban Arterials Incorporating Bluetooth, Weather, and Adaptive Signal Control Data, in: Transportation Research Board 97th Annual Meeting.

Yuan, J., Abdel-Aty, M., Wang, L., Lee, J., Yu, R., Wang, X., 2018b. Utilizing bluetooth and adaptive signal control data for real-time safety analysis on urban arterials. Transp. Res. part C Emerg. Technol. 97, 114–127.

Yuan, J., Mohamed Abdel-Aty, 2018. Approach-Level Real-Time Crash Risk Analysis for Signalized Intersections. Accid. Anal. Prev.

Yue, L., Abdel-Aty, M., Wu, Y., Wang, L., 2018. Assessment of the safety benefits of vehicles' advanced driver assistance, connectivity and low level automation systems. Accid. Anal. Prev. 117, 55–64. doi:10.1016/j.aap.2018.04.002

Zaki, M.H., Sayed, T., Khaled Shaaban, 2014. Use of Drivers' Jerk Profiles in Computer Vision–Based Traffic Safety Evaluations. Magy. Allatorvosok Lapja 136 10 , 579–587. doi:10.3141/2434-13

Zhang, B., 2015. Traffic Conflict Analysis Under Fog Conditions Using Computer Simulation.

Zhang, M., Khattak, A.J., 2018. Identifying and analyzing extreme lane change events using basic safety messages in a connected vehicle environment, in: 97th Annual Meeting of the

Transportation Research Board.

Zheng, J., Liu, H.X., 2017. Estimating traffic volumes for signalized intersections using connected vehicle data. Transp. Res. Part C 79, 347–362. doi:10.1016/j.trc.2017.03.007

Zhu, W.-X., Zhang, L.-D., 2014. An original traffic flow model with signal effect for energy dissipation. Int. J. Mod. Phys. C 25 7 , 1450018. doi:10.1142/S0129183114500181

Ziliaskopoulos, A.K., Waller, S.T., Li, Y., Byram, M., 2004. Large-Scale Dynamic Traffic Assignment : Implementation Issues and Computational Analysis 130 5 , 585–593.

Zitzow, S., Lehrke, D., Hourdos, J., 2015. Developing a Large-Scale Hybrid Simulation Model: Lessons Learned. Transp. Res. Rec. 2491, 107–116.